



University  
of Glasgow

<https://theses.gla.ac.uk/>

Theses Digitisation:

<https://www.gla.ac.uk/myglasgow/research/enlighten/theses/digitisation/>

This is a digitised version of the original print thesis.

Copyright and moral rights for this work are retained by the author

A copy can be downloaded for personal non-commercial research or study,  
without prior permission or charge

This work cannot be reproduced or quoted extensively from without first  
obtaining permission in writing from the author

The content must not be changed in any way or sold commercially in any  
format or medium without the formal permission of the author

When referring to this work, full bibliographic details including the author,  
title, awarding institution and date of the thesis must be given

Enlighten: Theses

<https://theses.gla.ac.uk/>  
[research-enlighten@glasgow.ac.uk](mailto:research-enlighten@glasgow.ac.uk)

"Scale Problems in Hydraulic Models where Density Spread is Simulated"

by

A.M.M. Hassan

Summary

This thesis is primarily concerned with the search for an appropriate criterion for the design of hydraulic models so as to simulate density spread. In an attempt to acquire an adequate knowledge of the physical behaviour of density spread, the special case of two dimensional spread in a rectangular flume as found in lock type exchange flow was chosen. A general review of work on such flows is given, followed by a derivation of the parameters pertaining to it. An experimental study of lock flows has led to confirmation of previous observation of the front and, seemingly for the first time as regards to hydraulic studies, to the finding of differential movements within and behind the fronts. This feature explains the great variations in the rate of decrease of front velocities within the range available in the flume; and this is shown to be related to the laminar or turbulent nature of the flow. The foregoing was confirmed by a study of the dilution in such flows.

A preliminary examination of the "dam-burst" was made together with some qualitative and quantitative studies of dam-burst analogy exchange flows. The fronts in the latter case were examined and were compared with those of lock exchange flow. Again, differential movements of water masses behind the front was observed.

Attention was then directed to the study of the three dimensional spreading of heated water in simple conditions. A reasonably good correspondence was achieved between a prototype of laboratory dimensions and a 1/5th model, for which

ProQuest Number: 10662272

All rights reserved

INFORMATION TO ALL USERS

The quality of this reproduction is dependent upon the quality of the copy submitted.

In the unlikely event that the author did not send a complete manuscript and there are missing pages, these will be noted. Also, if material had to be removed, a note will indicate the deletion.



ProQuest 10662272

Published by ProQuest LLC (2017). Copyright of the Dissertation is held by the Author.

All rights reserved.

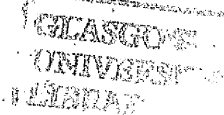
This work is protected against unauthorized copying under Title 17, United States Code  
Microform Edition © ProQuest LLC.

ProQuest LLC.  
789 East Eisenhower Parkway  
P.O. Box 1346  
Ann Arbor, MI 48106 – 1346

the vertical exaggeration was based on a Keulegan type congruency diagram.

The experimental work was carried out in a hydraulic circuit which was constructed for a previous basic study.

The critical review made and the model operations described have, in the opinion of the Author, pointed to the necessary adoption of Keulegan type congruency diagrams for the design of models involving density spread.



SCALE PROBLEMS IN HYDRAULIC  
MODELS WHERE DENSITY SPREAD  
IS SIMULATED

being

A thesis submitted for the degree of Master of Science  
in Engineering of the University of Glasgow.

by

A. M. M. Hassan, B.Sc.

April 1962.

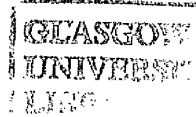
The thesis is bound in two Volumes

VOL. I

Thesis

2061

Copy 2



## CONTENTS

## ACKNOWLEDGEMENTS

	CONTENTS	page
1.	PREFACE	1
2.	INTRODUCTION	
2.1.	General review of density currents and stratified flows.	2
2.2.	Review of past work on heat dissipation models.	8
3.	THEORETICAL CONSIDERATIONS	
3.1.	The derivation of dimensionless numbers pertinent to the operation of non-homogeneous models.	14
3.2.	Comparison of the two methods for the study of scale exaggeration.	19
4.	HYDRAULIC APPARATUS	
4.1.	Description of the hydraulic circuit.	26
4.2.	Critical review of the apparatus competence	27
5.	RECORDING APPARATUS	
5.1.	The description and operation of the miniature current flowmeter.	29
5.2.	Velocity recording.	31
5.3.	Dilution recording.	32
6.	EXPERIMENTS WITH LOCK EXCHANGE FLOWS IN RECTANGULAR FLUME.	
6.1.	Introductory.	33
6.2.	The velocity study of density-current tip.	35

6.3.	Observational study of the differential movements of water well behind the tip.	36
6.4.	Measurements of velocity in regions well behind the front.	43
6.5.	Small scale dilution study.	47
7.	STUDY OF THE DAM-BURST	
7.1.	The ideal dam-burst (air and water).	54
7.2.	The dam-burst analogy.	55
7.3.	Some theoretical consideration.	59
8.	SIMPLIFIED OUTMALL STUDY	
8.1.	Introductory.	64
8.2.	Model-prototype similarity with regards to the limits of spread.	
8.3.	Model-prototype similarity with regards to through velocity.	
8.4.	Model-prototype similarity with regards to thermal vertical stratification.	68
9.	CONCLUSIONS AND RECOMMENDATION	
9.1.	Conclusions	72
9.2.	Recommendations	73
10.	REFERENCES	
10.1.	References for Chapter 2.	76
10.2.	References for Chapter 3.	78
10.3.	References for Chapter 6.	79
10.4.	References for Chapter 7.	80

## Vol. II

	page
Table 2.1.	83-84
Table 2.2.	85
FIG. 2.1. Temperature-density relation for fresh water.	86
" 2.2. Concentration-density relation for salt water solution (NaCl). Values from international critical tables.	87
" 3.1. Variables pertaining to lock flow.	88
" 3.2. Keulegan's results for channel and sea experiments.	89
" 4.1.1. Down stream end of the flume with draft excluders in open position, (Photograph)	90
" 4.1.2. Pumping system (Photograph)	90
" 4.1.3. Down-pipe controls (Photograph).	91
" 5.1.1. Angled thermometer and circular perspex tube in position to record temperatures of stratified layers.	91
" 6.1.1. Keulegan type congruency diagram.	92
" 6.1.2. Effect of reflection on front velocity	93
" 6.1.3. Surface tension variation for saline and thermal density differences.	94
" 6.2.5. Typical plots of advance of front - laminar.	95
" 6.2.6. Typical plots of advance of front - turbulent.	96
" 6.2.7. Viscosity of fresh water.	97
" 6.2.8. Typical calculation of front coefficient of proportionality and densimetric Reynold's number.	98
" 6.2.9. Front coefficients of proportionality of lock flow.	99
" 6.2.10. Saline coefficient of proportionality.	100

		page	
FIG.	6.3.11.	Starting conditions.	101
"	6.3.12.	Distortion of coloured prism.	101
"	6.3.13.	Overtaking of the front by coloured water from behind.	102
"	6.4.14.	Typical flowmeter recordings.	103
"	6.4.15.	Calibration of the miniature flowmeter.	104
"	6.4.16.	Velocity variation of water behind the front.	105
"	6.4.17.	Velocity variation of water behind the front.	106
"	6.4.18.	Velocity variation of water behind the front.	107
"	6.4.19.	Velocity variation of water behind the front.	108
"	6.4.20.	Velocity variation of water behind the front.	109
"	6.4.21.	Impression of velocity gradient at a section.	110
"	6.4.22.	Rate of transit of floats.	111
"	6.4.23.	Rate of transit of floats.	112
"	6.4.24.	Rate of advance of front.	113
"	6.4.25.	Rate of advance of foremost dye traces.	114
"	6.4.26.	Comparisons between variations of velocity of front and foremost dye traces.	115
"	6.4.27.	Rate of advance of front.	116
"	6.4.28.	Rate of advance of foremost dye traces.	117
"	6.4.29.	Variations of overflow front velocity	118
"	6.4.30.	Comparisons between variations of velocity of front and foremost dye traces.	119
"	6.5.31.	Dilution against depth at underflow fronts.	120

	page
FIG. 6.5.32.	Dilution against depth at underflow front. 121
" 6.5.33.	Dilution against depth at underflow flow 122 and at an extended part of it
" 6.5.34	Dilution against depth for samples along 123 an extended underflow.
" 6.5.35.	Dilution against depth for samples along 124 an extended underflow.
" 6.5.36.	Dilution against depth for samples along 125 an extended underflow.
" 6.5.37.	Rate of advance of front 126
" 7.1.1.	The St.-Venant wave profile resulting from 127 the sudden destruction of a dam.
" 7.1.2.	The outset of an ideal dam-burst. 128
" 7.1.3.	Developed stage of an ideal dam-burst. 128
" 7.2.4.	Dam-burst analogy - overflow. 129
" 7.2.5.	Dam-burst analogy - underflow. 130
" 7.2.6.	Dam-burst analogy - overflow at an 131 initial stage.
" 7.2.7.	Dam-burst analogy overflow at a developed 131 stage.
" 7.2.7.A	Dam-burst analogy underflow at various 132 stages. (Photographs). } a) at the starting conditions. b) at initial stage. c) at a developed stage. d) at a more developed stage. e) the form of interfacial layer at back 133 regions being similar to that of the ideal dam-burst as given by the St.-Venant theory.
" 7.2.8.7.2.8.	Typical rate of advance of dam-burst analogy 134 fronts.
" 7.2.9.	Dam-burst analogy overflow-underflow 135 coefficients of proportionality.
" 7.2.10.	Composite diagram of coefficients of 136 proportionality.

	page
FIG. 8.1. General view of tank and rear flume (Photograph).	137
" 8.1.A Simplified outfall.	138
" 8.2. Model/prototype similarity in basic outfall studies - through velocities.	139
" 8.3. Model/prototype similarity in basic outfall studies - through velocities.	140
" 8.4. Model/prototype similarity in basic out- fall studies.	141
" 8.5. An early stage of spreading of outfall heated water (Photograph).	137
" 8.6. A more developed stage of spreading of outfall heated water.	142
" 8.7. Fully developed stage of spreading of outfall heated water.	142
" 8.8. Model/prototype similarity in basic outfall studies - through velocities.	143
" 8.9. Model/prototype similarity in basic outfall studies - through velocities.	144
" 8.10. Model/prototype similarity in basic out- fall studies - through vertical thermal stratification.	145

## ACKNOWLEDGEMENTS

The Author wishes to express his gratitude to the head of the department of Mechanical, Civil and Chemical Engineering, Professor Adam T. Thomson, D.Sc., Ph.D., A.R.C.S.T., M.I.C.E., M.I.Mech.E., for the opportunity to carry out this work and for facilities granted within the department. Also, he is indebted to Professor William Frazer, B.Sc., Ph.D., A.R.C.S.T., A.M.I.C.E., A.M.I.Mech.E., Professor of Civil Engineering, for his generous allocation of space in the Civil Engineering Laboratory and for his interest and encouragement throughout the investigation. He, also, wishes to record his grateful thanks to D. I. H. Barr, B.Sc., Ph.D., D.R.T.C., A.M.I.C.E., M.ASCE., for his constant guidance and assistance throughout the investigation and preparation of the thesis. Mr. R. T. McCrone and the staff of the Civil Engineering Laboratory are also sincerely thanked.

The work was carried out while the Author was receiving a Port of Basrah-Iraq scholarship, for which financial assistance he is most grateful.

## 1. PREFACE.

1.1. For three or four years previously, basic studies had been carried out in the College concerned primarily with similarity in heat dissipation and recirculation models, and the better understanding of stratified flows and density currents in general. In order to further understand the physical behaviour of the phenomena and to check the suitability of the design method as obtained from the previous work, it was felt that further basic research on non-homogeneous flow was greatly needed. It was, thus, especially suitable to the author to embark on the basic study as certain facilities in the College were already built while the progress of <sup>a</sup> large scale ad-hoc investigation directly concerned with the basic study could be followed during his period of study.

1.2. Although the direct application of the present study is to heat dissipation and recirculation models, it could also be of special interest to the author's future work. For instance, the author will be dealing with the river "Shatt-El-Arab" which is the only navigable river in Iraq. This river is tidal, being connected to the Persian Gulf, and is, also, silt laden necessitating a large annual outlay on dredging operations in order to provide a navigable channel for the ocean-going ships.

1.3. It has been known that the movement of saline underflow water in estuaries, being generally opposed to the direction of fresh water current downstream, could cause the transportation of sediments back to their original places prior to dredging. If this is the case, then the knowledge gained from the present basic study may be useful to the author in his future work.

2.

## INTRODUCTION,

2.1. General review of density currents and stratified flows.

2.1.1. The presence of non-homogeneity in water may or may not cause difference of density. For example, varying temperature, varying salinity or varying turbidity (presence of silt in suspension) generally results in difference of density. Figure

2.1 shows the temperature-density relation for fresh water.

Fig. 2.2 shows the relation of density difference to the amount of dissolved common salt ( $\text{NaCl}$ ). The density caused by turbidity varies with the amount and specific gravity of the particles present in turbid water.

2.1.2. On the other hand chemical traces either naturally occurring or associated with waste water disposal, bacterial waste pollution or radio active waste pollution may not cause discernable density difference. Wherever non-homogeneity occurs with density difference, density currents are likely present in the form of superimposition of motion on the already existing motion, or lack of motion.

2.1.3. Density currents are of importance to the science of engineering especially in dealing with problems such as the transport of sediments and the pollution of harbours, estuaries, rivers and the like.

2.1.4. In hydraulics literature, many attempts have been made to provide an apt and relevant definition of a density current. For example, "A density current is the movement without loss of identity by turbulent mixing at the bounding surfaces, of a

stream of fluid, under, through or over a body of fluid, with which it is miscible, and the density of which varies from that of the current, the density difference being a function of differences in temperature, salt content and/or silt content of the two

2.2a

fluids". More especially "The term density current . . .

refers to a flow of water maintained by gravity forces through a main body of water such as Lake Mead and remaining separated therefrom because of the difference in density between the

2.2b 2.3  
current and the lake." But essentially, as Keulegan states,

a density current flow is always controlled, although to a lesser extent, by the same gravitational situation as that existing at the free surface of a body of water in contact with air. In other words, all free-surface hydraulic and wave phenomena can occur at the interface of the two adjacent strata. The effective gravitational coefficient as regards the interfacial movements can be taken as  $g' = \frac{\Delta\rho}{\rho} g$ , where  $\rho$  and  $\Delta\rho$  are the average and differential density respectively. This will be amplified in (3.1).

2.1.5. It is here suitable to draw a distinction between density currents and stratified flows. In the commonly found examples of stratified flows, vertical exchange motion is impeded by the density difference, whereas in density currents, horizontal exchange motion is caused by the density difference. Furthermore, the velocity distribution at a section taken through a stratified flow can in certain circumstances be the same as that of a homogenous unidirectional flow.

2.1.6. A good example of an intermediate case between stratified flows and density currents is the well-known "salt-wedge". Such a type of flow exists with the salt water intrusion of inland waterways. The intrusion, as a density current, moves up river until conditions such as river configuration, flow of fresh water down-stream and the magnitude of mixing become effective in preventing the underflow density current from further up-stream advancement. At this stage, the stationary underflow is known as saline wedge, and this is capable of moving up or down stream if any, or all, of the above mentioned factors are varied.

2.1.7. Although, for many years, small scale studies of non-homogenous water movements have been carried out and related to large scale movements by oceanographers,<sup>2.4</sup> it is only recently that civil engineers have shown keen interest in the subject. The interest has been fostered by the direct bearing of these phenomena on a number of problems encountered in the field of engineering.

2.1.8. It appears, however, that the subject of study of densimetric flows is, relatively speaking, new and that most of the available information has been drawn from qualitative studies. Moreover, due to the presently incomplete knowledge of mixing, interfacial friction and the relative importance of inertial forces of the two layers in contact, the qualitative studies, so far carried out,<sup>2.5,6</sup> have produced little progress. This situation might be attributed to the introduction of a number of

unwarranted assumptions regarding the above mentioned parameters.

2.1.9. Observations of large scale occurrences of density current have been reported on various occasions. Without undue repetition, the following examples are briefly mentioned:-

(1) Thermal density variation.

6.9  
It has been known that the effect of recirculation of heated water in the cooling system of a power station may cause a considerable loss of efficiency, and also, by the resulting variation of temperature, tends to affect marine life <sup>2,7,8</sup> in the region. This thesis is concerned with the basis of the model approach to the solution of such problems.

(2) Saline density variation.

The saline water intrusion of inland water is a common place occurrence in practically every tidal river. In the attempt to prevent such an occurrence, the alternative means of either deepening a waterway <sup>2.9</sup> or of obstructing <sup>2.10,11,12</sup> the fresh water flow does not always yield satisfactory results, as there has been adverse effects associated with both of these solutions. In the second example cited, reduction in drainage flow has resulted from the development of landward irrigation projects, and this has caused a deterioration in the quality of water available for local irrigation.

2.10,11

in the Sacramento-San Joaquin Delta, California.

Also, despite the various barrier schemes constructed so as to limit intrusion and to reduce fresh water flow, the port and city of Calcutta are, at present, affected by increasing salinity and siltation in the River Ganges. Hence, the water supply intake and the navigation channel are both being threatened. As an example of the effect of deepening of a waterway, the water supply intake of the city of Gothenburg was affected by salinity and it was found appropriate to move the intake further upstream. It seems, therefore, that since no effective or economically feasible means of preventing intrusion have yet been found, its occurrence, though regretted, should necessarily be accepted.

(3) Turbid density variation.

The physical nature of the suspended sediment is of considerable importance as a cause of density currents because some of the suspended sediments, being very fine, stays in suspension at low stream velocity and, thus, cause small density difference.

The movements of turbid water through Lake Mead (Hoover Dam Reservoir) provides a typical example of this kind of density current. It was found during construction in 1935 that under critical

2.2(a,b),13

discharge, water was unexpectedly turbid and was estimated that some 6,000,000 tons of silt, or about 2.5% of the average annual load of silt brought to the lake by Colorado River, passed through the temporary openings. Obviously such by-passing is beneficial as it tends to maintain the initial storage capacity of the lake. However, that suitable discharge appeared to be responsible for the present prevalent belief that normal flow of spilled water over a dam must be arranged so that as much silt as possible should be discharged.

2.14 Creek had put forward such a proposition some years prior to the observation of the above cited example.

## 2.2      Review of past work on heat dissipation models

2.2.1.    Modern steam generating stations may draw vast quantities of water from estuaries or rivers for condensing purposes. 1000, 2000 cusecs or even more is intended for stations now under construction. In condensing the steam a temperature rise of  $15^{\circ} - 20^{\circ}\text{F}$  is incurred, and it is important that the discharged water is not recirculated for reasons as explained in 2.1.9. The first obvious remedy of making the outlet point (station outfall) far from the inlet point (intake) can be very costly, and it has been found advisable in many occasions to study the problem in a model. It is hoped that, through such type of investigations, the restriction of recirculation may be attained at the least cost possible. Table 2.1 shows the main details of such models which involved tidal flows. Some of these have been specially built, and some were in existence for other purposes and this is indicated. Table 2.2 shows some brief details of the steady state river models, the design of which is not considered in this thesis.

2.2.2.    In non-steady state tidal models, the flow of a given quantity of water must necessarily be governed by the time scale as well as the velocity scale, both of which are based on the Froude criterion. When the standard Froude criterion is used for the overall currents, the common practice has been that the initial temperatures of prototype heated and colder water, and also the net density variations were adopted

in the model. This course is justified in 3.1.

2.2.3. Normally, the intention in such type of model studies has been that the following aspects of flow should be simulated as closely as possible both at slack water and when superimposed on the general tidal flows:-

- (1) The longitudinal travel and lateral spread of isolated heated currents over the colder river, estuary or sea water.
- (2) The intake of water from stratified layers.
- (3) Turbulent mixing.

For the simulation of the above mentioned factors, two methods have already been devised. These are:-

- (1) The theoretical method in which the principle of dimensional analysis is used to find the best suitable vertical distortion.
- (2) The empirical method which provides a set of experimental congruency diagrams from which vertical exaggeration is obtained.

More details together with a critical review of the two methods is given in 3.2.

2.2.4. It should be noted that, unlike the well established practice of modelling structures constructed in homogenous flow, such as weirs, bridges, dams and the like, very little has as yet been reported on model-prototype comparisons in the case of heat dissipation studies.

2.2.5. Of the models listed in table 2.1, more details are

available concerning that for the Kincardine power station than for others. It is suitable to draw upon the details of this model study in order to illustrate the overall picture of such studies. A fixed boundary model was constructed for part of the width of the River Forth at Kincardine. A  $\frac{1}{44}$  horizontal scale, which was dictated by the space available for model river bed, and a vertical scale of  $\frac{1}{48}$  were chosen. With the vertical exaggeration of 5, the resulting flow in the model was fairly turbulent. Since no information is given in the paper as to the basis of adopting such an exaggeration; it seems, however, that it was arbitrarily chosen.

2.2.6. It was found necessary to simulate only part of the tidal cycle - the latter part of the ebb and the ensuing slack. Certain peculiarities occur in the normal currents at this stage and good agreement was achieved in the model. The intake was fixed by the suitable deep water near the station and away from navigation. Recirculation resulting from each of several outfalls placed successively nearer to the station was studied. Subsequently, the outfall at a full size distance of approximately 2740 ft. from the intake was chosen. This outfall position produced not only an allowable degree of recirculation, but, also, a considerable saving in culvert length in comparison with the outfall previously intended.

2.2.7. It is interesting to note that diminishing stratification, hence more recirculation, took place in the model at lower basic

temperature. Heat losses to atmosphere and river bed were tested and proved to cause negligible effect on model-prototype similarity.

2.2.8. In the Kincardine model, it was hoped that three kinds of water movements were simulated. These are (1) normal currents, (2) density currents, and (3) turbulent mixing. As for (1) and (2) their simulation was based on Froude and densimetric Froude number ( $V_r = \sqrt{D_r \times d_r}$  where  $V_r$ ,  $D_r$  and  $d_r$  are velocity scale, vertical scale and variation in density scale) respectively. It was not claimed that similarity as regards to turbulent mixing had been achieved. As yet only a few reports on prototype verification of the model findings have been published.

2.2.9. The Civil Engineering section of the Royal College of Science and Technology has designed two heat dissipation models for the proposed power stations at Cockenzie and Methil on the River Forth on behalf of the South of Scotland Electricity Board.

The two models have been constructed by the S.S.E.B.,  
but only the Cockenzie model has as yet been operated.

2.2.10. The Cockenzie model is a fixed boundary model 60 ft.  
x 35 ft. embracing some  $\frac{2}{3}$  miles of coastline centred  
approximately on Cockenzie Harbour. Once more, the Froude  
criterion was adopted to simulate flow phenomena with the  
proposed prototype thermal and saline density differences.

adopted in the model. For prototype flow such as the one occasioned in the Firth at Cockenzie and on the basis of Keulegan type congruency diagram (3.2), the vertical exaggeration needed to simulate density spread should be between six and eight and accordingly an exaggeration of seven was used. From considerations of land area available for river bed and the desire to have a reasonably large circulating water flow the horizontal scale of  $\frac{1}{250}$  was chosen which led to a vertical scale of  $\frac{1}{56}$ .

Arrangements have been made to simulate the ebb and flood of the tidal currents over the full tide range. The model flow of circulating water (0.025 cusec.) is derived from the discharge scale using full load prototype flow of 1340 cusecs. Arrangements have been made to pass this quantity of water through electric water heaters and back to the model via a V-notch weir where flow measurement is made. The electric heating arrangement is capable of providing the model circulating water with a temperature increment of  $18^{\circ}\text{F}$ . In order to obviate the distortion resulted from the introduction of a flow of water over an outfall weir into a model with an exaggerated vertical scale, the model outfall was built using the vertical scale for both the vertical and horizontal dimensions in the direction of flow, but adhering to the horizontal scale ratio of  $\frac{1}{250}$  across the line of flow.

Thus geometric similarity within the outfall structure

in the direction of flow is obtained and, hence, correct flow conditions at the point of confluence with the distorted model proper. As far as the outfall, where the flow is predominately horizontal, distortion is permissible, but for a vertical intake shaft placed in such a model, the resulting flow in the vicinity is no longer horizontal. However, strict adherence to the horizontal scale in determining the cross section area of the shaft would result in very much exaggerated vertical velocities.

Indeed, it is very difficult to predict the effect of distorting the intake of stratified water, because with an increasing vertical velocity, there is an pronounced tendency of pulling down the overflow heated layers. On the other hand, the decrease in shaft width to total depth ratio might minimise the above mentioned tendency. However, a compromising arrangement was reached by employing a 3 inch shaft which gave slightly more vertical velocity than that given by Froude scale. Although the shaft, or shafts, will be out of scale in the horizontal direction, the surrounding bottom slopes are sufficiently gentle for this to be insignificant.

Having calibrated the model and determined the stream line patterns on the basis of float and tide observations made at Cockenzie in 1960/1961, a reasonable compromise in choosing the off shore boundary was attained. A number of tests have so far been run so as to determine economical positions of the intake and outfall while suffering only a moderate degree of recirculation.

### 3. THEORETICAL CONSIDERATIONS

3.1. The derivation of dimensionless numbers pertinent to the operation of non-homogeneous models.

3.1.1. While classical hydrodynamics treats water as an ideal fluid, modern fluid mechanics realizes the appreciable effects of viscosity, surface tension and elasticity on modifying the basic flow pattern expressed in a mathematical form. In the attempt to include the above mentioned parameters in the previous classical hydrodynamics, it was found essential that the several variables should be organised dimensionally in small numbers of significant parametric groups. That this was possible is due to the fact that in any mathematical equation of motion, in order to be physically correct, every term of it when reduced to basic dimensions of length, time and mass must contain identical powers of each of the respective dimensions i.e. both sides of the

equation are dimensionally homogeneous. After Buckingham<sup>3.1</sup> (1915) the  $\pi$ - theorem has become the principle tool of dimensionless analysis.

3.1.2. For illustration of the theorem, it seems desirable to use it for the dimensionless groupings of parameters which may be pertinent to the densimetric flow in rectangular channel. The equation of motion of a density current could be written as:

$$(H, B, l, l_0, \Delta\varrho, V_a, V_o, V, \nu, \gamma, \rho_m) = 0$$

Where the aforementioned variables are defined in the following table:-

Notation	Quantity	MIT System Dimensions
H	Total depth	L
B	Channel Width	L
$\ell$	Travel length	L
$\ell_0$	Lock length	L
$\Delta \rho$	Density difference	$M/L^3$
$V_d$	Densimetric velocity	$L/T$
$V_0$	Initial velocity of front	$L/T$
V	Velocity of front at distance $\ell$ from the gate	$L/T$
$\nu$	Coefficient of kinematic viscosity	$L^2/T$
$\gamma$	Weight density	$M/L^2 T^2$
$\rho_m$	Mean density $\frac{2\rho + \Delta \rho}{2}$	$M/L^3$

$V_d$ , the densimetric velocity, suggested by Keulegan, is a characteristic velocity which if occasioned by a density flow would give a densimetric Froude number (which is defined later)  $F_d = 1$ . Fig. (3.1.1) shows the variables diagrammatically.

Let  $H, \Delta \rho, V_d$  be some relevant variables representing the geometric, kinematic and dynamic parameters respectively. Since there are 11 independent variables and 3 fundamental dimensional units, therefore, the number of dimensionless PIS =  $11 - 3 = 8$

$$\text{i.e. } f(\pi_1, \pi_2, \dots, \pi_8) = 0$$

$$\begin{aligned}
 \pi_1 &= H^{x_1} \Delta e^{y_1} V_\Delta^{z_1} B^{-1}, & \pi_2 &= H^{x_2} \Delta e^{y_2} V_\Delta^{z_2} \ell^{-1} \\
 \pi_3 &= H^{x_3} \Delta e^{y_3} V_\Delta^{z_3} \ell_o^{-1}, & \pi_4 &= H^{x_4} \Delta e^{y_4} V_\Delta^{z_4} V_o^{-1} \\
 \pi_5 &= H^{x_5} \Delta e^{y_5} V_\Delta^{z_5} V^{-1}, & \pi_6 &= H^{x_6} \Delta e^{y_6} V_\Delta^{z_6} V_m^{-1} \\
 \pi_7 &= H^{x_7} \Delta e^{y_7} V^{z_7} y^{-1}, & \pi_8 &= H^{x_8} \Delta e^{y_8} V^{z_8} C_m^{-1} \\
 \pi_1 &= L^o T^o M^o + (L)^{x_1} (\frac{M}{T})^{y_1} (\frac{L}{T})^{z_1} (L)^{-1} \\
 o &= x_1 - 3y_1 + z_1 - 1 \\
 o &= -z_1 \\
 o &= y_1 \\
 \therefore \pi_1 &= \frac{H}{B}
 \end{aligned}$$

Similarly, by inspection,  $\pi_2$ ,  $\pi_3$ ,  $\pi_4$ ,  $\pi_5$ , and  $\pi_7$  equal to  $\frac{H}{L}$ ,  $\frac{H}{L}$ ,  $\frac{V_o}{V}$ ,  $\frac{V}{V}$  and  $\frac{\Delta e}{C_m}$  respectively.

$$\pi_6 = L^o M^o T^o = (L)^{x_6} (\frac{M}{T})^{y_6} (\frac{L}{T})^{z_6} (\frac{L}{T})^{-1}$$

$$o = x_6 - 3y_6 + z_6 - 2$$

$$o = -z_6 + 1$$

$$o = y_6$$

$\therefore \pi_6 = \frac{H \cdot V}{\rho}$  densimetric Reynold's number. Following the same process as above  $\pi_8 = \frac{\Delta e V^2}{g H}$ . Since  $\pi_8$  is dimensionless, therefore it could be written as:

$$\pi_8 = \frac{\Delta e V^2}{g H} \cdot \frac{C_m}{\Delta e} = \frac{V_o C_m}{g \Delta e H} = \frac{V_o^2}{g \frac{\Delta e}{C_m} H} \text{ densimetric Froude number.}$$

$$\text{Hence } \left( \frac{B}{H}, \frac{\ell_o}{H}, \frac{\ell}{H}, \frac{V_o}{V}, \frac{V}{V_\Delta}, \frac{\Delta e}{C_m}, R, F \right) = 0$$

3.1.3. Geometric similarity exists when all corresponding linear dimensions ( $\frac{B}{H}$ ,  $\frac{\ell_o}{H}$ ,  $\frac{\ell}{H}$ ) in model and prototype bear an equal relationship.

Kinematic similarity exists when the ratios of the

components of velocity ( $\frac{V_o}{V_s}, \frac{V_s}{V_d}$ ) at all homologous points in two geometrically similar systems are equal.

Dynamic similarity between geometrically and kinematically similar systems requires that the ratio of all homologous forces ( $\frac{\Delta C}{\Gamma_m}, R_s, F_s$ ) in the two systems, be the same.

Of course, the above stated conditions are for an ideal similarity. Due to the impossibility of scaling down the properties of water such as density, viscosity, surface tension, the correct reproduction of all the force actions in a model is unattainable. Therefore, the procedure is to reproduce the action of the presumed dominant force.

3.1.4. At the outset of an exchange flow, gravitational forces assume a dominant role. Therefore, as far as model-prototype initial velocities are concerned, the Froude densimetric number ( $F_d$ ) seems to be the correct criterion for simulation. Thereafter, viscosity and, especially, mixing effectively cause the marked diminution of velocity and its simulation is no longer based on one criterion. However, the experimental congruency diagram such as those proposed by Keulegan could be a correct and reliable criterion for achieving simulation thereof. For further discussion of the above, see (3.2).

3.1.5. On the other hand, in the design of heat dissipation models where density spread is superimposed by normal free surface flows of tidal currents and the like, it has invariably been assumed that both standard Froude criterion and densimetric Froude ( $F_d$ ) or Richardson (Ri) criterion should be satisfied

as explained below:-

$$\frac{V_p}{V_m} = \sqrt{\frac{L_p}{L_m}} \quad (\text{standard Froude criterion})$$

$$\frac{\rho_p V_p^2}{g \cdot \Delta P_p L_p} = \frac{\rho_m V_m^2}{g \cdot \Delta P_m L_m} \quad (F_a, \text{ or Richardson, model law})$$

$$\frac{\rho_p}{\Delta P_p} = \frac{V_m^2}{V_p^2} \cdot \frac{L_p}{L_m} \cdot \frac{\rho_m}{\Delta P_m} = \frac{\rho_m}{\Delta P_m}$$

$\rho_m = \rho_p$  as water is usually used in both model

and prototype.

$$\therefore \Delta P_m = \Delta P_p$$

3.2. Comparison of the two methods for the study of scale exaggeration.

3.2.1. 1). The analytical method:-

Professor Gibson<sup>3.2</sup> had used the principle of dimensional homogeneity in problems involving the transference of heat between two flowing fluids separated by some division. He assumed that radiation effects were negligible and introduced the following as pertinent variables to the problem:-

$$H = \text{the flow of heat per unit time (energy/unit time)} \\ = M I^2 t^{-3}$$

$T$  = the temperature difference

$K$  = the conductivity of the fluid

$\rho$  = the density of the fluid

$C$  = the specific heat of the fluid

$\mu$  = the viscosity of the fluid

$\ell$  = some representative linear dimension

$v$  = the velocity

3.2.2. Professor J. Allen<sup>3.3</sup> extended Gibson's analysis to the study of the actual simulation of heat dissipation in a model; and suggested that the flow in the model, like that in prototype, should essentially be turbulent on the basis of the

following formula:-  $\frac{H_p}{H_m} = x^{5/2}$ . The validity of this

formula was tested in a natural model of scale 1:150, which produced agreement within  $0.2^{\circ}\text{F}$  at most of the points selected for comparison. It should be noted, since only  $\frac{1}{7}$ th of the river width was included, the diminution of velocity of the

extended spread did not appear to have been considered; and thus exchange due to extended spread was not investigated.

Recently, the Hydraulic Research Station, 3.4 Wallingford, used the dimensional analysis for the operation of a heat dissipation model for a power station being built on the Severn estuary.

3.2.3. Following the argument given by the Hydraulics Research Station, the equation of motion could be written as:-

$$f(H, T, K, \rho, g, \mu, e, v, g) = 0$$

Since  $T$  is not reducible in terms of fundamental units of  $M, L, t$ , the dimensional analysis yields the following 5 pi groups:-

$$f\left(\frac{H}{\rho e^2 v^3}, \frac{\mu}{\rho e v}, \frac{KT}{\rho e v^3}, \frac{\sigma T}{v^2}, \frac{e g}{v^2}\right) = 0$$

$$\frac{H}{\rho e^2 v^3} = \phi\left(\frac{v e}{\nu}, \frac{\mu e T}{\rho e v^3}, \frac{\rho e v^3}{K T}, \frac{\sigma T}{v^2}, \frac{v^2}{e g}\right)$$

Since heat losses through radiation is negligible, heat flow is directly proportional to temperature difference.

$$\text{i.e. } \frac{H}{\rho e^2 v^3} = \frac{\sigma T}{v^2} \phi\left(\frac{v e}{\nu}, \frac{\mu}{K}, \frac{v^2}{e g}\right)$$

Reynold's number  $\frac{v e}{\nu}$  and Prandtl number  $\frac{\mu}{K}$  are neglected for the case of a jet striking a mass of water and the case of same fluid with same temperature difference is considered.

$$H = \sigma e^2 T v \phi\left(\frac{v^2}{e g}\right)$$

This demonstrates that the simulation of heat transference is based on Froude Criterion.

If  $p$  and  $m$  denote prototype and model respectively,

$$\text{then } \frac{H_p}{H_m} = \frac{\rho_p}{\rho_m} \frac{L_p^2}{L_m^2} \frac{V_p}{V_m} \frac{\sigma_p}{\sigma_m} \frac{T_p}{T_m}$$

$$\frac{H_p}{H_m} = \frac{L_p^2}{L_m^2} \cdot \frac{V_p}{V_m} - (1) \quad (\text{Since Prandtl number is the same})$$

If one thinks of heat dissipating through a parallelogram of horizontal and vertical sides equal to  $x$  and  $y$  respectively, then the ratio of heat flowing horizontally is equal to  $xy \cdot y^{1/2}$  and that flowing vertically is equal to  $x^2 \cdot \left(\frac{V_p}{V_m}\right)^{1/2}$ . In the Report of the Director of Hydraulic Research, 1960 the following assumptions were made:-

- 1) the vertical velocity in a model is numerically equal to that in a prototype.
- 2) the ratio of flow of heat in the horizontal direction is equal to that in the vertical direction.

$$\text{i.e. } x^2 \cdot 1 = xy \cdot y^{1/2}$$

$$\text{Hence vertical exaggeration} = \frac{x}{y} = x^{1/2} - (2)$$

3.2.4. It seems that if assumption (1) was correct, any attempt to model a vertically flowing, turbulent jet into stratified fluid would almost certainly fail. Yet, on the other hand, there have been cases 3.5, 3.6 where a flow ejected from a jet was successfully reproduced in a small model being operated on the basis of Froude densimetric criterion from which model velocity given by  $\frac{V_p}{\left(\frac{\Delta \rho}{\rho} gy\right)^{1/2}}$  is not only true for horizontal motion but is also equally true for vertical motion. Moreover, if vertical velocities in model

and prototype were, in fact, equal, then the corresponding vertical mixing would necessarily be similar. In other words, the simulation of vertical mixing would only be attained by the introduction of the relevant vertical exaggeration ( $x^{\frac{1}{3}}$ ). But mixing has been adequately simulated in a non distorted model as typified by the model operated by Gibson in Manchester. On the contrary, it appears that the introduction of the suitable exaggeration is essential only where the need arises to simulate such aspects of an extended densimetric spread as, in particular, the diminution in velocity of the spread.

Furthermore, equation (2) in effect states that as long as the horizontal scale ratio is kept constant, there is only one vertical exaggeration (equal to  $x^{\frac{1}{3}}$ ). It appears, however, that there is no allowance whatever to the size of the model.

But it has been shown by Keulegan that if the horizontal scale of a model of a large prototype is increased, there will come a stage when it is irrelevant to introduce an exaggeration as demonstrated by Fig. 3.2.

3.2.5. As far back as 1932, O'Brien and Chernoff put forward the following model law:-

$$\frac{L_o}{d^{2.5} S^{0.5}} = \frac{l_o}{d^{2.5} S_s^{0.5}}$$

Where  $L_o$ ,  $d$ ,  $S$  denote linear dimension, water depth and salinity in a prototype and the terms on the left side denote the same things in the model.

If  $S_s' = S_s$  then

$$\frac{L_o'}{L_o} = \frac{d}{d'}^{2.5}$$

$$\text{i.e. } \frac{1}{x} = \left(\frac{1}{y}\right)^{2.5}$$

$$\text{and exaggeration} = \frac{x}{x'}^{3/5} = x^{6.5} \quad - (3)$$

It should be remembered that equation (3) was arrived at by the unwarranted assumption that the kinematic viscosity (in  $K = \frac{\nu L_o}{V_{od}^2}$ ) was of the same nature as eddy viscosity being of constant value independent of initial velocity ( $V_0$ ), depth (d) and lock length ( $L_o$ ); and also the factor  $(C_2 + C_1)$  was suppressed.

With such an assumption, it had been found that the time of travel of a body of water in the model would have been greater than the corresponding time in prototype. Since such a result is obviously illogical, it suffices to undermine its validity.

### 3.2.6. 2) The empirical method:-

Keulegan's experimental study on lock exchange flow resulted in a type of congruency diagram (Fig. 6.1.1) which shows that, provided geometric similarity between depth (H) breadth (B) and lock length  $l_o$  is preserved between model and prototype, congruency exists if equality of the parameter  $\frac{V_{od}}{C_m}$  is maintained.

Although Keulegan type of congruency diagram has primarily been intended for lock exchange flow, it could be used as a basis for modelling any densimetric spread if recordings were available for the case of infinite width, non reflected wave.

3.2.7. It is very unfortunate that such Keulegan congruency diagrams have not yet been extended fully to cover a wide range of densimetric Reynold's number ( $KR_\Delta$ ) and Fig. 6.1.1 is the only information available for the required case cited above. As a hypothesis, based on Keulegan's results from his channel and sea experiments (Fig. 3.2), it could be said that if Fig. 6.1.1 is extended to cover much higher values of  $KR_\Delta$  for the infinite width, non reflected wave case, the lines corresponding to velocity ratios would be flattened out. This suggests the existence of a complete congruency between two flows despite there might be some relative difference in their sizes.

3.2.8. For better illustration of the usage of a Keulegan type of congruency diagram for the evaluation of the suitable vertical exaggeration, the following account is given below:-

- 1) In order to evaluate  $KR_\Delta$  relating to a prototype flow, one has to predict an approximate value of the outfall water depth (h). The corresponding total depth (H) in lock exchange flow, on which the congruency diagram was based, is twice the predicted depth (h). Substituting H in  $V_\Delta = \left\{ \frac{\Delta \rho}{\rho_m} gh \right\}^{1/2}$ , the value of the latter is calculated and hence  $KR_\Delta \left( \frac{K \cdot V_\Delta H}{\sqrt{g} h} \right)$ , where K is assumed to be equal 0.5) is evaluated.
- 2) Referring to Fig. 6.1.1,  $\frac{L}{H}$  corresponding to the calculated  $KR_\Delta$  at velocity ratio  $\frac{V}{V_0}$  preferably equal to 0.9 is obtained. Let it be equal to  $X_p$ .
- 3) Vertical exaggeration  $\frac{x}{y} \left( \frac{1}{x}, \frac{1}{y} \right)$  are horizontal and vertical scale ratios respectively) defined as: model travel length ratio divided by prototype travel length ratio and multiplied by

exaggeration would give 1.

i.e.  $\frac{X_m}{X_p} \cdot \frac{x}{y} = 1 \quad \text{--- (4)}$

where  $X_m$  is model travel length ratio  $\frac{L}{H}$ .

4) Having assumed a suitable value for  $y$ , two values of  $X_m$  are consequently obtained; one from equation (4) and the other from Fig. 6.1.1. If these values are equal then that particular value of  $y$  will give the best vertical exaggeration by this criterion.

3.2.9. It should be born in mind that the arguments put forward in evaluating equations (2) and (3) appear to be unjustified.

4. HYDRAULIC APPARATUS4.1. Description of the hydraulic circuit

4.1.1. The hydraulic circuit had been constructed for a previous basic study on density currents. A brief description of it is given below:-

An 17.5 ft. by 1.5 ft. by 0.9 ft. deep level bottomed flume was mainly constructed of resin bonded plywood, with the exception of the front side in  $\frac{1}{8}$  inch perspex so as to allow direct vision. (Fig. 4.1.1) At the end near the pumping system, a fixed wooden gate could be fitted and at the other extreme end a weir gate was erected to control water level in the flume and to discharge water through a 2 ft. opening into the tank (described below).

4.1.2. An 18 ft. by 7.25 ft. by 1.75 ft. deep tank and its guiding walls were built in 9 inch brickwork. At one end of the tank, a 2 ft. opening led to a sump 1.7 ft. below floor level. From the sump water was lifted by an 0.75 cusec. capacity "Siegmund" pump and passed, via branched connection, to a constant head tank and, through a 6 inch diameter delivery pipe, to a V-notch tank. In the constant head tank, excess water passed over a 4.5 ft. long weir and led back to the sump. Fig. 4.1.2 shows the pumping system. Water from the V-notch tank fell into a stilling basin and was led along the flume, the fixed end being removed in this case.

4.1.3. A reasonably fast drainage of the tank was carried out by pumping water from the sump into the constant head tank from which water was led through a 2 inch diameter pipe to waste.

4.1.4. Two mixing tanks of 25 and 12 cubic feet capacity (8.94 and 4.835 sq. ft. surface area respectively) were sited on the internal half floor above the main laboratory. Hand operated mixing paddles were fitted inside the tanks for the purpose of producing uniformity in temperature, or salinity, of the water in the tank. Water from the mixing tanks could be led into the flume or the tank through a flexible down-pipes (1½ ins. and 1 inch.) which were fitted with a regulating valve, an on-off control valve and a drain valve (Fig. 4.1.3.).

4.2. Critical review of the apparatus competence.

4.2.1. Although the present hydraulic circuit has served, on the whole, its purpose reasonably well, the need for relatively larger apparatus (especially the flume) has been realized during every stage of experimentation. Indeed, any attempt towards supplementing the Keulegan type of congruency diagram so as to cover a higher range of KR will undoubtedly be frustrated in the absence of a much longer flume. In the available 17.5 ft. long flume a compromising arrangement was made by positioning the barrier near one end and allowing the front, under study, to proceed along the longer part. In so doing the observation of a reasonable development of the flow was attainable.

4.2.2. It should be noted that as the time taken to fill and empty the available flume was fairly short, a repetitive type of study such as the observational (6.3) was made possible. In contrast to this, it would not only be laborious to fill and empty a much longer and wider flume, but it would also be very time consuming; and subsequently the study of a certain feature

quantitatively would appear to be a very difficult undertaking.

4.2.3. As regards to the tank, while its range was reasonably adequate for the type of experiments carried out, its width was not (see Chapter 3). As the study of the unchecked sideway spread is greatly desirable, it would be better to arrange for a wider tank than the available. Moreover, in the spread study (chapter 8) the balancing of surface tension difference, using a wetting agent, resulted in a large amount of foam to form in the tank and other parts of the circuit. Since normal surface spread was greatly disturbed by the presence of foam, it was necessary to wait until they had disappeared - a process which took a very considerable time - before any test was carried out. It would be possible to altogether eliminate foam's formation, if a circuit with bottom withdrawal after any drop was, instead, designed.

## 5. RECORDING APPARATUS

### 5.1. The description and operation of the miniature current flowmeter.

The miniature current flowmeter - of the type developed at the Hydraulic Research Station, Wallingford, and manufactured by Armstrong Whitworth Aircraft Ltd. - is designed for measuring very low rates of flow, as low as 0.89 inch. per second, of conductive fluid. Also, it is capable of withstanding flows as high as 5 ft. per second.

5.1.1. The measuring head consists of a five bladed Cobex plastic rotor mounted on a hard stainless steel spindle. Frictional torque is extremely low, because the spindle terminates in an adjustable jewel bearings and the whole setting is protected by a stainless steel frame fixed to a stainless steel tube. A gold wire, being insulated from the tube, passes down inside it and finishes about 1 m.m. from the rotor blade tip. The gold wire is connected to an electronic measuring unit via a co-axial cable. The principle of the instrument is that of the gold wire passing of a rotor blade changes the capacitance of a bridge circuit, thus causing an electric impulse which is amplified and displayed on a dekatron counter unit.

5.1.2. For better operation of the instrument, the sensitive balancing of voltage was carried out by carefully following the instructions supplied by the manufacturer. When the instrument in operation, a count of pulses are shown on the "dekatron". This count of pulses can be produced either continuously or intermittently by setting up the "10 seconds/run" switch to either

of them. While the latter setting was discarded because it failed to demonstrate a meaningful velocity variation, the former setting was used in measuring velocity of water following the front in the following manner:-

- (1) While the measuring head was immersed in the water filling the longer reach of the flume, the voltage was balanced as mentioned above.
- (2) Having cleared the "dekatron" from any residue of pulses, the instrument was switched on "run" count of pulses.
- (3) When the density current reached the location of the measuring head, the flow of pulses started to appear. The times corresponding to the start and end of 10 pulses were noted as "tick" (in line with the second hand of a stop clock) on a circular disc of paper attached to the face of a stop clock. This process of time recording continued till the front reached the far end barrier of the longer reach.
- (4) The results thus obtained were plotted against time (sec.) from the lifting of the barrier (Fig. 6.4.14). Also from these results, the number of pulses per 10 seconds were calculated in order the linear velocity (inch/sec.) could be obtained from the calibration chart (Fig. 6.4.15).

5.1.3. It is worth noting that the instrument was firstly recalibrated. In an open channel, a given uniform flow was set up and the rate of travel of a small wooden float was

recorded for 3 and 4 different distances. The mean value was obtained corresponding to the surface velocity of the flow. Thereafter, the instrument measuring head was just immersed beneath water surface in the same flow and the number of pulses per 10 seconds was recorded directly from the "Dekatron". In the same way as above, an average value of 3 or 4 direct recordings of pulses was obtained. It would be reasonable to assume that the average value of pulses should correspond to the average linear velocity of the wooden float. The same procedure was repeated for different flows. Results, shown in Fig. 6.4.15, are recorded in Vol. II

Section

5.1.4. If fluid other than water is used, the Dummy probe should be inserted into the wheatstone bridge circuit of the system. Although the instrument is designed for the above mentioned arrangement, somehow, when deploying saline water, it has been found difficult to control the voltage within the suitable range (8 - 11 volts) demanded by the instruction. Therefore, thermal density difference was used (6.4.a) in preference to salinity.

## 5.2. Velocity recording:

By the colouring of the water in the flume's shorter reach, the advance of the fronts can be observed. In the present study, a stop clock was used with a circle of paper (of diameter just less than the markings) stuck to its face. As either of the fronts passed foot, or  $\frac{1}{2}$  foot, marks, a tick was made at the position of the second hand with a number assigned to it corresponding to the consecutive foot marks. Although this process might appear, the speed, together with the reasonably crude

satisfactory results of it justifies its use.

### 5.3. Dilution recording:

As the dilution study (6.5 and 8.3) was primarily concerned with thermal density difference, direct measurements of temperature using a mercury thermometer appeared to be the obvious choice. Although the normal mercury bulb thermometer was accurate (after calibration) and simple to read, it tends to average out varying temperature both in dimension and time because of the bulb size and its comparative slow response. In the measurements to be made, the length of the bulb would have been inconvenient with a normal thermometer.

5.3.2. Instead, the angled mercury thermometer (Fig. 5.1.1) was used and later observed to be reasonably sensitive towards quite a small vertical variation in temperature. Furthermore, because of the bulb (0.232 inch in diameter and 0.625 inch long) being at right angle to the calibrated stem, the temperature recording seemed to be confined to a localised layer whose thickness was in the same order as the bulb's diameter and thus the study of layers stratification was made possible.

5.3.3. Parallel to Keulegan method of isolating different water samples from the bulk of water in the flume using barriers, circular perspex tubes (Fig. 5.1.1) were presently used for the purpose of isolating different samples on which temperature recordings were carried out. That the water inside the tube appeared to reach stable stratification shortly afterwards and continue like this for a considerable time, indicated the general usefulness of deploying the above mentioned tubes.

## 6. EXPERIMENTS WITH LOCK EXCHANGE FLOWS IN RECTANGULAR FLUME.

### 6.1. Introductory:

When a gate or other division, which has separated bodies of still water at the same surface elevation but with slight variation in density, is removed an exchange flow occurs; the less dense water is seen to flow over the denser water and in opposite direction to it. In full scale circumstances, while the flow of the former is visible, the flow of the latter is not. Studies of densimetric exchange flows, mostly conducted in a level bottomed rectangular channel, have been reported intermittently over the last thirty years or so. Since the frontal surge possesses a kind of individualistic shape, much attention has been concentrated on observing its motion in experiments carried out in a comparatively short flume. Experimental results, together with some analytical work, were first reported by O'Brien and Chernoff<sup>6.1</sup> in 1932. Since then, several authors<sup>6.2-5</sup> have considered the problem; but in each case, the study started with the assumption that the initial velocities of the underflow and overflow fronts were equal. This symmetrical assumption led to the evaluation of the front initial velocity ( $V_0$ ) as:-

$$V_0 = 0.5 \sqrt{(\Delta \rho g H / \ell)} \quad (\text{The symbols are defined in Chapter 3.})$$

However, much valuable experimental information has been gathered by Keulegan<sup>6.6-7</sup> who firstly considered the problem from the theoretical standpoint.<sup>6.5</sup> Keulegan, in dealing with a comprehensive series of experiments, concentrated on the motion of the saline underflow front for which he was able to show that,<sup>6.6</sup>

provided geometric similarity between depth(H) breadth(B) and lock length  $l_0$  is preserved between two cases, congruency exists if equality of the parameter  $\frac{V_{0H}}{V_m}$  is maintained. This is illustrated by Fig. 6.1.1. He also dealt in detail with the effect of channel width and the wave reflection from the lock end. As for the channel width, he found that, apart from the case of an extremely narrow channel, the side walls had no effect on the initial front velocity, but for breadth to depth ratio less than 6, the side wall appreciably affected the rate of decrease of velocity of an unchecked front.

6.1.1. As for the effect of waves reflected from one end, as shown in Fig. 6.1.2, Barr recently described reflection as "an intermediate stage between a front and a wave, less liable to suffer diminution of velocity than a front". If the diminution of underflow, say, velocity occurs, for any reason, the reflection eventually overtakes it and, due to the subsequent decrease in the underflow total depth, causes further marked decrease in velocity over and above the normal decrease in the absence of reflection. It was noted that while saline density difference causes practically no difference in surface tension between two bodies of water, comparable thermal density difference causes an appreciable difference in surface tension. The effect is illustrated in Fig. 6.1.3.

6.1.2. In the study of overflow front at the College, it was invariably found that the initial velocity of saline overflow, the fresh water advance, was about 12% faster than the underflow; as for the thermal overflow, the effect of surface tension, in the

form of a drawing forward of a surface layer ahead of the frontal tip, tended to make its initial velocity to be greater than that of saline overflow. However, the existed difference in surface tension was obviated by the addition of a wetting agent to the colder water and the test of surface tension was made by sprinkling aluminium powder on the water contained in the mixing tanks, and using a reciprocal process of touching the water surface in one tank by a drop abstracted from the other using a dropper. In so doing, general similarity with saline overflow coefficient of proportionality was found. For the thermal underflow, the balancing of surface tension was immaterial since its effect at the interface was quite minute.

#### 6.2. The velocity study of density-current tip.

Lock type exchange flows, similar to those described by Keulegan and Barr, were carried out in the level smooth bottomed flume (18.5 ft. long, 1.5 ft. wide, and 0.9 ft. maximum depth). The intention was to supplement the distribution of K-KR<sub>A</sub> as obtained by Keulegan and Barr for the front of saline underflow and of thermal overflow respectively. With the thin (1 m.m.) vertical barrier in its position at 5.5 ft. from one end, the flume's two reaches were filled with dissimilar bodies of water up to same level. Usually the water in the shorter reach was coloured with potassium permanganate so as to facilitate the process of tracking the frontal tip. On removing the barrier swiftly upwards, an exchange flow was set up with the coloured tip advancing along the flume's longer reach; its rate of advance

being recorded as described in Chapter 5. Fig. 6.2.5 shows typical recordings of the rate of advance of the tip in a laminar case ( $KR$  up to 5,000) where the observed interfacial waves away from the frontal surge, are just on the point of breaking.

Fig. 6.2.6 shows the above mentioned typical recordings in a turbulent case ( $KR > 5,000$ ). The coefficient of proportionality ( $K$ ) together with the product of densimetric Reynold's number ( $KR$ ) were evaluated for each test, using Fig. 6.2.7 for obtaining the value of kinematic viscosity ; and a typical calculation is shown at the foot of Fig. 6.2.8. These values are plotted in Fig. 6.2.9. The pattern in which the present results scattered in relation to the lines relating the underflow and overflow for the range covered by Keulegan and Barr, appeared to be analogous to the manner in which their results scattered as demonstrated by Fig. 6.2.10. Although in each case the results showed considerable scatter, the best line drawn through the mean variation of a paired underflow results, or paired overflow, was often similar, suggesting the existence of a constant ratio, at least for the range examined, between the underflow and the overflow.

### 6.3. Observational study of the differential movements of water well behind the tip.

6.3.1. Most previous efforts on lock type experiments, both at the College and elsewhere, have been concentrated on observing the behavior of the underflow front and to a lesser extent the behavior of the overflow tip. To make such kind of study possible, water on one or other side of the vertical barrier was

coloured with a dye. In the previous work at the College, potassium permanganate was found appropriate; and the usual practice has been to colour water in the shorter reach, so that to allow the front of either the overflow or the underflow to advance in the longer reach. This unsymmetrical arrangement allows a reasonable progress of the studied flow (underflow or overflow) without its obstruction and hence a reflection. Of course, the other reflection does have some effect, but care was taken to discard such aspects of the results as were so affected. Furthermore, the advancing coloured, say, underflow, both to the eye and even more so to the camera, is dominant and the dilution of it can be quite marked before it is visually obvious. On the other hand, the overflow front of clear water can be quite difficult to observe, because some of the overlying coloured water is soon drawn into the swirling tip.

6.3.2. In an exchange flow, the two distinct types of mixing are:- mixing at the front and mixing at the interfacial boundary; the former is thought to be predominate in laminar cases, since the interface is so stable that it acts as a barrier against exchange of water of different densities. In turbulent cases, the combination of the two types causes mixing. Prandtl<sup>6.10</sup> suggested that the front of denser or lighter water, or air, travels along in a sort of "rolling up" motion. The result of such a motion is that some of the less dense water is drawn into the underflow front which will be consequently diluted and come to be much slowed. The circumstance of increasing depth and density difference leads to more turbulent conditions in which

the general pattern of movement of the tip is thought to be similar to the laminar case. Since the breaking of waves in regions behind the front is a characteristic feature of turbulent flows, the interfacial layers no longer have distinct existance. Hence there exists, along the interface, a continuous process of water exchange between the underflow and overflow - a process that speeds up dilution.

6.3.3. Since little or, perhaps, no examination had been made on water velocities in regions behind the front as against the considerable studies of the frontal surge that have been made by many authors, the study of flow pattern of water masses behind the front seemed to be quite desirable. The overall colouring of either the dense or less dense water, as explained before, tends to have prevented any visual impression of the internal velocities. Therefore, it was thought suitable to perform some lock type experiments with partial colouring of water on one side of the barrier.

6.3.4. In an attempt to elucidate clearly the observational results obtained, it seems convenient to describe only one of the many tests carried out on the underflow when it was partially coloured in the manner that follows:-

With the main barrier in its position, the flume was filled, in the usual way, with uncoloured water on both sides up to a predetermined level. Two additional barriers were placed vertically at one foot and two feet from the main barrier position and in the shorter length of the flume containing the more dense water. Water entrapped between the two additional barriers was

coloured leaving the rest uncoloured. Fig. 6.3.11 shows the starting conditions. Thenafter, the two additional barriers were lifted gently upwards so as to prevent local disturbances and to obtain a well defined prism of coloured water.

Immediately afterwards, the main barrier was lifted away so as to initiate the exchange flow.

6.3.5. While the underflow front, being uncoloured in this case, started to move away from the starting position; the coloured prism was not affected by the exchange flow until the overflow tip reached its location. Fig. 6.3.12. Subsequently, the well-defined coloured prism was broken up in such a manner that most of coloured was left moving behind the underflow tip, while some little amount of it was swept into the lower layer of the overflow under the action of the interfacial drag. Fig. 6.3.13. Thus after the displacement of the prism the underflow consisted of an uncoloured front followed by a coloured region of water. That there was in the underflow stream some coloured water easily observed, it seemed suitable to follow the path of that visible portion in order to find the manner in which it was going to be distributed along the flume, especially before the front had reached the end barrier (A).

6.3.6. The exact flow-behaviour of the coloured water was greatly dependent on the nature of flow under study; that is to say, whether the flow was more laminar or more turbulent. In more laminar flow with the type of colouring cited above, the tendency of overtaking the front by the coloured water was not so pronounced as compared with overtaking in more turbulent flow.

Furthermore, in more laminar flow, the coloured water, having reached the rear of the frontal surge, seemed to stay there for some time without any further advance into the front. In turbulent flow, the coloured water did not only reach the rear of the frontal surge, but overtook and became part of the tip. Thereafter was rolled up into the interfacial boundary and thus discarded to upper regions of the following masses of the underflow stream.

6.3.7. In the turbulent, the phenomena of undiluted water in the form of bands, or layers, coming from behind, being shifted to the back along the interface, was, of course, a continuing process up to the time the front reached the end barrier. It seems that although there was appreciable mixing at the front, much of the diluted water was discarded; and the proportion of "fresh" saline water coming from behind was not very much less than the diluted water leaving the frontal region. It follows that the front was little diluted. For a given travel length as compared with laminar case, this is demonstrated in Fig. 6.2.6 which shows that there is little, if any, drop in the initial velocity of the front. Indeed it seems likely in a full size lock exchange flow of the same nature as the experiments mentioned above, the front would continue to move for quite a distance with its initially acquired velocity. It seems also probable that the proportion of water in laminar flow, discarded from the front is very much less than that remained there. From continuity considerations of the water masses in the frontal region, the slightly diluted water supplied by the stream had,

in effect, no chance to advance into the front which consequently became, together with a foot or so immediately behind the rear of it, very diluted. This explains the sharp drop in the initial velocity of the front so commonly observed in laminar flows, as shown in Fig. 6.2.5. Actually at very low dimensional Reynold Number, although there was no distinguishable forward movement of the front for an hour or so after its apparent stoppage, it was observed that the front would reach the other end barrier if it had been left in the flume overnight. This suggests that the front continues to advance so long as there exists even the slightest possible density difference between the underflow and the overlying water.

6.3.8. The other method, adopted for the study of the manner in which coloured water was distributed in the flume, took place after settling, that is after allowing sufficient time for water in the flume to reach stable stratification with all movements due to reflected waves at end barrier vanished.

It might seem rather a crude way of comparing distribution of certain proportion of water in flows which were quite different in nature; but it could be justified, if one considered that the flows were carried out in the same flume, with water at the same depth and under the same laboratory temperature. The first two conditions appeared to be important factors for conducting such kind of comparison. Moreover, the density difference, being the factor mostly affected by mixing, was the only variable left to change the circumstance of flow from laminar to turbulent.

The after settling results, as observed, for the two selected tests, are summarised below:-

In turbulent flows  $H = 0.34\text{ft}$ ;  $\Delta\rho = 0.0229$ ;  $R_\Delta = 13300$  the coloured water, started at -2 ft. as a thin layer stationed near the bottom, increased in thickness towards barrier (A). Between 6 ft. and 12 ft., the layer was 0.75 inches thick as against a small fraction of an inch in the proximitiies of the removable barrier. In general, therefore, in turbulent cases, water, initially lagging the front by some distance, ended in the front and in regions very near to it. As for a typical laminar case  $H = 0.34\text{ft}$   $\Delta\rho = 0.0024$ ;  $R_\Delta = 4146$  where overtaking was not appreciable, most of the coloured water was seen in regions not very far from the starting position (i.e. the layer was about 1.3 inches in the short reach as compared with 0.4 inches near the other end).

6.3.9. Other experiments of the same nature supported the aforementioned conclusion as regard to water behaviour in the back region and the existance of differential movements in any given densimetric flow; the extent of the latter seemed to depend greatly on the nature of the flow being turbulent or laminar.

#### 6.4. Measurements of velocity in regions well behind the front.

6.4.1. The bands, or layers of water cited in 6.3.3, which were observed to move longitudinally parallel to the flume's bottom well away from the interface, appeared to follow the front with relatively high velocity and to overtake the tip within the limit provided by the flume's longer reach (i.e.  $\frac{L}{H}$  up to 43 for the tests deployed). The study of the velocity distribution of these bands in relation to the front velocity seemed essential for the better understanding of the phenomena.

The study of velocity measurement was carried out as explained below:-

#### 6.4.2. (a) By Hydraulics Research Station miniature current meter.

The H.R.S. type miniature current flowmeter, available in the hydraulic laboratory, was used in the manner as described in (5.1.). The two positions chosen to place the measuring head were near the barrier position at 1 ft. and at 6 ft. away from the barrier, where the flow was thought to be fully developed.

Fig. 6.4.14 shows typical plots of the direct recordings. The item "time (in seconds) for 10 pulses" was converted, by direct proportion, into number of pulses per 10 seconds so as to obtain the corresponding linear velocity (in inches/sec.) from the calibration chart shown in Fig. 6.4.15. Runs B 4,5,6 - H = 0.8 ft.;  $\Delta \rho = 0.00314$  g.m./m.l. ; KR = 9614 - in which the rotar was placed along the flume's central line, at 1 ft. from the barrier were concerned with the dense water movements behind the underflow front. Results are shown in Fig. 6.4.16. Runs B 16, 18 - H=0.8 ft.;  $\Delta \rho = 0.0032$  g.m./m.l. ; KR = 10640 - whose results are shown in

Fig. 6.4.17, were intended to check the pattern of flow behavior as demonstrated by B 4,5,6. For all practical purposes, the two patterns appeared to show similarity in so far as most of the recorded velocities were well above the dotted line relating to the underflow frontal velocity. Fig. 6.4.18 shows the results of runs B 6,7 -  $H = 0.8$  ft.;  $\Delta\sigma = 0.00313$  gms./m.l.;  $KR_\Delta = 8418$  - which dealt with the underflow and with the rotar placed at 6 ft. from the barrier. For the two above mentioned positions, the axis of the rotar was at 1.5 inches above the bottom. This was adopted because the observational study (6.3) showed the bands centre point lay in the proximitiies of 1.5 inches height.

For the overflow, runs B 9,10,12 -  $H = 0.8$  ft.;  $\Delta\sigma = 0.0029$  gms./m.l.;  $KR_\Delta = 11670$  - dealt with the case in which the rotar was placed at 1 ft. from the barrier. Results are in Fig. 6.4.19. Runs B 13,14,15 -  $H = 0.8$  ft.;  $\Delta\sigma = 0.00306$  gms./m.l.;  $KR_\Delta = 10930$  - dealt with the case in which the rotar was placed at 6 ft. from the barrier position. Results are shown in Fig. 6.4.20. As before, it was found suitable to place the rotar with its axis at 1.5 inch. under the free water surface. The difference in surface tension associated with the difference in temperature was balanced in the usual way (6.1).

6.4.3. The plotted results seem to follow a regular pattern of variation approximating to a damped harmonic motion. This variation could be assumed to result from the swirling motion of interfacial eddies. To lesser extent, it could, also, be

assumed to result from the continuously observed changes in the instrument voltage. The latter appears to be greatly sensitive towards even the slightest variation in temperature usually occasioned with mixing. Nevertheless, if the best line is drawn through the scattered results, this line demonstrates that the bands follow the front with a velocity higher than that of the front which is shown as a dotted straight line drawn on the same figure. Therefore, it appears that the measured flow behaviour of water behind the front tends to be similar to the prediction drawn from the observational study (6.3).

#### 6.4.4. (b) By timing dye traces.

Although the miniature current flowmeter proved to be of great assistance to the study with regards to turbulent cases only, it failed to operate when the rotor was immersed in the laminar exchange flow, because water current impinging on the rotar was not adequate to set it in continuous motion; thus only an intermittent count of pulses was shown on the "dekatron".

6.4.5. Instead, perspex surface floats (cylindrical with diameter  $\frac{5}{8}$  inch, and with four vanes attached to the vertical side of  $\frac{3}{8}$  inch, height) were firstly used to study the laminar case. However, later observations, using potassium permanganate patches, showed that there existed along the depth of the overflow, and the underflow, a kind of velocity gradient as shown in Fig. 6.4.21. Since the use of floats was confined to the study of the overflow in which the approximate location of the bands was extended between  $\frac{1}{2}$  inch, and 1 inch under the free surface for the tested flows with total depth  $H = 0.5$  ft., the velocity distribution

as shown in Fig. 6.4.22, 6.4.23, appeared to be less than that of the front. In other words, they seemed to give no correspondence with the observational findings (6.3.)

6.4.6. Instead, the dye trace was employed in the following manner:- an exchange flow with  $H = 0.3$  ft. was set up with neither the overflow nor the underflow coloured. A little amount of solid potassium permanganate was released carefully at the free surface so as to fall vertically, under its own weight, to the bottom. In so doing, it left a coloured trace, which, initially, was seen to move as a vertical line for some time. Thereafter, the line trace was deformed in accordance with the velocity distribution whose impression is shown in Fig. 6.4.21. In following the foremost coloured trace, which seemingly related to the fast moving bands, the time of transit was recorded as described in (5.2). Figures 6.4.24, 6.4.25 show the rate of advance of the thermal overflow front and the foremost dye trace respectively for tests D 1, 2, 3, 4 -  $H = 0.3$  ft.;  $\Delta \rho = 0.003$  g.m./m.l.;  $KR = 2160$ . From Fig. 6.4.26, which shows the comparison between the aforementioned velocity variations, it appeared, however, that for the range  $\frac{L}{H}$  approximately equal to 17, the dye trace was advancing faster than the front. Beyond that range, the velocity distribution showed that the rate of decrease of the frontal velocity was much less than that of the bands. This seemed to show a resemblance with the observational findings (6.3) regarding the more laminar type of exchange flow in that after the front had travelled some distance and, thus, became appreciably diluted, the foremost parts

of the extended bands, at that time, could not advance any further into the frontal surge; the effect of which was the marked diminution in the dye's forward movement. In order to obviate the scale effects resulting from the probable surface tension difference not being fairly balanced, similar process of dye tracking was carried out on saline overflow.

Tests D 5, 9, 13 and D 6, 7, 8, 10, 11, 12 -  $H = 0.3$  ft.

$KR_A = 2360$ ,  $\Delta \rho = 0.0024$  gms./m.l. - are plotted in Figs. 6.4.27, 6.4.28 respectively.

6.4.7. Comparing Fig. 6.4.26 with Fig. 6.4.30, there seemed to exist an overall agreement especially in regard to the rate of advance of the foremost dye trace being greater than that of the front within the range  $\frac{L}{H} = 17$ ; and beyond it being much less.

The data of the above mentioned tests are listed in Volume II  
Section  
Chapter 12.

### 6.5. Small scale dilution study.

From consideration of the previously observed rate of decrease of the frontal velocity 6.6, 6.9 and the findings of the present study regarding the differential movements of water masses in the extended parts of an exchange flow, it could be presumed that for the same relative travel length, the front in a flow with high densimetric Reynold's number ( $KR_A$ ) is much less diluted than that in a flow with low densimetric Reynold's number.

Moreover, the diluted water having been discarded from the front, (a feature very pronounced in turbulent cases) appears to be left behind in layers lying near and parallel to the interface. It was thus in these layers that most of the diluted water was

expected to be found.

6.5.2. In order to check the presumption mentioned above and to study the dilution pattern along the total depth ( $H$ ) for the front and for some selected points on the extended flow in lock experiments, direct dilution measurements in the form of temperature variations, seemed useful to be included in the presently described study.

6.5.3. Temperature recordings were made, using the angled thermometer and circular tubes as described in (5.3). The studies were restricted to the arrangement where the underflow tip advanced along the longer reach of the flume (13 ft.) and a range of densimetric Reynold's number was covered. In each case, the isolation of samples was carried out when the advancing underflow tip had travelled a maximum of 9 ft. from the starting position. This was necessary in order to obviate the undesirable effects of the reflected waves at the end barrier, whose presence would considerably affect the natural pattern of dilution. Provided care was taken in inserting the tube into the water so as to rest on the flume's bottom, the water entrapped inside reached a state of stability shortly afterwards. The extent to which the stratified layers were stable was examined by conducting the temperature recordings in two stages, each of which took about 5 minutes to accomplish. The first stage was carried out from surface to bottom and the second was carried out in the reverse direction. For a given layer, it was found that, despite the disturbances caused by the movements of the thermometer, the recordings of the second stage showed an overall agreement

with those of the first stage. This meant that the stratified layers were fairly stable at least for the time the recordings were taken. Therefore, the present method of using a tube to isolate a sample from the main flow appears to be reasonably satisfactory for the study of dilution being incurred on the extended parts of an exchange flow.

6.5.4. To minimise the heat losses from the free surface of water, the temperature of the less dense water was chosen to be of same order as that of the laboratory atmosphere. The more dense (colder) water was drawn from the main at temperature around  $60^{\circ}\text{F}$ . and the scale effects resulting from the difference in surface tension between the two bodies of water was balanced in the usual manner (6.1). The difference in temperature of about  $7^{\circ}\text{F}$ , or so, causes a small density difference ( $\Delta\gamma = 0.0008 \text{ gms./m.l.}$ ). Therefore, when dilution of a turbulent case was examined, a measured quantity of salt was added to the cold water in the small tank where the underflow water was thoroughly mixed using the varies arrangement described in (4.1). Since the dense water was made completely homogeneous with regard to uniformity in temperature and salinity, it could be assumed that the measured pattern of dilution in the form of temperature variation gave a reasonable picture of overall dilution affecting the total density difference ( $\Delta\varrho$ ).

6.5.5. Experimental results were plotted in the form of temperature dilution ( $t$ ) versus depth ( $h$ ) ( $t = \frac{T-T_1}{T_2-T_1} \%$ ; where  $T$  is the recorded temperature of a layer situated at a given depth ( $h$ ), and  $T_1, T_2$  are cold and warm water temperatures respectively).

## 6.6

It seems suitable when discussing temperature dilution incurred on the underflow front, to speak of the continuously decreasing density factor  $f$  which is by  $\frac{\Delta Y}{\Delta Y} = 1$  at the outset of an exchange flow ( $\Delta Y'$  is the varying density difference due to the measured temperature rise;  $\Delta Y$  is the constant density difference due to the initial temperature difference  $T_2 - T_1$ ).

As  $\Delta Y'$  is inversely proportional to  $(T - T_1)$  and  $\Delta Y$  is directly proportional to  $T_2 - T_1$ , it follows that the value of  $f\%$  is proportional to  $(100 - t\%)$  i.e. if  $t = 30\% f = 70\%$ , for the underflow and for the overflow  $f\% = t\%$ .

6.5.6. Figures 6.5.31 and 6.5.32 show the dilution pattern of samples taken from the crest of the underflow fronts whose foremost tips had reached 1.5, 4.5, 9 feet from the barrier position. Points which are represented by ( $\Delta$ ) relate to flows associated with comparatively high ( $KR_\Delta$ ); and the more laminar flows are represented by ( $\bullet$ ). As a basis of comparison, let dilution at 1 inch above the bottom surface be considered.

Values of ( $f$ ) at this height for tests E 36,39 with  $H = 0.6$  ft,  $R_\Delta = 12,820$  are: 85%, 82% and 80% for fronts at 1.5, 4.5 and 9 feet respectively. The corresponding values for tests E 35,40 with  $H = 0.6$  ft,  $R_\Delta = 6445$  are 81%, 80% and 76% i.e. the difference in the values of ( $f$ ) being 2%, 2% and 4% respectively. For other layers which were situated well into the underflow region, i.e. away from the interface, the graphs show the same pattern of variation as the one cited above. However, it seems that the above quoted values for ( $f$ ) tend to demonstrate the expected increase in dilution in regard to distance travelled and

its bearing on the observed diminution of the frontal velocity.

On the other hand, in tests E 37, 38 with  $H = 0.3$  ft.,  $R_A = 4505$ , shown in Fig. 6.5.31, values of  $(f)$  corresponding to the layer situated at 1 inch above the bottom and taken from fronts at 1.5, 4.5 ft. are 74% and 56%; as against 78% and 66% for tests E 33, 34 with  $H = 0.3$  ft.,  $R_A = 2140$ . As before, the pattern of variation in  $(f)$  as typified by that for the above mentioned layer, applies to other layers in the underflow front. However, it was thought that the marked departure, as demonstrated by the above quoted values of  $f$ , from the prediction mentioned in (6.5.1) might be related to the hypothesis that the observed interfacial eddies in an exchange flow of transitional nature, i.e. neither laminar nor turbulent, were of considerable size in comparison with  $H = 0.3$  ft. Therefore, it seemed possible that the unexpected pattern of dilution was caused by the intrusion of a considerable amount of the ambient water, at higher temperature, deep into the underflow front. Moreover, it could be that only flows with relatively great depth showed agreement with the previous studies regarding the dilution of the front; and, also, agreement with the observational findings as discussed in (6.3). Fig. 6.5.33 shows the dilution pattern for the still more turbulent case:  $H = 0.6$  ft.,  $\Delta \rho = 0.01179$  and  $0.01186$  gm./ml.;  $R_A = 24,080$ . The two samples were taken at 1.5 and 8 ft. (the location of the crest) from the barrier, at the instant the frontal tip had reached 9 ft. Apart from severe mixing in the proximities of the interface at 8 ft., the marked differences in  $(f)$  for layers lying between the flume's bottom and 1 inch above it, seemed to demonstrate the effect of the oncoming bands of

36

slightly diluted water at the front. This water was seen to be discarded to the rear portion of the extended underflow. Furthermore, the bands were seen to move parallel to the flume's bottom at a height approximately within the range mentioned above.

It should be emphasised that the sample taken at 1.5 ft. was not affected by the reflected overflow front at the upstream barrier, which at that particular instant, had not yet returned to the main barrier position.

6.5.7. Comparing tests E (14, 15, 16, 17, 18) -  $H = 0.6$  ft.,  $\Delta \rho = 0.0008$  gm./m.l.,  $R_A = 6445$  - shown in Fig. 6.5.34, and tests E, 20, 21, 22, 23, 25 -  $H = 0.6$  ft.,  $\Delta \rho = 0.0034$  gm./m.l.,  $R_A = 12,820$  - shown in Fig. 6.5.35 values of  $(f)$  at 1 inch above the bottom for the samples at 3, 4.5, 6.5 ft. from the barrier, are:- 91%, 87%, 79% relating to the latter group of tests; and 84%, 79%, 76% relating to the former group. Similar pattern of variation appeared to exist for other layers situated away from the interface. Parallel to the above cited pattern of dilution regarding the front, it appeared that for the same travel length, the extended more turbulent flow was less diluted than the extended more laminar.

6.5.8. Supposing that the flow with  $H = 0.3$  ft.,  $R_A = 2140$ , shown in Fig. 6.5.36, had been intended as a model, on the basis of Froude law, to the flow with  $H = 0.6$  ft.,  $R_A = 6445$ , shown in Fig. 6.5.34, a vertical exaggeration of 1.4 would be required for horizontal scale of  $\frac{1}{3}$ , leading to 1.5 ft. in the former flow corresponding with 4.5 ft. in the latter flow. From Fig. 6.5.37

the prototype front velocity at 4.5 ft. = 0.073 ft./sec.; while the corresponding model front velocity ( $V_m = \frac{V}{\sqrt{\frac{A_e}{A_m}}}$ ) = 0.04 ft./sec., the observed model front velocity at 1.5 ft. from the barrier (fig. 6.5.47) = 0.038 ft./sec. This could be assumed as a reasonable simulation to the prototype velocity.

The extent to which model/prototype similarity in regard to dilution at corresponding layers, were examined as follows:-

<u>Prototype</u>	<u>f%</u>	<u>Model</u>	<u>f%</u>
Full size depth		Corresponding depth	
0.5 inch	15	0.234 inch	12
0.8 "	20	0.372 "	15
1. " "	21	0.460 "	17
1.5 "	25	0.7 "	20
2. "	32	0.93 "	28

The above results appeared to be reasonably similar.

6.5.9. From previous study and this, the introduction of a vertical exaggeration seems essential in order to simulate mixing and hence spread, in general. Furthermore, there seems to be always one exaggeration that gives best simulation.

## 7. STUDY OF THE DAM-BURST.

### 7.1. The ideal dam-burst (air and water).

If a sudden burst of a dam should occur, the resulting flow would be highly unsteady and rapidly varied with a positive wave advancing over dry land and a negative (dying) wave propagating upstream into the still water. Although rare, such an occurrence has a profound effect on human lives and property, and thus aroused much interest with regard to its hydraulics.

St. Venant considered the problem in two dimensions with the usual approximation involving small curvature, the case of a very long wave; and produced the following general equation of free surface profile:

$$\frac{x}{t\sqrt{gh}} = 2.5 \sqrt{\frac{y}{h}} \quad (1)$$

The symbols used are shown in Fig. 7.1.1.

7.1.1. Ritter, having applied certain expression of St. Venant, obtained the following:-

$$U = \frac{g}{2} \left( \frac{x^2}{t} + \sqrt{2h} \right) \quad (2)$$

$$C = \frac{1}{2} \left( 2\sqrt{2h} - \frac{x}{t} \right) \quad (3)$$

where  $U$  is the front velocity and  $C = \sqrt{gy}$  is the wave celerity.

7.1.2. For any fixed time ( $t$ ), equation (3) yields equation (1) which represents a parabolic surface profile with the negative wave propagating upstream with velocity  $-\sqrt{gh}$  and the positive wave advancing downstream with velocity  $2\sqrt{gh}$ . Although the above stated equations showed reasonable agreement with the

experimental work of Schoklitsch in regard to the propagation of the negative wave, the observed forward velocity of the positive surge was about 40% less than the corresponding

theoretically obtained velocity.

### 7.2

7.1.3. When Dressler introduced the canal frictional resistance, almost perfect agreement with Schoklitsch's results was achieved. Also, if the bed frictional resistance  $R$  is neglected in Dressler's momentum equation, Ritter's equations (2 and 3) will result, suggesting that friction was the cause of the above cited disagreement of 40% and that St. Venant's procedure was adopted.

7.1.4. Some ideal dam-burst experiments were carried out by the author in a closed flume (16 ft. long by 4 inches square) but with the pressure inside at atmospheric by means of a number of holes drilled in the ceiling. The free surface profile at and near the negative wave, instead of being concave downwards as given by the theory, was invariably observed to be concave upwards as shown by Figures 7.1.2 and 7.1.3. Indeed, this was so even with the case of a shallow depth where the relative time required to lift the water-tight barrier was very small.

## 7.2 The dam-burst analogy:-

7.2.1. It has been observed that the flow behaviour resulting from the sudden burst of a dam, which had separated two miscible, or immiscible, liquids of different densities, was similar to that of the extreme, ideal dam-burst of air and water.

### 7.3

Very recently Abbott, in his dealing with the spread of paraffin oil on water, investigated the dam-burst case with regard to the motion of the front. He worked mostly from the theoretical standpoint, and he suggested, in the light of experiments carried out by him and Schoklitsch, that the front

equation of motion should be neither in accordance with the St. Venant "envelope" front theory nor with the elementary stability conditions proposed by Rossby and Craya. Instead, it should take the form

$$U_f = K \{ g(1-\lambda) h_f \}^{1/2} \quad (4)$$

where:  $U_f$  is the paraffin oil front velocity (assumed to be constant for short travel length);  $1-\lambda = \frac{\rho_p - \rho_w}{\rho_p}$ ,  $\rho_p, \rho_w$  are density difference and water density respectively;  $h_f$  is the paraffin overflow depth and  $K$  is a factor introduced by him on the ground the flow in a region behind the front is critical.

7.2.2. Abbott conducted a series of experiments in the form of a forced, sustained overflow and obtained an evaluation of the value of  $K$  as unity. Equation (4) will be used later to evaluate the coefficient of proportionality of the dam-burst analogy case.

7.2.3. An experimental study of a case analogous to a dam-burst in the form of a layer of water superimposed on other layer of different density to it but of equal density to water on the other side of the barrier was carried out in the 17.5 ft. long flume. Fig. 7.2.4 and 7.2.5 show the starting condition of the overflow and underflow cases respectively. The instability of the interface between the two dissimilar bodies of water in the shorter reach, necessitates the adoption of the following process of filling the flume, although it was very time consuming.

7.2.4. Case 1 - the overflow - was attained by:

- 1) With the main barrier in its position, the flume's shorter and longer reaches were filled with fresh

(coloured) and saline water up to 0.3 ft. deep respectively.

- 2) The valve feeding the longer reach with saline water was opened for a very low discharge ( $1.46 \times 10^{-3}$  cu.ft/sec)
- 3) When the level of saline water reached about  $\frac{1}{16}$  inch, or so, above the initial 0.3 ft. depth, the barrier was lifted gently and gradually up to  $\frac{1}{2}$  inches so as to allow saline water to seep through to the shorter reach where it lay under the fresh water at the flume's bottom. It took about 30 minutes for a distinct common layer to form along the entire length of the shorter reach.
- 4) The process of slow rate of filling continued until the total depth reached 0.8 ft. The valve was turned off at the instant the barrier was lowered to rest on the bottom.
- 5) Having allowed sufficient time for local disturbances to die out, the main barrier was lifted so as to initiate exchange flow, and the front rate of advance was recorded in the usual way. Figs. 7.2.6 and 7.2.7 show the overflow at the initial and the developed stages respectively. See also Fig. 7.2.7.A

7.2.5. Case 2 - the underflow was attained by a process similar to the above mentioned with the exception of the following:- the whole flume was firstly filled with fresh water up to 0.5 ft. The main barrier was placed in its position; then the pipe feeding the shorter reach with saline water (coloured) was

lowered down to  $\frac{1}{8}$  inch. above the bottom. Thereafter, both valves were opened for low discharges and aiming at keeping same water level on both sides of the barrier throughout the filling process.

7.2.6. Fig. 7.2.8 shows some of the typical recordings of the rate of transit of the underflow and overflow tips along the flume's longer reach. Fig. 7.2.9 shows the results of plotting the coefficient of proportionality of the front velocity against the product of K and the densimetric Reynold's number. The term  $KR \left( \frac{V_{OH}}{V_m} \right)$  was obtained by substituting the relevant depth (h) which corresponded to the thin layer initially in the shorter reach, i.e. either 0.3 or 0.15 ft. in the cases studied. The two lines, shown in Fig. 7.2.9 were drawn on the basis of pairing the points from the mean value in the manner adopted for the lock exchange flows. Since these lines appeared to be nearly parallel to the already established lines relating to the front velocity in a lock exchange flows, it suggested the existence of a close similarity in the variation of the initial velocity coefficient as between the latter and the case of dam-burst analogy. However, it should be emphasised that the evaluation of the coefficient of proportionality for this case is not conclusive. An extensive series of experiments, covering as wide a range as possible, should be carried out so as to firmly establish its position. Because of the laborious process of filling the flume and the considerable time it took, that few tests were carried out. Nevertheless, the distribution clearly demonstrates that the (K) values were greater than even that of the overflow in lock exchange flow. Moreover, the

dam-burst overflow seemed to be at a constant ratio higher than the underflow. Fig. 7.2.10 shows a composite diagram of K-KR<sub>a</sub> for the underflow and overflow in both exchange and dam-burst flows.

7.2.7. Experience showed that as long as the depth of the underlying layer of denser water was equal or greater than that of the overlying layer, the latter did not have any distinguishable effect on the initially acquired velocity of the overflow.

### 7.3. Some theoretical consideration.

Following the same method used by O'Brien and Chernoff for the theoretical evaluation of the overflow and underflow initial velocity in the lock exchange flow, an approximate value of the overflow and underflow initial velocities and, hence, the coefficient of proportionality K for the case of the dam-burst analogy are given below.

The following assumptions were made:-

- 1) that at any section the rate of flow of water in the opposite directions were equal.
- 2) that the depth of the overflow current was half the initial depth prior to the lifting of the barrier.
- 3) that the treatment was with respect to the flow at its initial stage only. Thus, one could assume that the overflow and underflow travel distance (x) after an infinitesimal time from the onset of the flow to be equal.

7.3.1. In the lock type exchange flow, if the overflow initial velocity equal to that of the underflow, then each of them would

equal to

$$V_0 = 0.5 \sqrt{\frac{\Delta \rho}{gH}} gH^{7.4} \quad - (2)$$

From assumption (1) the underflow initial velocity

$$V = \frac{h}{2(H-h)} V_0 \quad - (2)$$

where  $V = \frac{dx}{dt}$  is the overflow initial velocity.

Referring to Fig. 7.2.4, at the instant the barrier was removed, there was an unbalanced force to the right equal to

$$\frac{\rho_2 H^2}{2} - \left( \frac{\rho_2 H^2 - 2Hh(\rho_2 - \rho_1) - h^2 \Delta \rho}{2} \right) = \Delta \rho \cdot h \left( H - \frac{h}{2} \right)$$

This net force causes the rate of change of momentum of the water mass confined within the block ABCD.

i.e.

$$\Delta \rho \cdot h \left( H - \frac{h}{2} \right) = \frac{d}{dt} \left[ \frac{(H-h)\rho_2}{2} \frac{2x}{g} \frac{h}{2(H-h)} \frac{dx}{dt} + \rho_1 \frac{h}{2} \frac{2x}{g} \frac{dx}{dt} \right]$$

$$\frac{\Delta \rho \cdot h(H-h)}{2} = \frac{d}{dt} (x \frac{dx}{dt}) 2gh\rho_m$$

$$\frac{\Delta \rho \cdot g(H-h)}{2} = \frac{d}{dt} (x \frac{dx}{dt})$$

$$\frac{\Delta \rho \cdot g(H-h)}{2} t + A = x \frac{dx}{dt}$$

$A = 0$  for  $x = 0$  at  $t = 0$

$$\frac{\Delta \rho \cdot g(H-h)}{2} \frac{t^2}{2} = \frac{x^2}{2} + B$$

Similarly  $B = 0$

$$x = \pm t \left\{ \frac{\Delta \rho}{2\rho_m} \cdot g \left( H - \frac{h}{2} \right) \right\}^{\frac{1}{2}}$$

$$v = \frac{dx}{dt} = 0.71 \left\{ \frac{\Delta \rho}{\rho_m} g \left( H - \frac{h}{2} \right) \right\}^{\frac{1}{2}} \quad (3)$$

This is equivalent to Keulegan's densimetric velocity with the exception of the depth being less than the total depth and of the K value being greater.

Provided  $H > h$ , the initial velocity given by equation (3) is always greater by that given by equation (1). Furthermore,

$$v = \frac{h}{2(H-h)} \cdot v = 0.71 \left\{ \frac{\Delta \rho}{\rho_m} g \frac{h^2}{2(H-h)} \right\}^{\frac{1}{2}} \text{ which is much less than the}$$

underflow initial velocity in the lock exchange flow.

It could be argued that the kinetic energy absorbed in moving the underflow water in the dam-burst case was much less than the comparative in the lock exchange case, therefore the energy available for the movement of the overflow water was much greater in the dam-burst case; and this could explain the acquirement of the overflow front with, relatively, such a high velocity.

7.3.2. Equation 4 with  $K = 1$  could be written as :-

$$U_f = \left\{ g \left( \frac{\Delta \rho}{\rho_0} \right) h \right\}^{1/4} \quad - (5)$$

Although the above equation was derived for the special case of a forced, sustained paraffin oil flowing over water, one could assume, on the basis of the previous experience<sup>7.5</sup>, that the behaviour of paraffin front at an appreciable distance away from the source would behave as a pure density current. In the presently studied cases of the dam-burst analogy, severe mixing was present, and subsequently the diminution of velocities, the validity of equation (5) seemed to be restricted to the flow at its earliest stage. If  $h$  was the overflow initial depth and  $h_f$  is the depth when the flow was developed, then  $h_f$  is approximately equal to  $2h$ , and equation (5) is written as:-

$$V_o = K' \left\{ g \left( \frac{\Delta \rho}{\rho_m} \right) 2h_f \right\}^{1/2} \quad - (6)$$

$K'$  is a coefficient whose value for water varying in density, does not equal unity as for the paraffin case. Equation (6) is a form of Keulegan densimetric velocity ( $V_o = K \sqrt{\frac{\Delta \rho}{\rho_m} gh}$ ). If  $U_f$  and  $\frac{\Delta \rho}{\rho_0}$  in equation 5 is equal to  $V_o$  and  $\frac{\Delta \rho}{\rho_m}$  in equation 6 then from equations 5 and 6,  $K = \frac{1}{\sqrt{2}} = 0.708$  (c.f. with equation 3 page ).

From Fig. 7.2.10, the experimental value of the coefficient of proportionality is about 0.613. The difference in the value of coefficient of proportionality of about 15% between theory and practice might be partly due to  $h_1$  being actually less than  $\frac{h}{2}$ , and, doubtless, partly caused by the unduly simplifying assumptions made.

## 8. SIMPLIFIED OUTFALL STUDY.

### 8.1. Introductory:-

8.1.1. The final stages of the project were oriented towards the study of three-dimensional spread, still in simplified conditions, but of the same general form as the spread which is known to occur in heat dissipation models and, presumably, in the prototype thereof.

8.1.2. As described in 4.1, a 17.5 ft x 7.5 ft. tank (Fig. 8.1) was available, and this was used for the prototype. An 0.5 ft. wide introduction box was placed in one end as shown in Fig. 8.1a, which, in addition, shows the starting position of a run. When a flow of fresh water was led into the box, it was forced to flow over saline water at the entry region, and thereafter assumed to proceed as a pure density current.

8.1.3. A section of the flume was used for the model. Since the flume was 1.5 ft. wide, it was convenient to work to a one-fifth horizontal scale.

### 8.2. Model-prototype similarity with regards to the limits of spread.

8.2.1. With saline water filling the tank up to 0.83 ft. deep, a sustained overflow water was introduced along the introduction box. The outfall water was coloured with potassium permanganate so as to clearly observe the sideway spread and, more important, to record the rate of travel of the coloured water foremost tip in the manner cited in 5.2. The guide lines painted in the bottom and along the side walls of the tank made this undertaking easy. The series of tests in the tank commenced with the

deployment of fresh water discharge equal to 0.045 cusec, but later observations showed that <sup>the</sup> water surface was hardly moved by such <sup>a</sup> low discharge. Therefore, it was found necessary to increase <sup>the</sup> discharge to 0.08 cusec as a compromise between providing enough inertial forces to set the water surface in a marked motion and keeping the effect of forced flow necessarily localised in proximities of the entry region. The density difference employed in the above mentioned test series was ranging between 0.0018 and 0.002 gm./m.<sup>3</sup>.L. and was altogether due to salinity.

8.2.2. The pattern of flow behaviour of the fresh coloured water was similar to that of a horizontally flowing plume, with sideway spread symmetrically gaining in width as the foremost tip was moving away from the source. At the ratio  $\frac{L}{H}$  approximately equal to 6, the sideway spread had hit the side walls; thus the observation of further modes of unchecked spread was prevented and this tended to contribute in increasing the velocity of the foremost tip.

8.2.3. Fig. 8.2 shows the tip velocity variation for the case where the outfall water was discharged at 0.045 cusec. It had been shown that in order to simulate such a flow in a  $\frac{1}{5}$  model, 1.95 distortion was required.

Fig. 8.3 shows the rate of advance of the tip (as a line starting from the origin) in cases where the discharge was equal to 0.08 cusec. In both cases there was a marked decrease in the tip velocity which suggested that the resulting flows

were more of laminar nature.

8.2.4. In designing the model, the vertical exaggeration obtained on the basis of Barr's Keulegan - type congruency diagram (Fig. 6.1.1) at velocity ratio = 0.9 (shown dotted) was equal to 2.0. However, with outfall discharge increased to 0.08 cusec. in the prototype (instead of 0.044 used previously), 1.85 distortion was found most suitable in that the general sequence of events in the model appeared similar to the full size tests in regard to the limit of spread. Observation of the 1.85 exaggeration model as regards centre line front travel are shown in Fig. 8.4, having been brought to the full size basis for comparison. These results show a reasonable agreement with the prototype results (shown as a continuous line). Fig. 8.4 also demonstrates the usual effect of unbalanced surface tension in providing a higher rate of advance (shown as a dotted line) when thermal density variation was substituted.

The manner in which the fresh water was spreading on the saline water is typified by Figs. 8.5 - 7 which show the particular spreading in the 1.85 model at three different stages.

8.3. Model/prototype similarity with regards to through velocity.

8.3.1. The term "through velocity" is related to the recorded rate of advance of the faster moving bands of water (cited in 6.3 and 6.4) which were, once again, observed in the present three dimensional study in the tank. The manner in which through velocities were observed is as follows:

- 1) The tank was filled with saline uncoloured water up to 0.83 ft. deep. Sufficient time was allowed for disturbances caused by the filling to die out.
- 2) Outfall water in the 8.94 sq. ft. mixing tank was coloured with fluoresceine. A test commenced when outfall water (having greenish colour) started to flow from the introduction box into the tank.
- 3) After some chosen time interval from the start of the test, a little amount of fresh water, coloured with potassium permanganate was gently poured into the introduction box. This was necessary in order to ensure that this water, being differently coloured and thus easily observed in isolation, become part of the outfall water and, hence, took the pattern of flow as outfall water similarly orientated. The differently coloured water was seen to move with a relatively greater velocity than the front and eventually to overtake the front and continue to indicate the limit of spread.

8.3.2. The flow behaviour of "through velocity" is demonstrated in Fig. 8.3 which shows results of tests G 13 - 14, 10 - 12, 17 - 18, 15 - 16, and 18 - 20 respectively, corresponding to the above mentioned coloured fresh water, poured in at 15, 25.5, 35, 45 and 75 seconds from the start of each test.

8.3.3. A similar type of experiments were carried out in the one-fifth size model with 1.85 exaggeration. Model test results, having been brought to the full size basis for comparison, are

shown in Fig. 8.8. For all practical purposes, similarity was achieved as compared with the full size "through velocities" (shown as continuous curves which were brought forward from the original curves drawn on Fig. 8.3).

8.4. Model/prototype similarity with regards to the thermal vertical stratification.

8.4.1. Further experiments as described in 8.2 and 8.3 were carried out in the tank with the exception that the temperature of the outfall water was adjusted to be about  $7^{\circ}\text{F}$  higher than that of the basic saline water in the tank. For reasons of direct/model/prototype comparison, the overall density difference between the two dissimilar bodies of water was kept in the same range mentioned in 8.2.1; and the difference in surface tension was balanced in the usual way.

8.4.2. In each run, it was possible to separate three samples from the bulk of water using the perspex tubes. These samples were, for reason of easy access to them, chosen along the tank's centre line at 1 ft., 5 ft. and 11 ft. from the introduction box. At each of these positions a piece of perspex (of size just enough to close the tube's bore) covered with a layer of vaseline (used as water sealing) was placed at the bottom of the tank.

8.4.3. In the usual way, each test commenced with outfall water allowed to flow into the tank. After the limit of spread had reached the other end of the tank, the source of supply of outfall water was turned off and immediately afterwards the perspex tubes

were carefully lowered to properly rest on the perspex "footings". Provided care was taken in gently lifting the sample to one of the bridges built across the tank, proper sealing and hence stable stratification were attained. The latter was examined in the same manner as explained in 6.5.3 using the angled thermometer.

8.4.4. Since the outfall water was of negligible volume in comparison to that of the basic saline water, and initially identified with a small temperature difference ( $7^{\circ}\text{F}$ ), it was, in the case where water depth in the introduction box was equal to 0.163 ft., very susceptible to the mixing caused by spread. The effect of such mixing seemed to have removed any measurable temperature difference. On the other hand, it appeared unwise, in the light of the relatively large surface area of water in the tank and the considerable time required to examine mixing in each run, to use large difference in temperature as the resulting heat losses through evaporation could hinder the study of natural mixing associated with spread in general.

8.4.5. When water depth in the introduction box was doubled (0.326 ft.) by dropping the base of the introduction box, the rate of advance of the limit of spread together with through velocities were decreased as shown in Fig. 8.9. This pattern of flow resulted in a reasonable variation in temperature taking place in the total depth of 0.83 ft.

8.4.6. A similar procedure was adopted for the study of vertical stratification in the model of 1.85 distortion. Fig. 8.10

shows model/prototype similarity with regards to the three selected places. It appeared that there existed a reasonable degree of similarity at 5 ft. and 11 ft.; and that at 1 ft. was rather erratic. This, however, was expected since the oncoming forced current tended to inhibit the occurrence of normal stratification. It should be noted that, with water depth in the introduction box equal to 0.326 ft., similarity with respect to the limit of spread and the through velocities was, in contrast to the case of 0.163 ft., less pronounced as shown in Fig. 8.11. Prototype and model tests recordings are listed under letters G and H respectively in Chapter 12, Vol. II.

8.4.7. Parallel to the two dimensional study cited in 6.5, the introduction of the best suitable vertical exaggeration seemed, once more, essential in order to achieve proper similarity of flow aspects resulting from three dimensional densimetric spread. Moreover, it is suggested that the phenomena of through velocities could be taken as an extra criterion of testing for complete similarity.

8.4.8. It could be said, however, that the mechanism of spread in the tank was as follows:-

- (1) At the entry, the divergence of the edge lines corresponded largely to that of a jet.
- (2) Beyond the entry, the spreading was to greater extent due to internal gravitational advance.
- (3) Vertical mixing-in the form of water mass exchange taking place at right angle to the direction of

the main current - was present over the whole area covered by the flowing outfall water.

## 9. CONCLUSIONS & RECOMMENDATIONS.

### 9.1. Conclusions:-

9.1.1. The study of the fronts in lock type exchange flows has confirmed the previous findings regarding the overflow front coefficients of proportionality ( $K$ ) being of higher values than that of the underflow by about 12% and, also, the pattern of variations of  $K$  with respect to the densimetric Reynold's number as shown in Fig. 6.2.9.

9.1.2. Both qualitative and quantitative studies (as explained in 6.3 and 6.4 respectively) have indicated the existence of differential movements of water masses behind the front and the manner of such movements has been found to depend on whether the flow is turbulent or laminar. Observations of a turbulent case have shown that there exists for some period a continuous process of undiluted water flowing longitudinally parallel to the flume's bottom and away from the interface. This water has such a velocity that it eventually overtakes the frontal tip where it is swirled upwards and discarded to back layers lying near the interface. The process tends to minimise the dilution of a front; hence the manifestation of little diminution of the front velocity for the travel length ratio ( $\frac{L}{H}$  up to 20) available in the flume as shown in Fig. 6.2.6. In a laminar case, the tendency of overtaking the front by the faster moving water from behind, also seen in similarly situated layers, is less pronounced than that in a turbulent flow. Moreover, this water, having reached the rear of the frontal surge, remains there without further advance into the front. Such a behaviour

tends to cause appreciable dilution of the front; hence the marked rate of decrease of the front velocity as shown in Fig. 6.2.5.

9.1.3. The above cited results were checked by the study of temperature dilution incurred by the front and the above mentioned layers. In these regions, dilution was found less marked in turbulent cases as compared with laminar cases. Also, a study of the dilution has indicated that in order to simulate vertical mixing as caused by the particular case of longitudinal spread in the flume, a definitely determinable vertical exaggeration is needed. The results so-far mentioned are reported with detail in Chapter 6.

9.1.4. Both experimental and theoretical studies of a dam-burst analogy, in the form of a layer of water superimposed on an other layer of different density to it but of equal density to water on other side of the barrier, were carried out. These studies resulted in the finding of a similar variations of overflow and underflow front coefficient of proportionality with respect to densimetric Reynold's number as those of the comparable overflow and underflow in lock exchange flow. They are of higher values as shown in Fig. 7.2.10. The differential movements of water masses behind the front cited in 9.1.2 was also observed in such type of experiments.

9.1.5. Experimental studies of a simplified outfall in the form of fresh water led into an introduction box, forced to flow over saline water at the entry region and, thereafter, assumed

to proceed as pure density current, were carried out in a tank (see Fig. 8.1) and in a fifth scale model of the tank. The study has, once more, demonstrated the importance of distorting the model with a suitable vertical exaggeration in order to better simulate density spread in general. Vertical exaggeration of 1.85 was found to give better simulation of the spread than exaggeration of 2 obtained from the Keulegan type congruency diagram (Fig. 6.1.1). This marked difference in the value of distortion is perhaps due to the Keulegan type congruency diagram being based on lock experiments and thus associated with pure density spread, whereas in the outfall experiments the spread, especially at the entry regions, was not altogether densimetric but was forced. With 1.85 vertical exaggeration, a good degree of model-prototype similarity with regards to foremost tip velocity, through velocity and thermal vertical stratification was achieved as shown in Fig. 8.4, 8.8, 8.10 respectively.

## 9.2. Recommendations:

9.2.1. For all possible considerations discussed in 3.2 the adoption of Keulegan type congruency diagram for obtaining the best suitable vertical exaggeration of a model is logically the obvious choice and, therefore, it is recommended for the operation of future heat dissipation models. Hence the extension of such diagrams to cover higher ranges of densimetric Reynold's number is desirable and this should necessarily have a priority in any future basic study of density flows. Better still would be the construction of a Keulegan type congruency diagram based on the dam-burst analogy exchange flow. Although

this is tedious and time consuming, it provides better representative of the actual spreading of heated water over colder water in full scale circumstances.

9.2.2. As is shown in Chapter 8, aspects of through velocities are recommended as an extra criterions of achieving complete model-prototype similarity. This criterion might be useful in the special case of developed spread mechanism in three dimensions as prevails in the discharge of sewage waste disposals from a vertical pipe at the bottom of a body of water.

9.2.3. Photographs, as shown in Figs. 7.1.2. and 7.1.5 of water surface profile in the ideal dam-burst (air and water) show a marked departure, especially in the vicinity of the negative wave, from the shape given by the St. Venant theory. This aspect might provide useful scope for future research of this particular problem.

9.2.4. The physical characteristics of density currents as revealed by this study make it now possible to base theoretical studies on sounder footings. The resulting equations, which will involve unsteady flow will be extremely complicated, but, it is thought, not beyond the capacity of modern computer.

References for Chapter 2

- 2.1. International Critical Tables, McGraw Hill, N.Y., 1926.
- 2.2.a and b quoted by Howard C. S. "Density Currents in Lake Mead" Proc. Minnesota International Hydraulics Convention, 1953.
- 2.3. G. H. Keulegan "Wave Motion" Engineering Hydraulics, ed. H. Rouse Willey N.Y., 1950. p. 711.
- 2.4. H. U. Sverdrup et alia "The Oceans" Prentice Hall, N.Y., 1942.
- 2.5. J. B. Schiff and J. C. Schonfeld, "Theoretical considerations on the motion of salt and fresh water", Proc. Minnesota International Hydraulics Convention, 1953. p. 321.
- 2.6. G. H. Keulegan, "Second progress report on model laws for density currents" N.B.S. (hydraulics division) 1946.
- 2.7. R. V. Vliet, "Effect of heated condenser discharge water upon aquatic life". ASME, Paper No. 57 - PWR - 4, 1957.
- 2.8. C. V. Threiner "Cause of mortality of a mid-summer plant of rainbow trout in a southern Wisconsin Lake, with notes on acclimatisation and lethal temperatures". Frog. Fish Cult., Vol. 20, p. 279, 1958.
- 2.9. G. Blidberg "Gothenburg water-works and the salt sea water." Aqua 1957, No. 1, p. 16.
- 2.10. Interim report to the Californian State Legislature on the Salinity Control Barrier Investigation. State of Calif. Dept. of Water Resources, Div. of Resource Planning, Bulletin No. 60.
- 2.11. Progress report (and second progress report) on model studies of the Sacramento - San Joaquin Delta - Central Valley project, California. U.S. Bureau of Reclamation, Hydraulic Laboratory reports 142 and 155 (Unpublished).

- 2.12. D. Mookerjea "A comprehensive State water plan for the Hooghly and Calcutta Port." Bulletin of the Institution of Engineers (India). Vol. 8, No. 3., (1958) p.4.
- 2.13. N. O. Grover and C. S. Howard, "The passage of turbid water through Lake Mead". Tans. ASCE, Vol. 103, p. 720, 1938.
- 2.14. A. Smreek, "Experiments on the motion of water in the interior of large reservoirs. "Hydraulic Laboratory practice Ed. J. R. Freeman, ASME 1929, p. 510.
- 2.15. D. I. H. Barr, "A hydraulic model study of heat dissipation at Kincardine Power Station". Proc. Instn. Civ. Engrs., Vol. 10, p. 305. July, 1958.
- 2.16. W. Frazer et alia "Interim report on heat dissipation model of Cokenzie Power Station". The Royal College of Science and Technology, Civil Engineering Section, March, 1962.

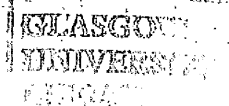
References for Chapter 3

- 3.1. G. Buckingham, "Model experiments and the forms of empirical equations", Trans. A.S.M.E., Vol. 37, 1915.
- 3.2. A. H. Gibson, "Application of the principle of dimensional homogeneity to problems involving heat transmission". The Mechanical Properties of Fluids p. 179. Blackie Ltd., 1925.
- 3.3. J. Allen "Scale models in hydraulic engineering", p. 63 Longmans London, 1947.
- 3.4. Director of the Hydraulic Research Station "The Severn Estuary". Hydraulics Research, 1960 p. 43.
- 3.5. P. Cooley and S. L. Harris "The prevention of stratification in reservoirs". Journal of the Institute of Water Engineers. Vol. 8. Nov. 1954, p. 517.
- 3.6. A. M. Rawn, F. R. Bowerman, and N. H. Brooks "Diffusers for disposal of sewage in sea water". Trans. ASCE Vol. 86, No. SA2, March 1960 p. 81.

- 6.1. M. P. O'Brien and J. Chernoff, "Model law for motion of salt water through fresh" Trans. ASCE Vol. 99, (1932). p. 1769.
- 6.2. H. Rouse et alia "Advanced mechanics of fluids" Wiley N.Y., 1959.
- 6.3. C. P. Linder "Intrusion of sea water in tidal sections of fresh water streams" Proc. ASCE, Hydraulic Div. Sept. No. 358, 1953.
- 6.4. J. B. Schiff and J. G. Schonfeld, "Theoretical considerations on the motion of salt and fresh water" Proc. Minnesota International Hydraulics Convention (5th I.A.H.R.) 1953.
- 6.5. G. H. Keulegan, "The problem of salt water intrusion in canal locks and the sufficient conditions for adequate model experiments" U. S. Depart. of Commerce, National Bureau of Standards Report (2nd in series on model laws for density currents), (1946), (Unpublished).
- 6.6. G. H. Keulegan, "An experimental study of the motion of saline water from locks into fresh water channels". Thirteenth progress report on model laws for density currents. U.S.N.B.S., March, 1957 (unpublished).
- 6.7. G. H. Keulegan "The motion of saline fronts in still water" NBS report 5831 (12th in series on model laws for density currents) 1958, (unpublished).
- 6.8. D. I. H. Barr "Some aspects of densimetric exchange flow" The Dock and Harbour Authority Vol. XLII, No. 94, Dec. 1961.
- 6.9. D. I. H. Barr "Aspects of the study of heat dissipation using models". Ph.D. thesis, University of Glasgow, 1960. p. 48.

References for Chapter 7

- 7.1. St. - Venant as reported by G. H. Keulegan "Wave motion", Engineering Hydraulics, ed. H. Rouse, Wiley N.Y. 1950. p. 711.
- 7.2. Dressler "Hydraulic resistance effect upon the dam-break functions." Journal of Research of the National Bureau of Standards - Vol. 49, No. 3. Sep. 1952.
- 7.3. M. B. Abbott "On the spreading of one fluid over another". Part II "The Wave front" La Houille Blanche Dec. 1961 No. 6, p. 827.
- 7.4. Rossby (G.G.) "On the vertical and horizontal concentration of momentum in air and ocean currents".  
- Craya (A.) - Critical regimes of flows with density stratification. Tellus, 3, 1951.



SCALE PROBLEMS IN HYDRAULIC  
MODELS WHERE DENSITY SPREAD  
IS SIMULATED

by

A. M. M. Hassan

Volume II.

The contents of both Volumes are listed at the front of Volume I. Pagination in Volume II continues from that of Volume I.

Thesis  
2061  
Copy 2

GLASGOW  
UNIVERSITY

## 11. FIGURES AND TABLES

(A full list of Figures and tables is included  
in contents at the front of Volume I.)

	page
Tables for Chapter 2	83
Figs. for Chapter 2	86
Figs. for Chapter 3	88
Figs. for Chapter 4	90
Figs. for Chapter 5	91
Figs. for Chapter 6	92
Figs. for Chapter 7	127
Figs. for Chapter 8	137

TABLE 2.1 HEAT DISSIPATION MODELS INVOLVING TIDAL FLOWS

<u>Model</u>	<u>Horiz. Scale</u>	<u>Vert. Scale</u>	<u>Specially conducted</u>	<u>Size of model and details</u>
At Manchester University basic studies	$\frac{1}{150}$	$\frac{1}{150}$	yes	Approximately 2.5 ft. wide with only part of $\frac{1}{3}$ mile width of tidal river actually modelled.
Antioch P.S. (U.S.A.)	$\frac{1}{100}$	$\frac{1}{100}$	yes	30ft. x 4 ft. with part width of tidal river modelled.
Kincardine P.S.	$\frac{1}{144}$	$\frac{1}{48}$	yes	30ft. x 15 ft. with whole width of tidal river modelled.
Berkeley P.S.	$\frac{1}{300}$	$\frac{1}{60}$	yes	Rather smaller than Kincardine model but again whole width of body of water modelled.
Bradwell P.S.	$\frac{1}{192}$	$\frac{1}{60}$	yes	As for Berkeley P.S.
Thames Model (North fleet and West Thurrock P.S.)	$\frac{1}{600}$	$\frac{1}{60}$	No	Recirculation studies for two power stations to be sited on the Thames were carried out in the Thames model while it was being operated with normal tidal conditions and salinity distribution simulated.
Pt. Augusta (Australia)	$\frac{1}{60}$	$\frac{1}{60}$	yes	Size not known. "Study of optimum location for flow cut-off walls between inlet and outlet ducting of condensate cooling water".
Severn	$\frac{1}{60}$	$\frac{1}{60}$	Two purposes (a) recirculation outfall structure, (b) bed movements.	Combined intake and outfall structure, operated with tidal flows simulated.

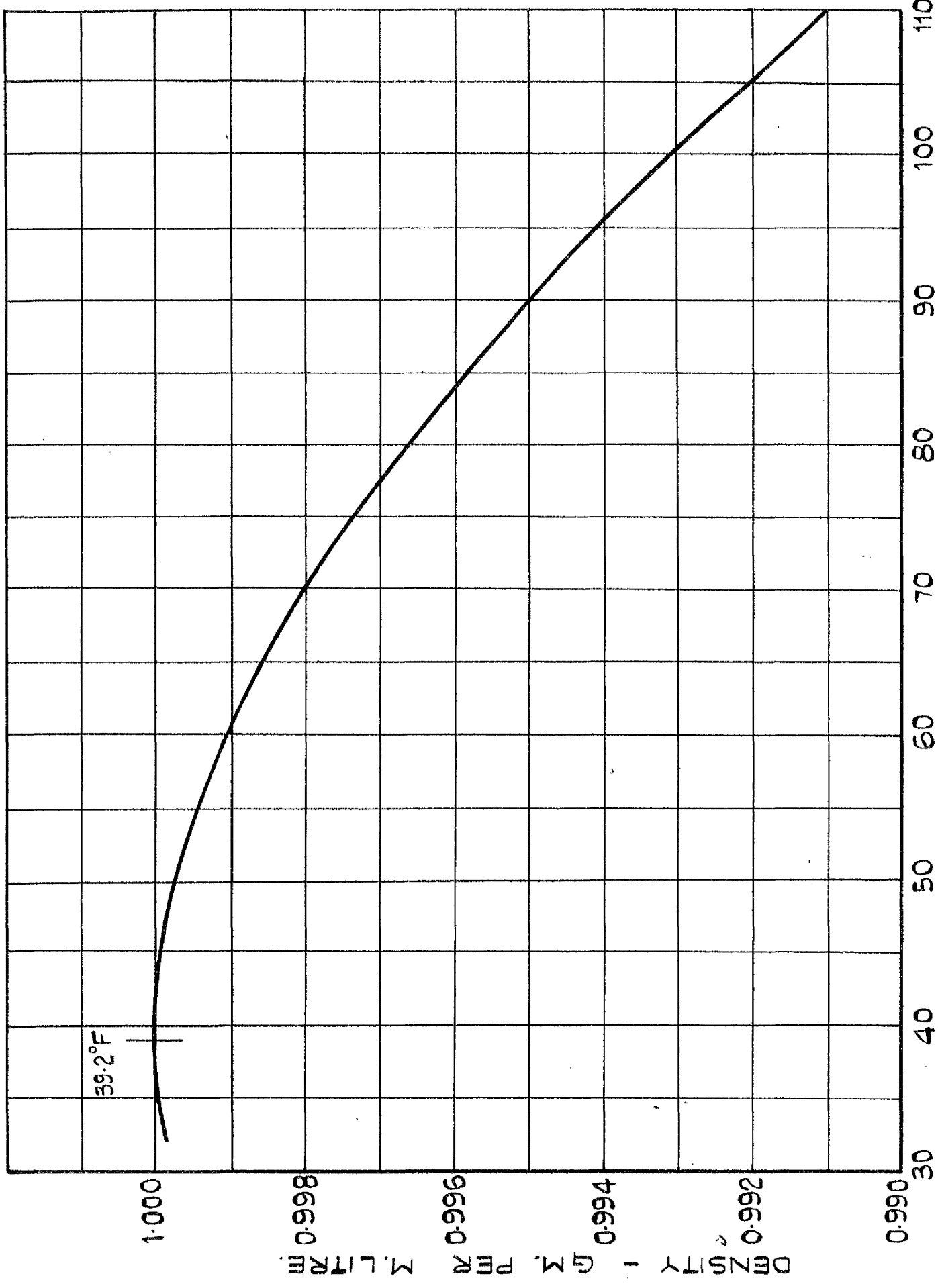
(TABLE 2.1 continued)

<u>Model</u>	<u>Horiz. Scale</u>	<u>Vert. Scale</u>	<u>Specially conducted</u>	<u>Size of model and details</u>
Severn	<u>1 480</u>	<u>1 60</u>	yes	Tidal model of large part of Severn estuary - 150 ft. long <del>or so.</del> Effect of heated discharge from several power stations to be studied.
Oockenzie P.S.	<u>1 250</u>	<u>1 36</u>		60 ft. x 35 ft. - small part width of estuary modelled.
Methil P.S.	<u>1 120</u>	<u>1 20</u>		60 ft. x 30 ft. - small part width of estuary modelled.
Deleware	<u>1 1000</u>	<u>1 100</u>		Recirculation study carried out in large existing tidal model.

TABLE 2.2 NON-TIDAL RIVER OR LAKE RECIRCULATION

<u>Model</u>	<u>Horiz. Scale</u>	<u>Vert. Scale</u>	<u>Notes</u>
Castle Donington P.S.	1 120	1 36	Length of River Trent modelled and recirculation studied using heated water
Alden Hydraulic Laboratory	-	-	At least three river model studies have been carried out. Vertical exaggeration 3 to 5 with normal Froude Law basis for velocity and heated water at 1:1 density differences.
White River	-	-	Purdue University - no details known.
Crawford P.S.	1 60	1 60	Model study of recirculation in Chicago Sanitary Canal.
Schylkill River	1 45	1 15	Recirculation studied in river model - no details known.
Olosglany P.S.	1 250	1 50	Model study for siting of baffle walls to give maximum cooling surface.

FIG. 2.1 - TEMPERATURE - DENSITY RELATION FOR FRESH WATER.



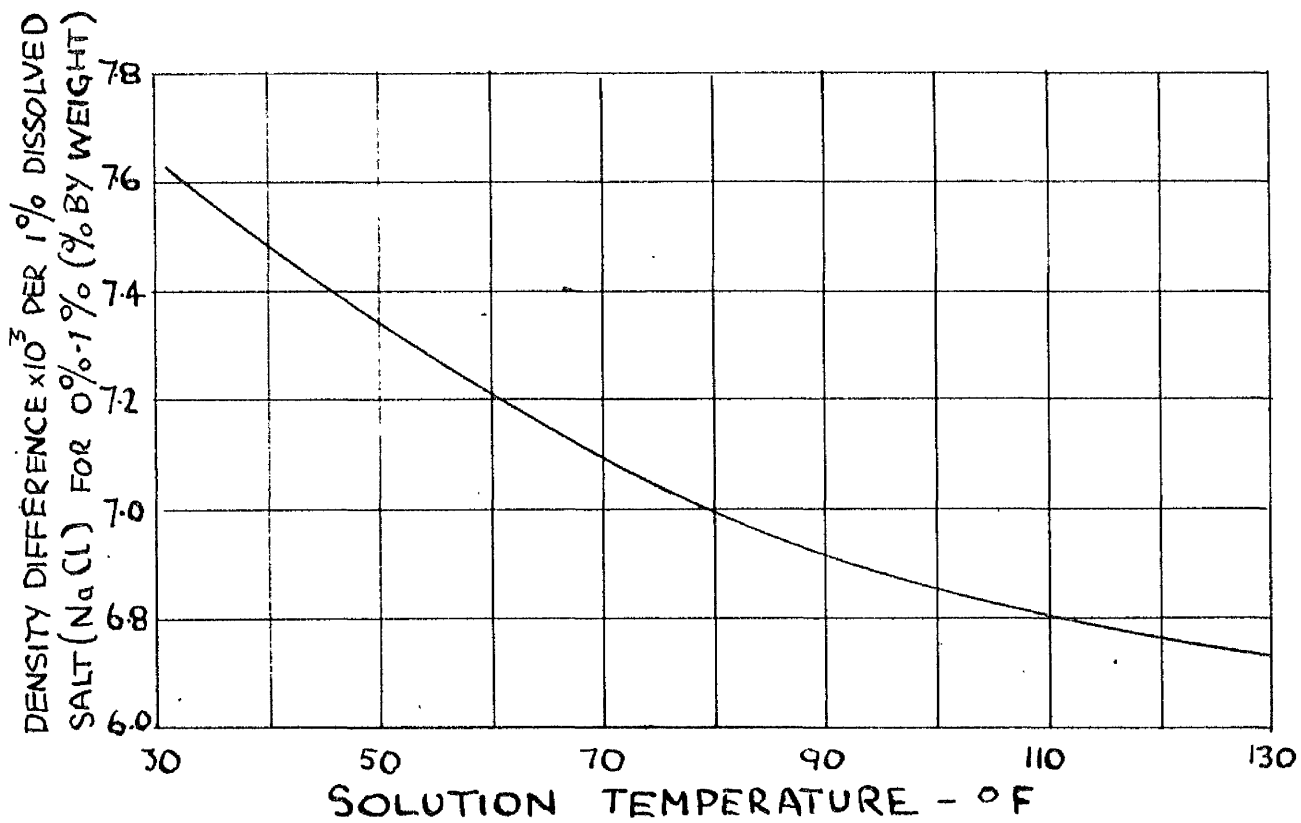
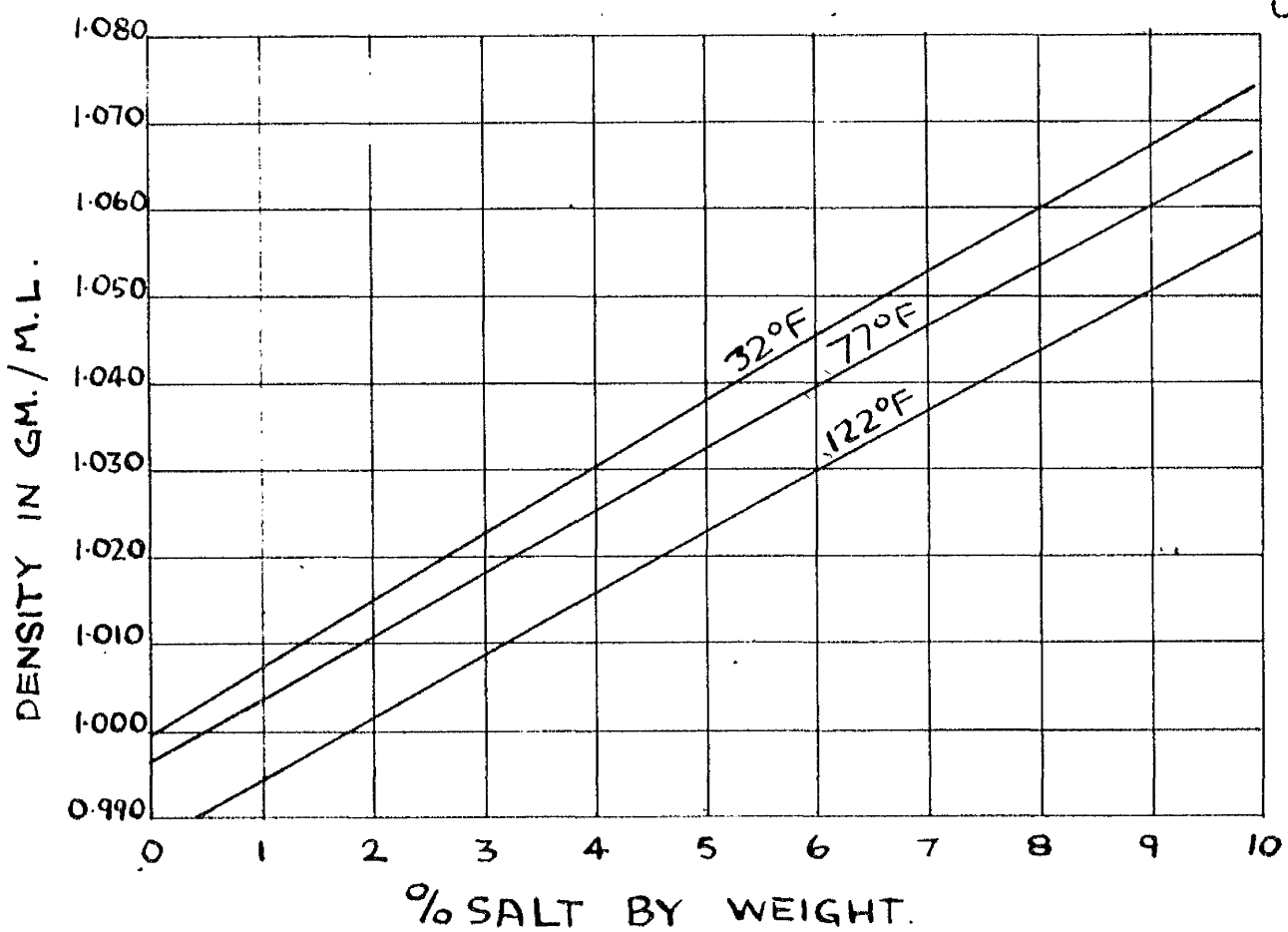


FIG. 2.2 CONCENTRATION-DENSITY RELATION FOR SALT SOLUTION (NaCl). VALUES FROM INTERNATIONAL CRITICAL TABLES.

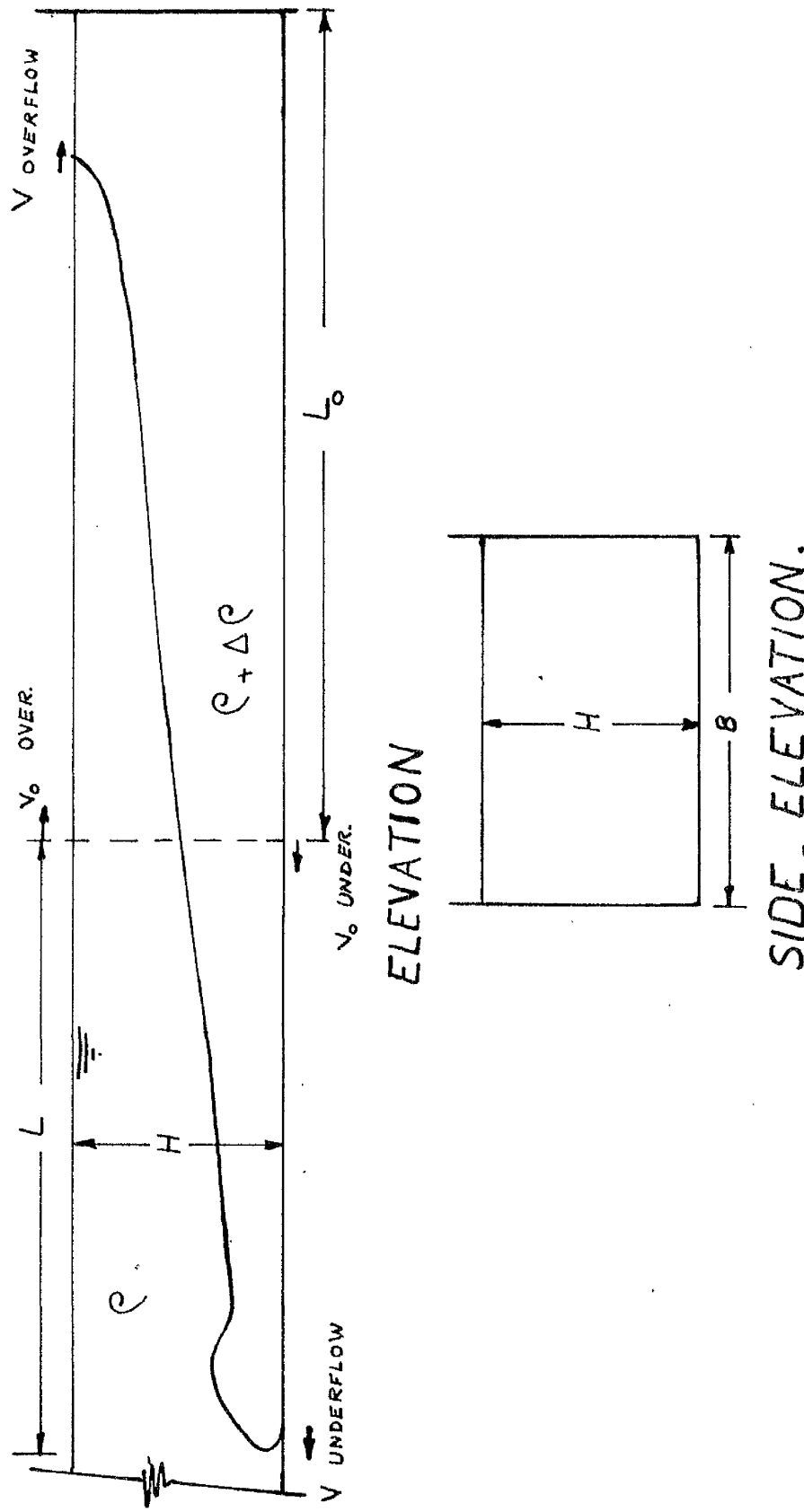


FIG 3.1 - VARIABLES PERTAINING TO  
LOCK FLOW.

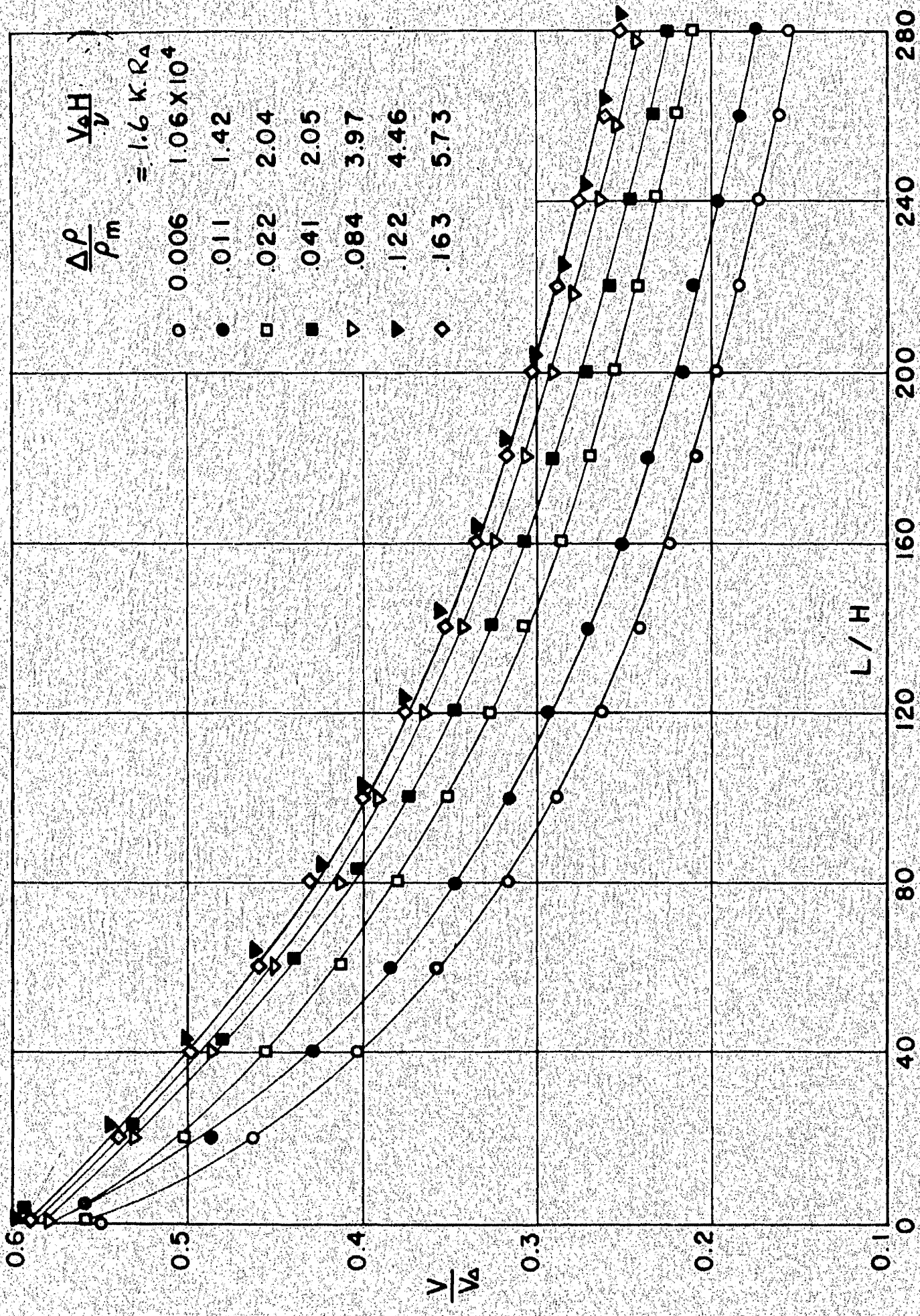


FIG. 24 VELOCITY OF SALINE FRONTS. SMOOTHED VALUES. CHANNEL H=11.2, B=11.3 cm  
 FIG. 3.2 - KEULEGAN'S RESULTS FOR CHANNEL AND SEA EXPTS.

FIG. 4.1.1 - Down stream end of the flume with draft excluders in open position.

FIG. 4.1.2 - Pumping system.

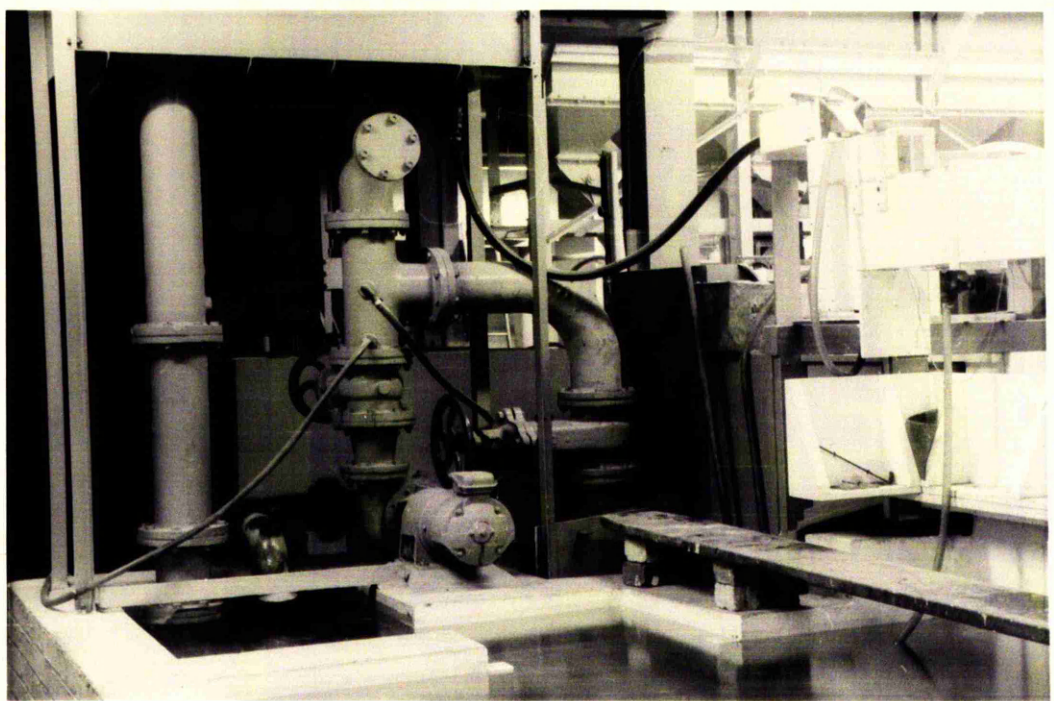
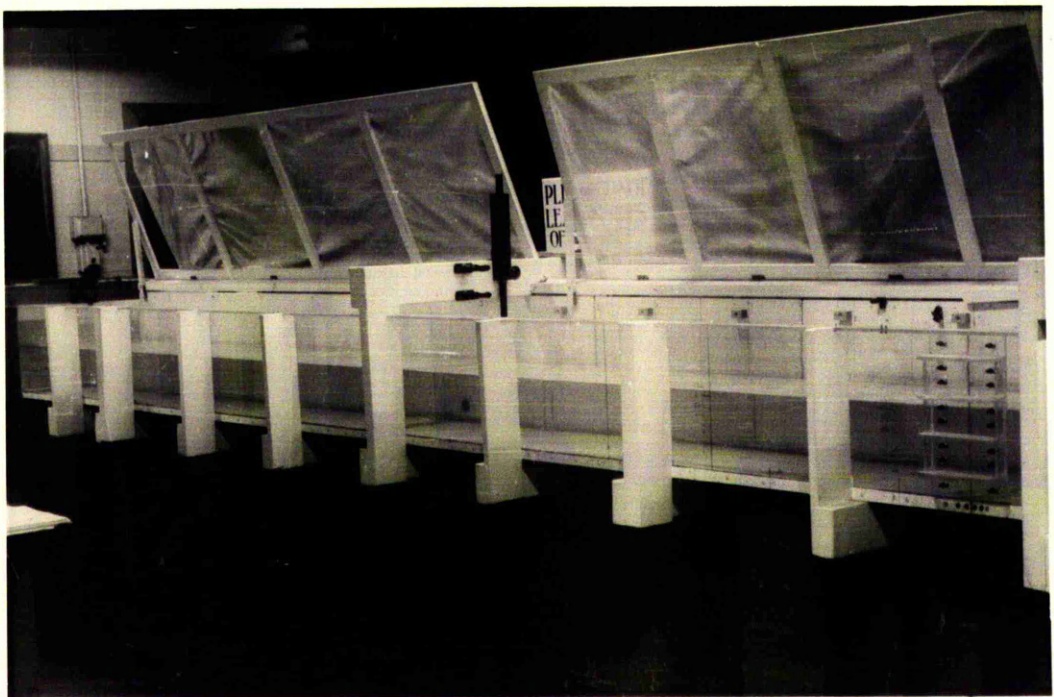
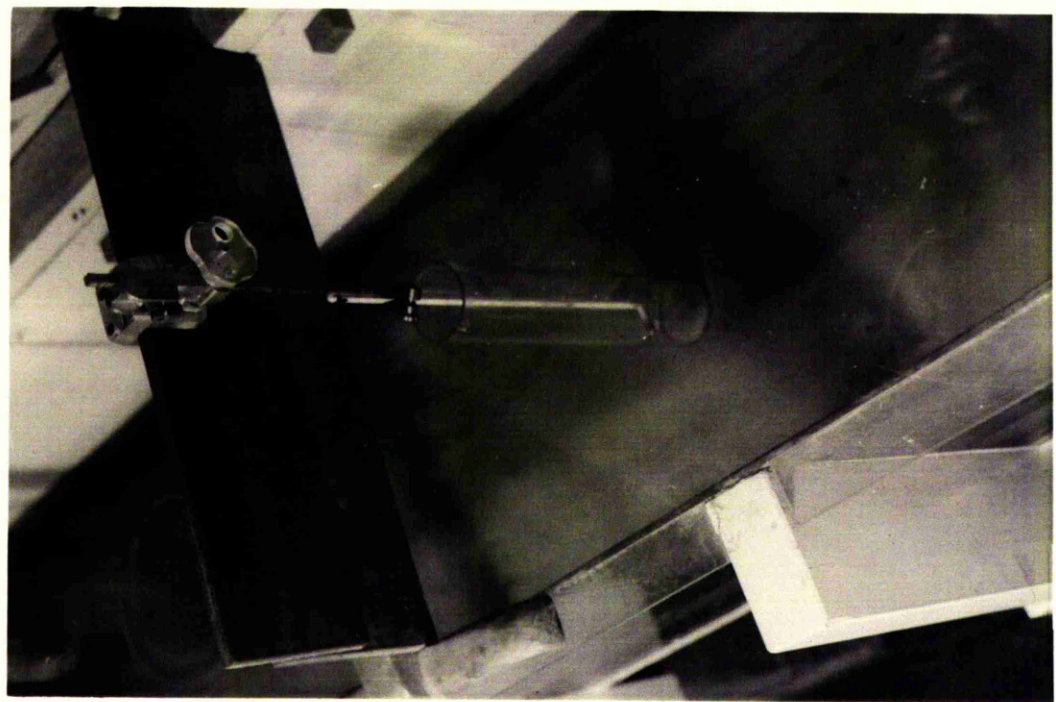
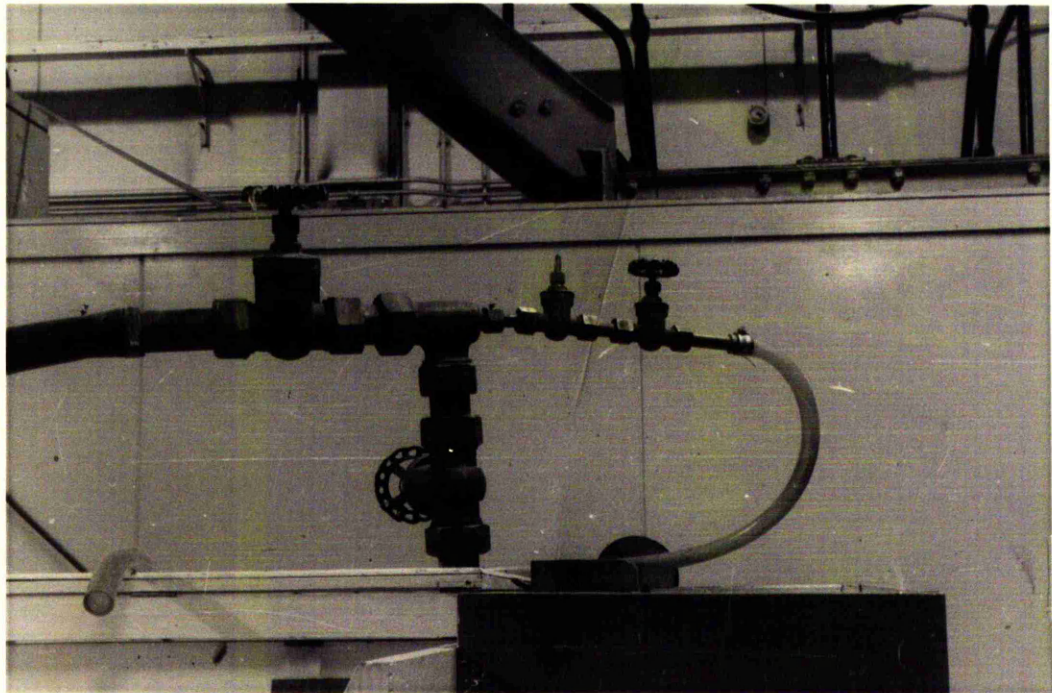


FIG. 4.1.3 - Down-pipe controls

FIG. 5.1.1 -- Angled thermometer  
and circular perspex tube  
in position to record  
temperatures of stratified  
layers.



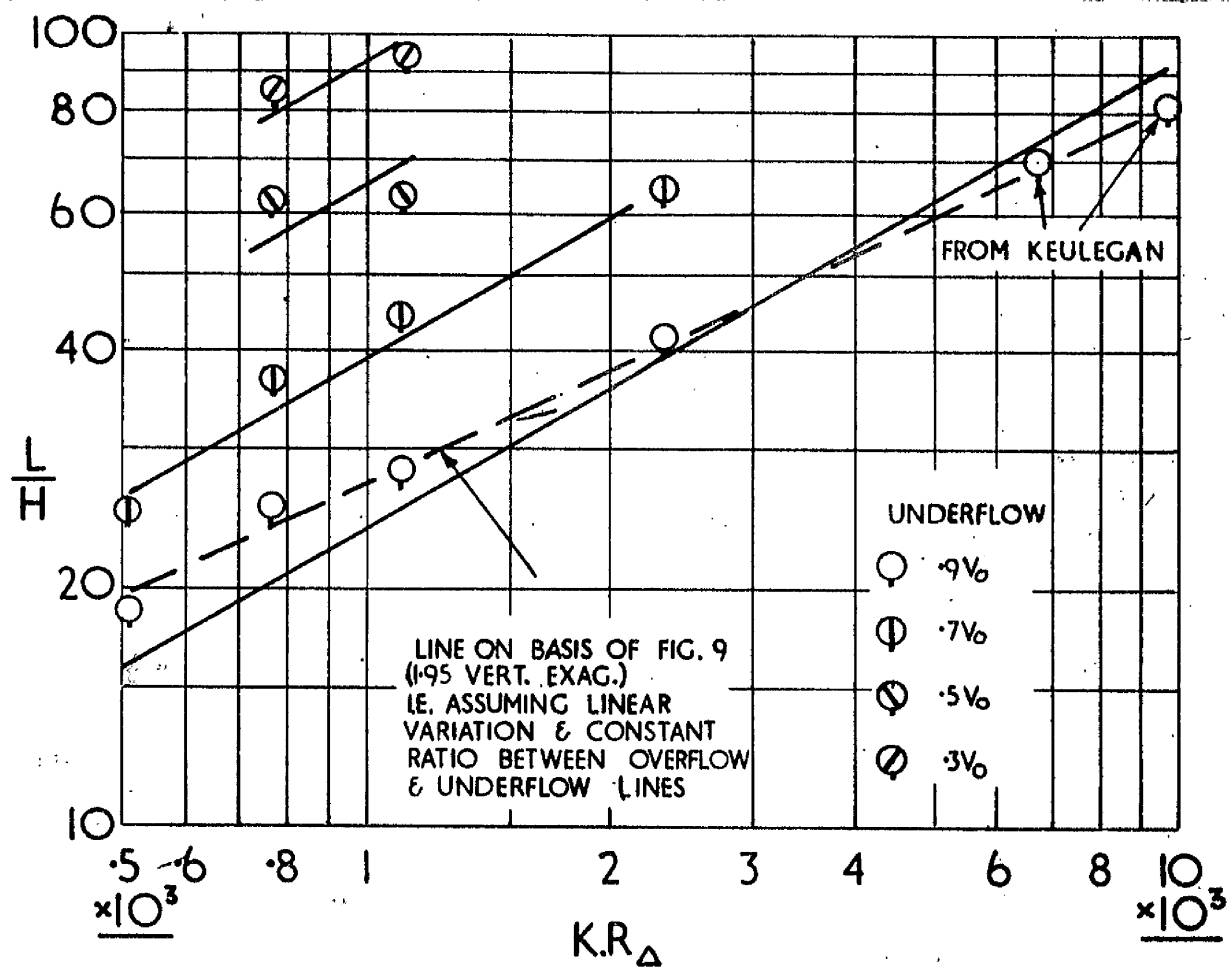
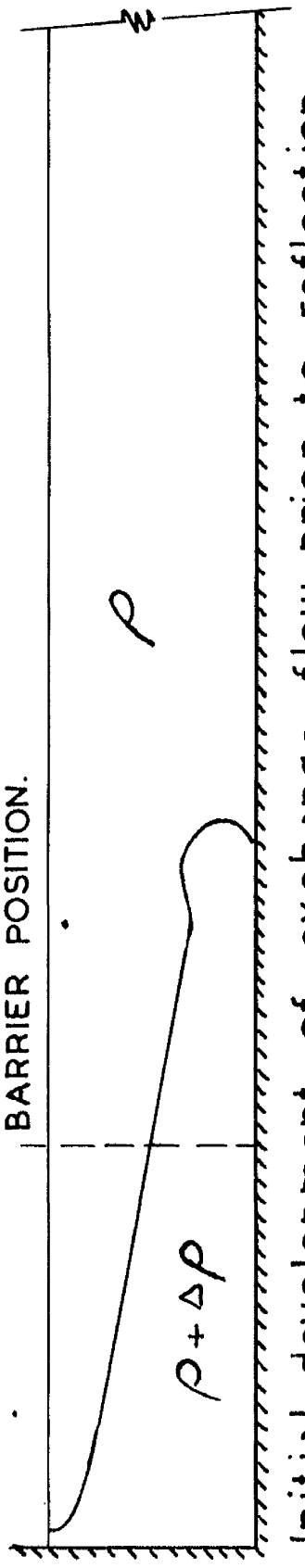
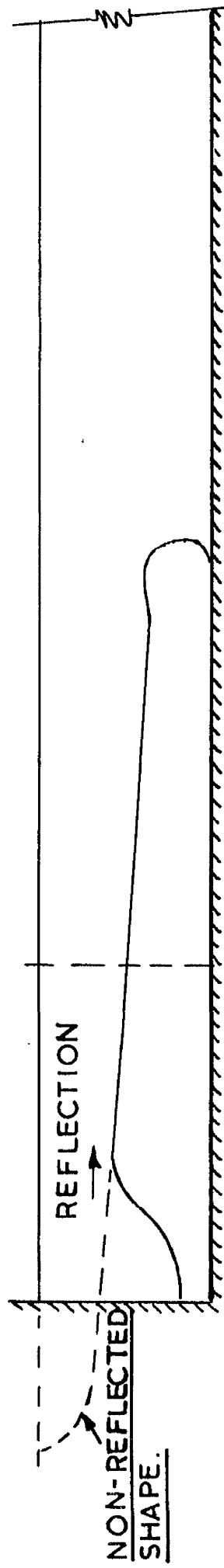


Fig. 6.11- KEULEGAN TYPE CONGRUENCY DIAGRAM.

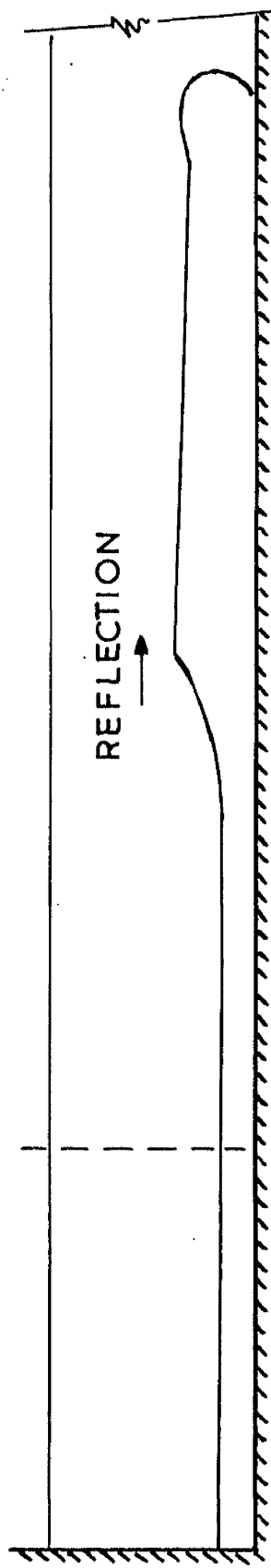
BARRIER POSITION.



(a) Initial development of exchange flow prior to reflection.



(b) Reflection due to overflow meeting end wall.



(c) As diminution of underflow velocity occurs reflection overtakes underflow & eventually further decreases its velocity.

FIG. 6.1.2 - EFFECT OF REFLECTION ON FRONT VELOCITY.

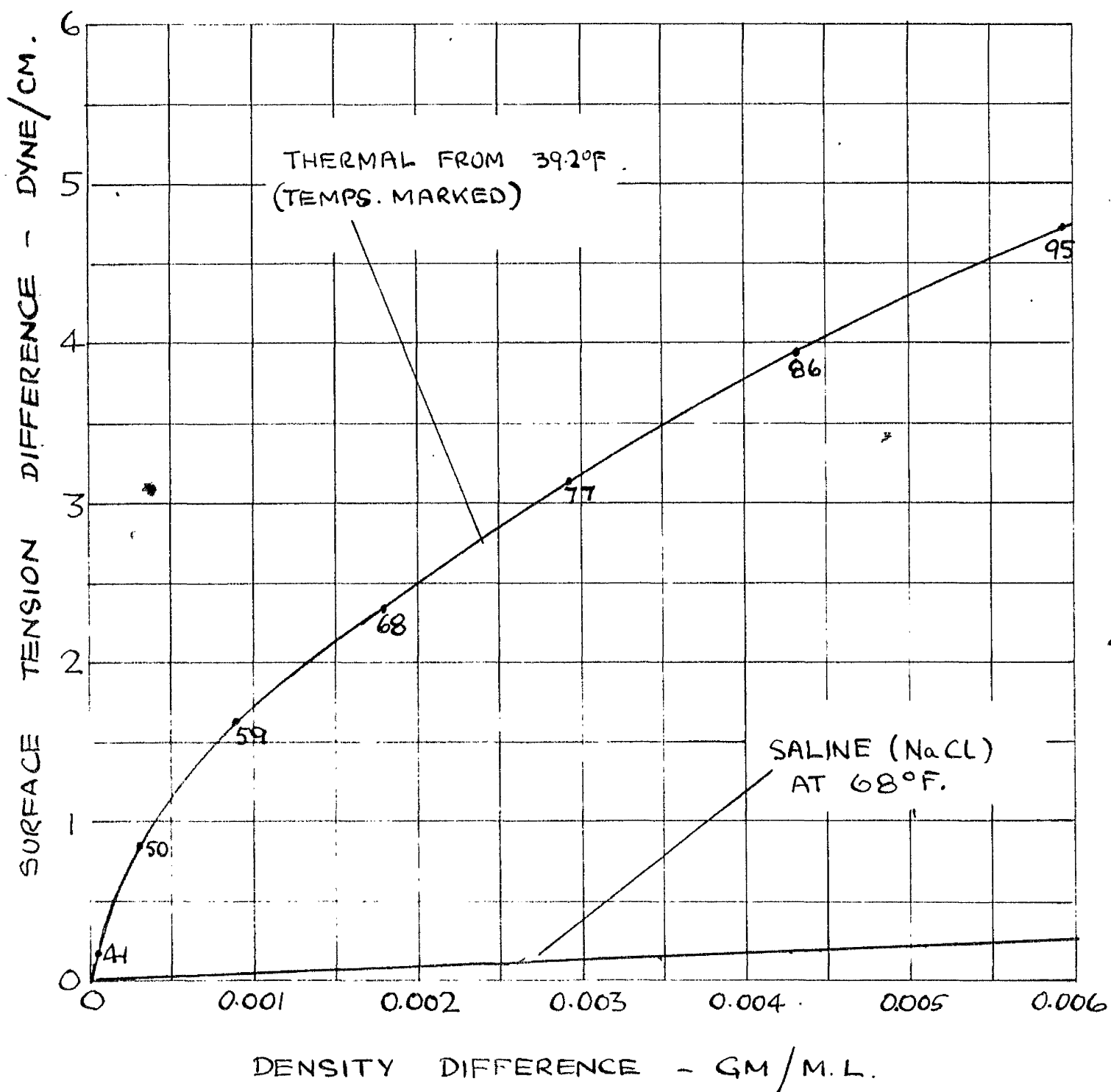


FIG. 6.1.3 SURFACE TENSION VARIATION FOR SALINE AND THERMAL DENSITY DIFFERENCES.

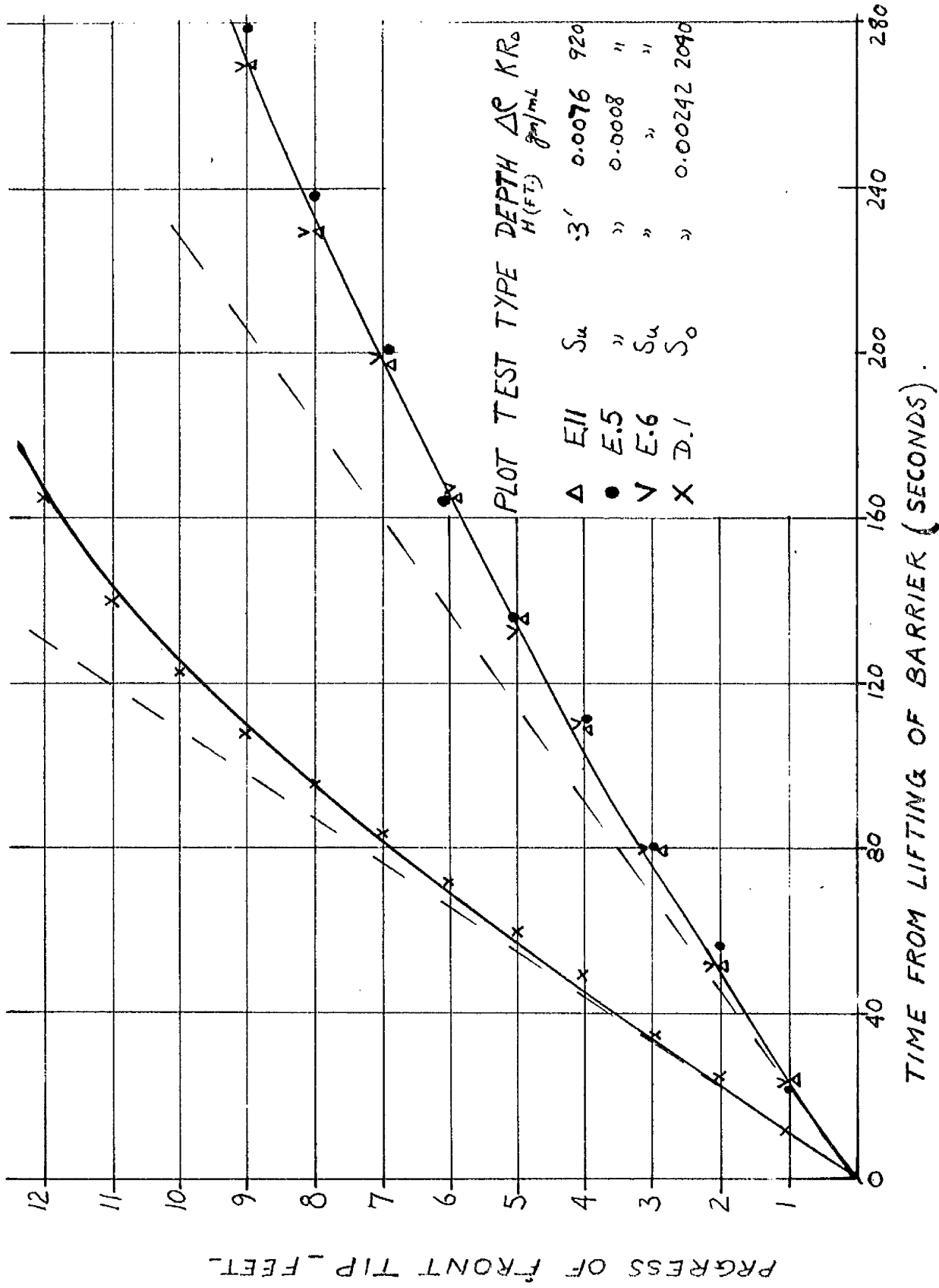
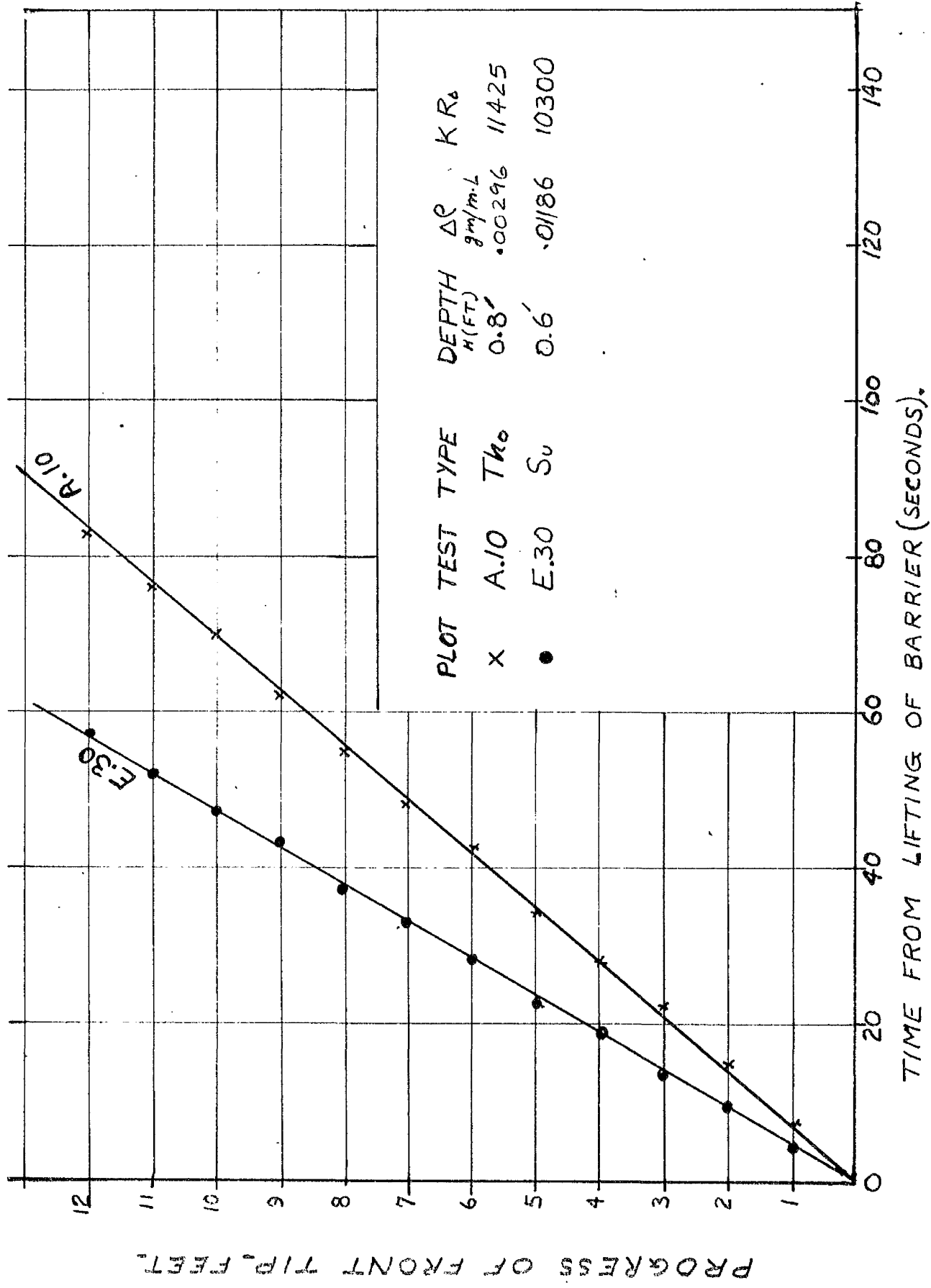


FIG. 6.2.5. TYPICAL PLOTS OF ADVANCE OF FRONT LAMINAR-



PROGRESS OF FRONT TIP. FEET.

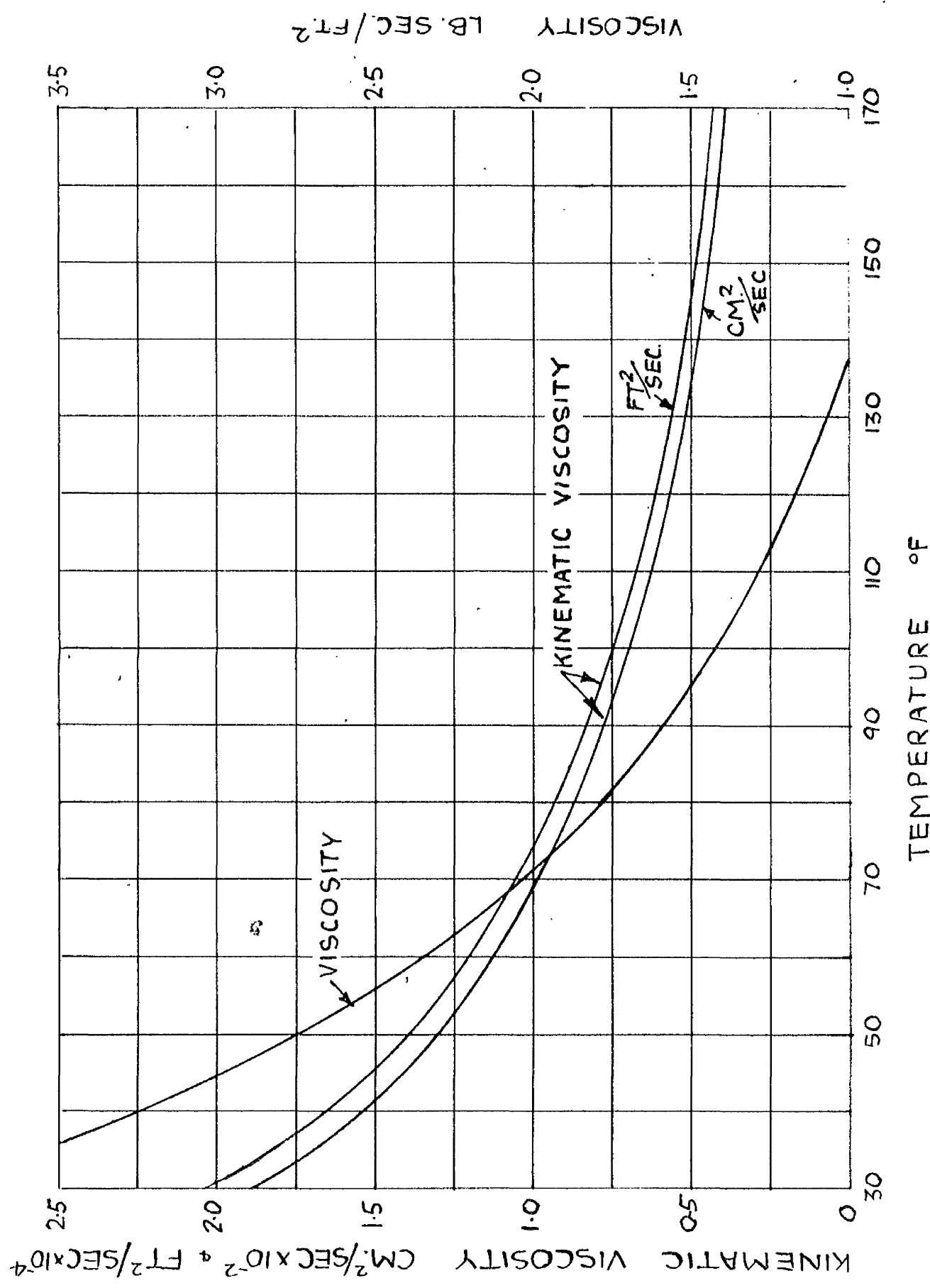


FIG. 6.2.7 VISCOSITY OF FRESH WATER.

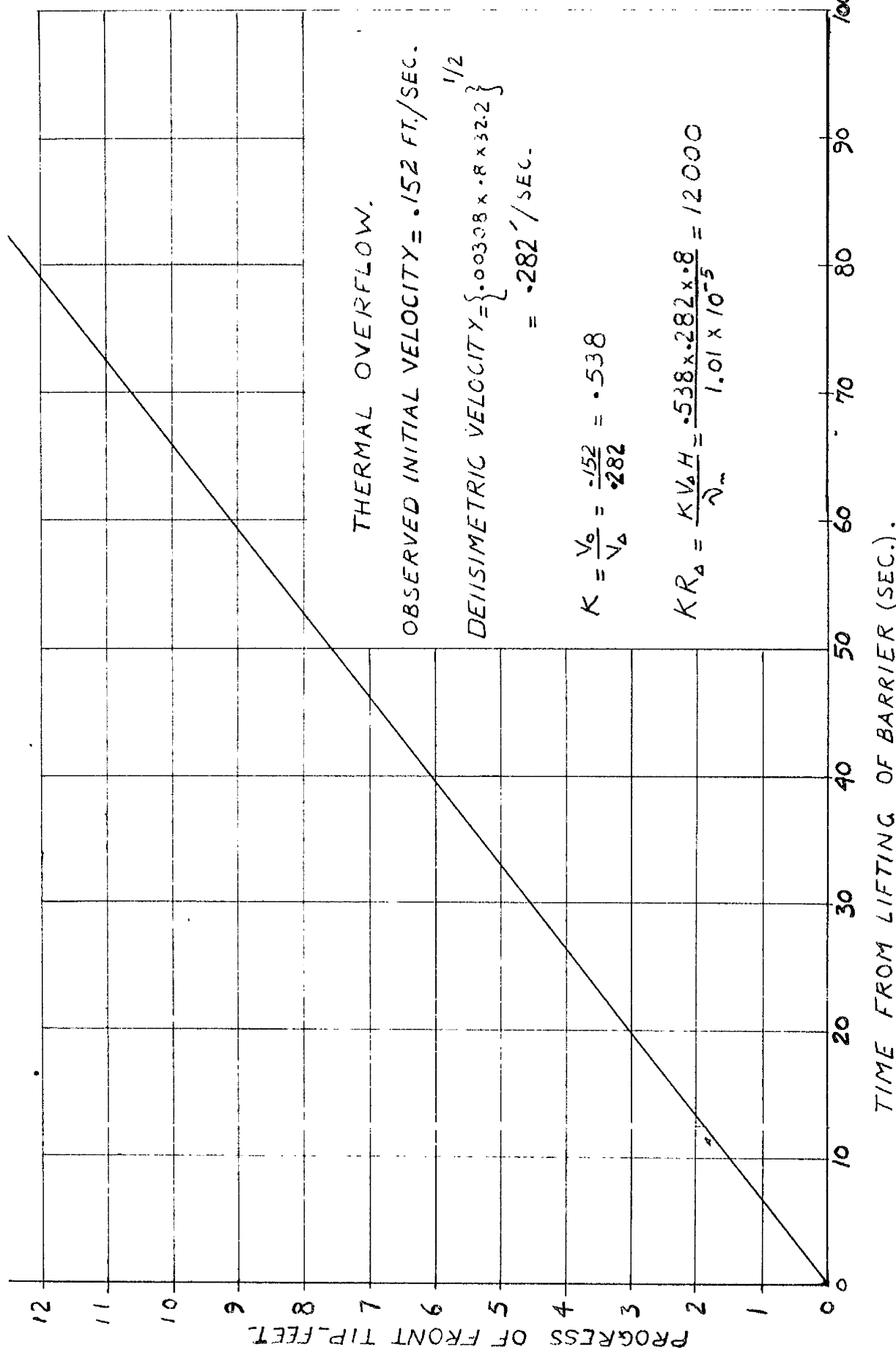


FIG. 6.2.8-TYPICAL CALCULATION OF FRONT COEFFICIENT OF PROPORTIONALITY & DENSIMETRIC RYNOULD'S NUMBER.

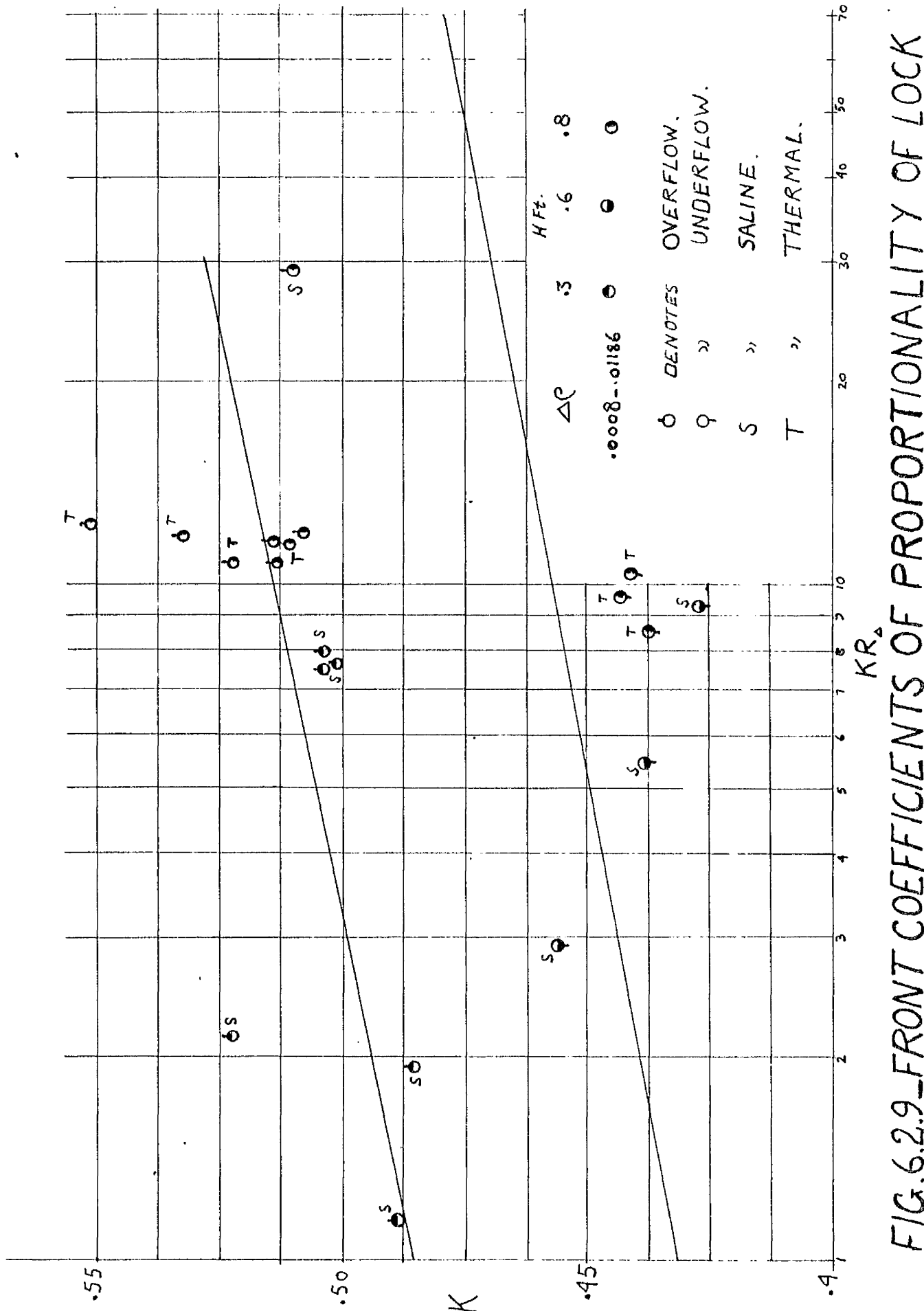


FIG. 6.2.9 FRONT COEFFICIENTS OF PROPORTIONALITY OF LOCK FLOW.

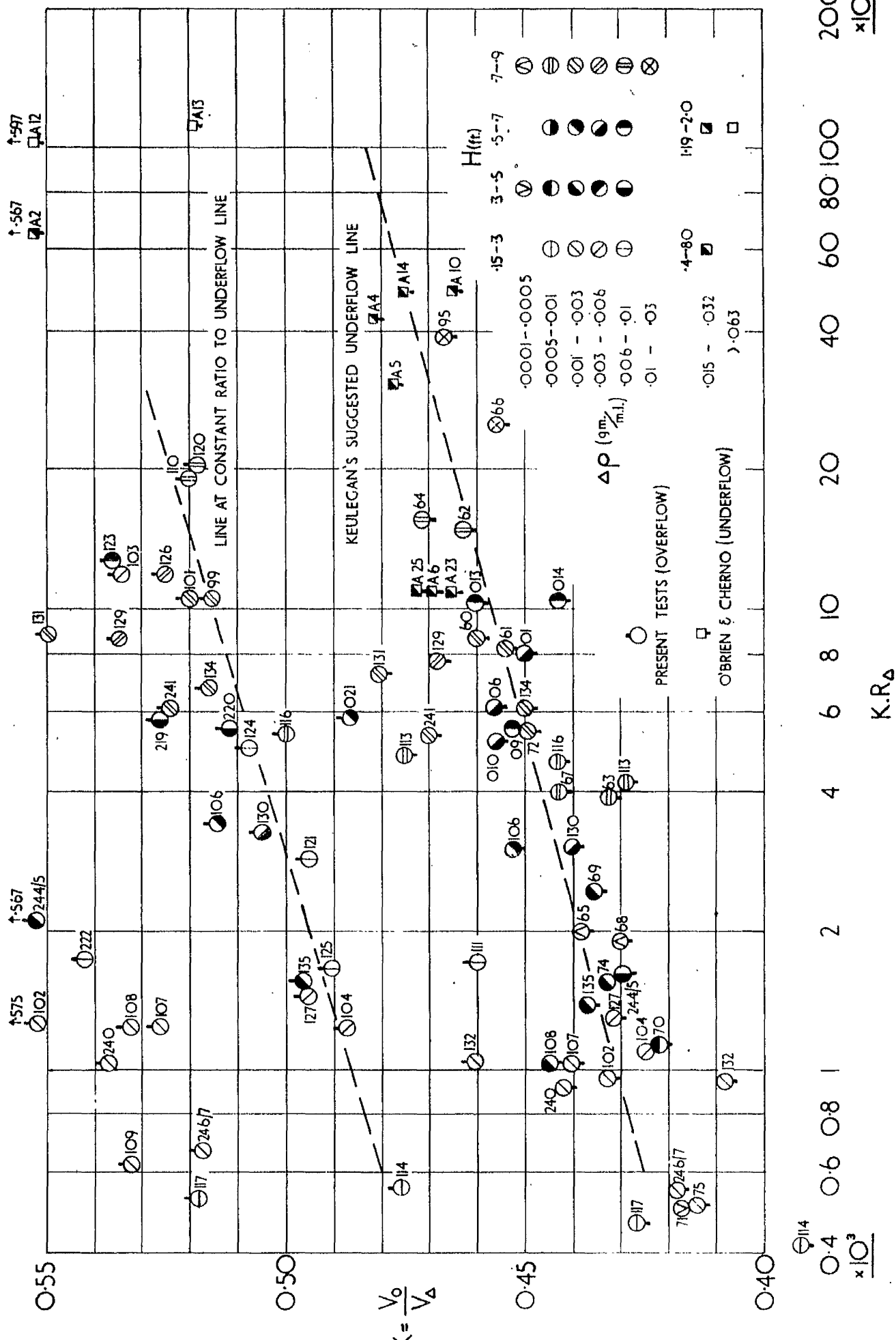


Fig.6.2.10 SALINE COEFFICIENTS OF PROPORTIONALITY.

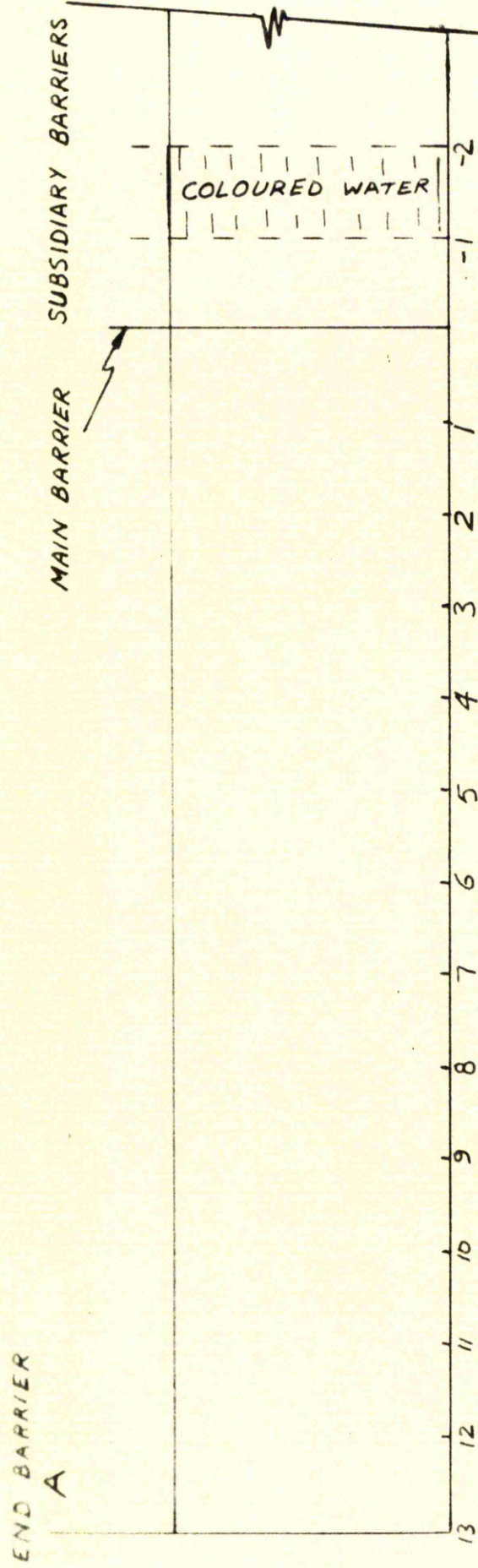


FIG. 63.11 - STARTING CONDITIONS.

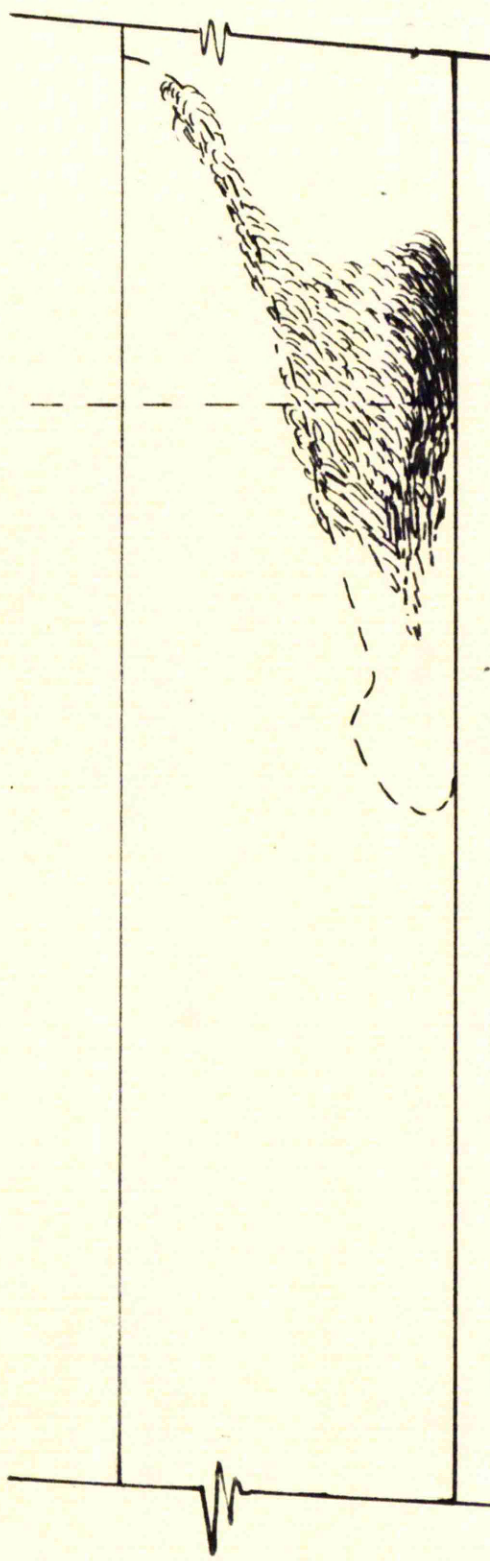


FIG. 63.12 - DISTORTION OF COLOURED PRISM.

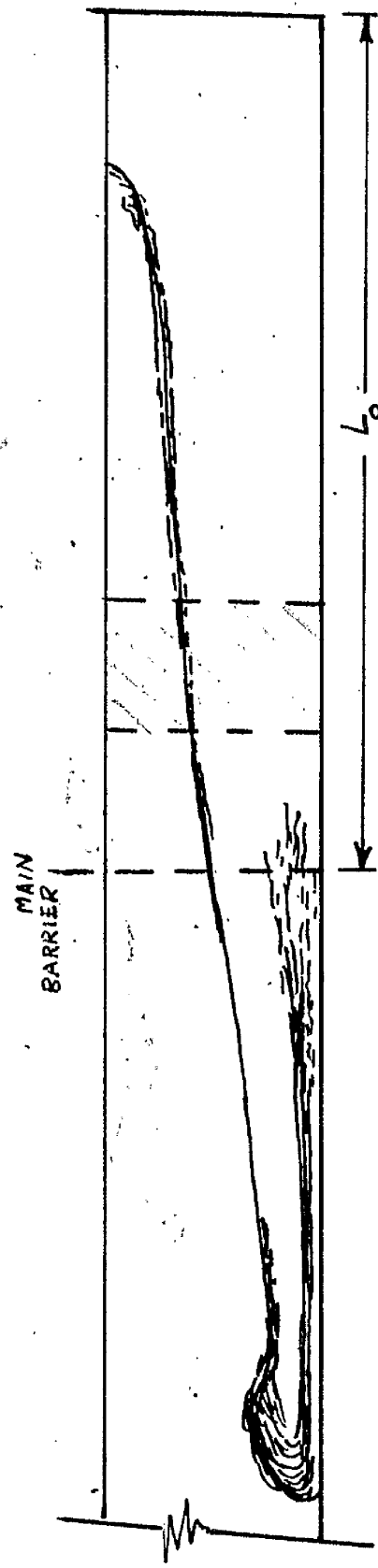


FIG. 6.3.13 - OVERTAKING OF THE FRONT BY  
COLOURED WATER FROM BEHIND.

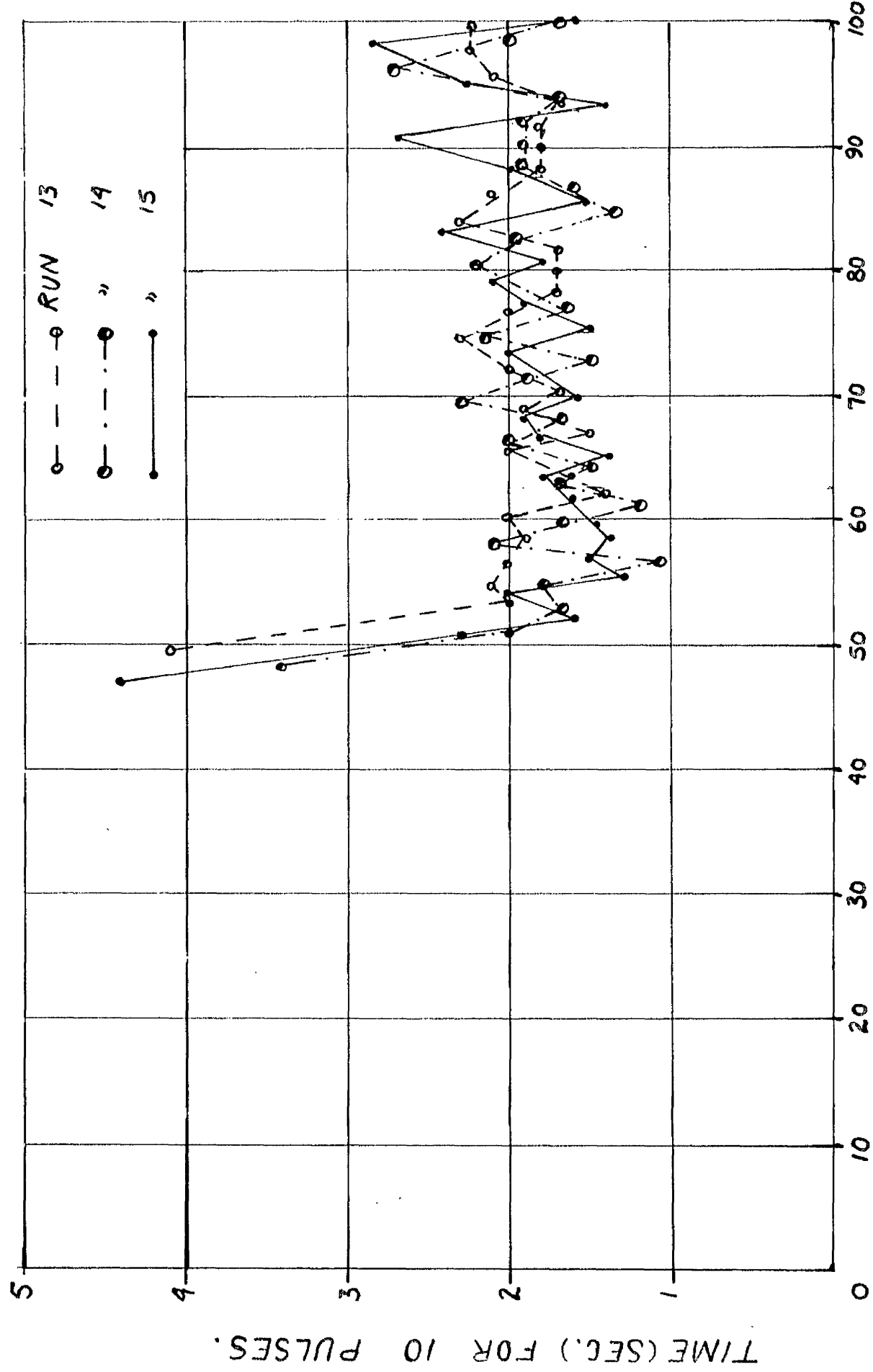


FIG. 6.4.14 - TYPICAL FLOWMETER RECORDINGS.  
TIME (SEC.) FROM LIFTING OF THE BARRIER.

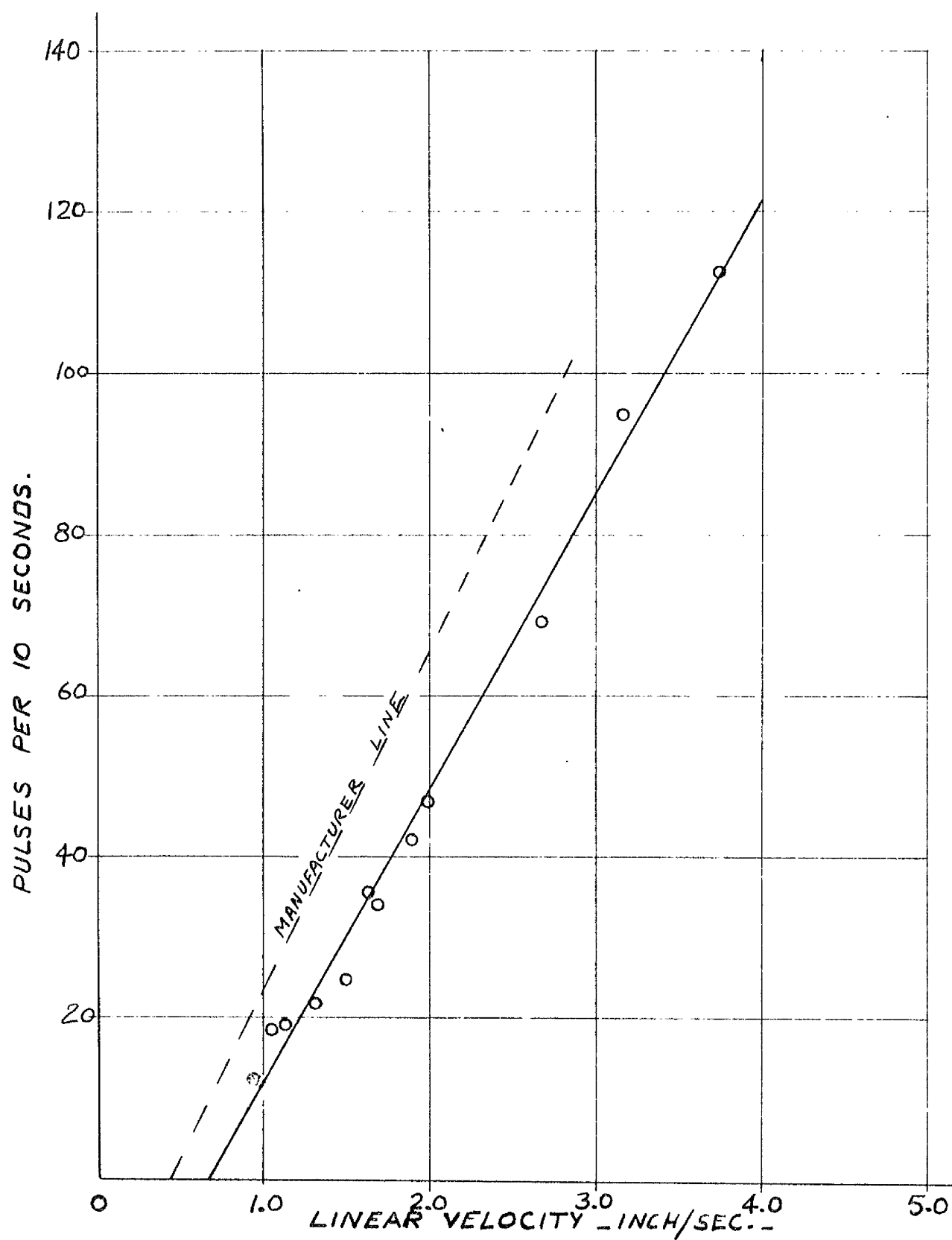


FIG.6.4.15\_CALIBRATION OF THE MINIATURE FLOWMETER.

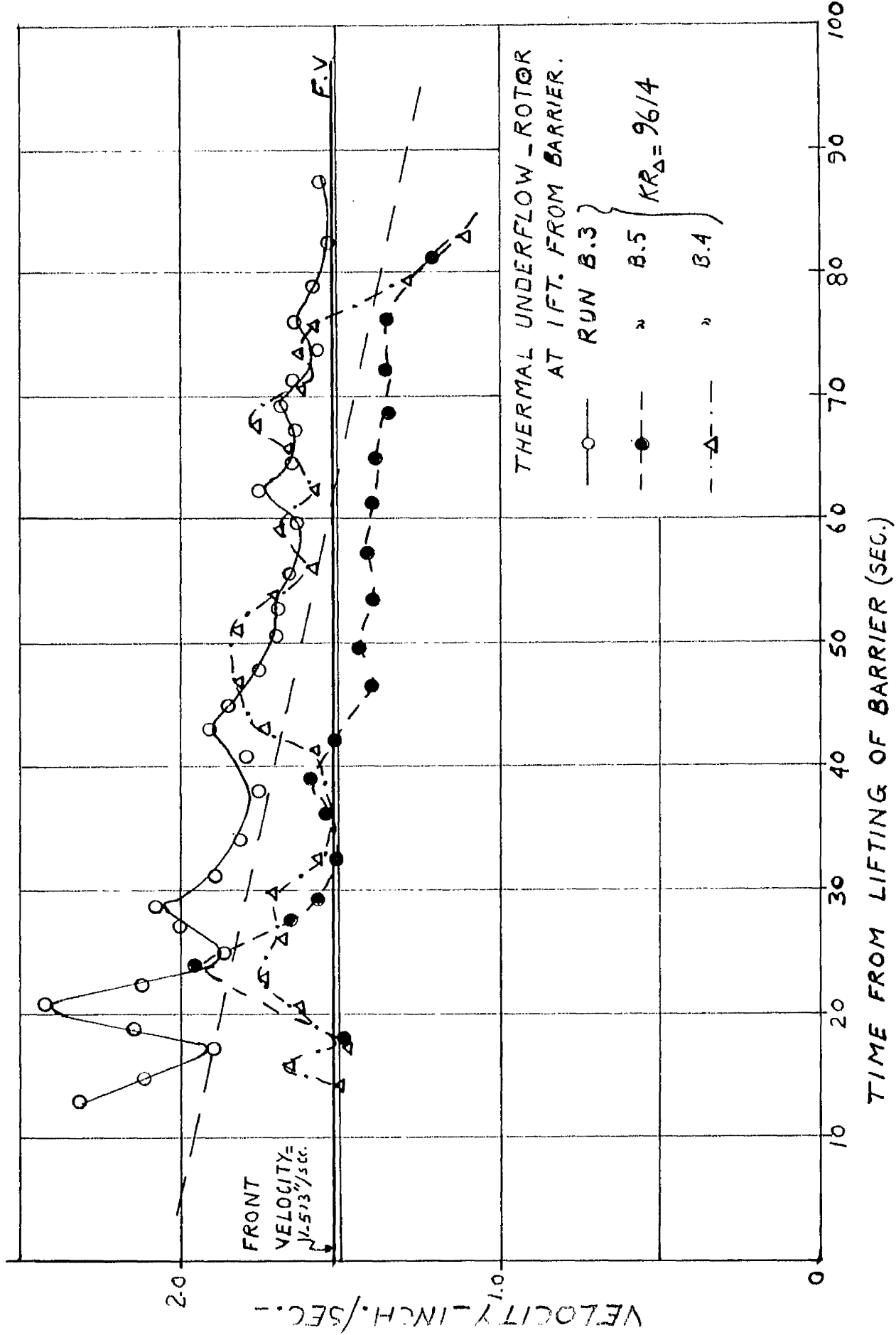


FIG. 6.4.16-VELOCITY VARIATION OF WATER BEHIND THE FRONT.

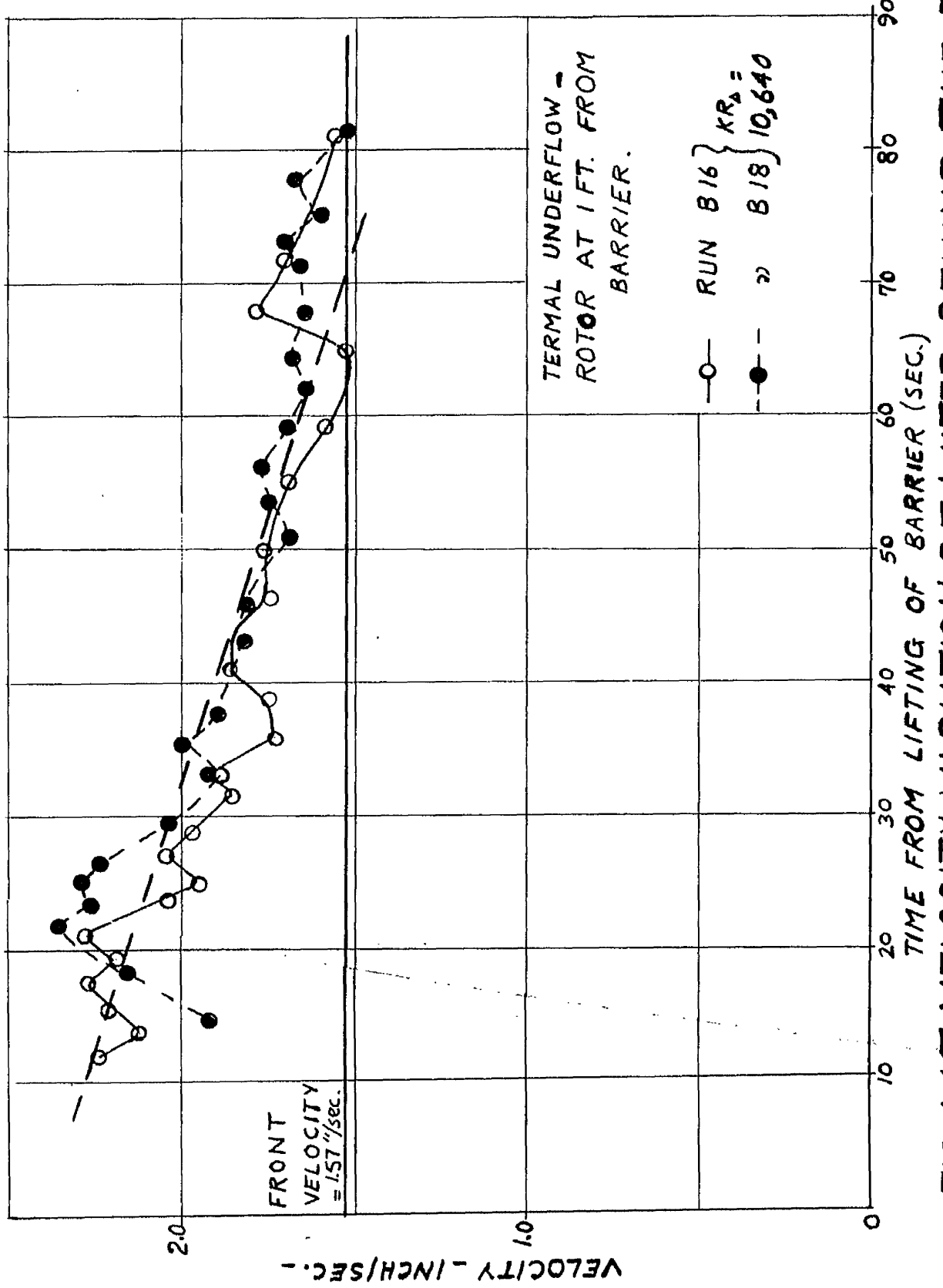
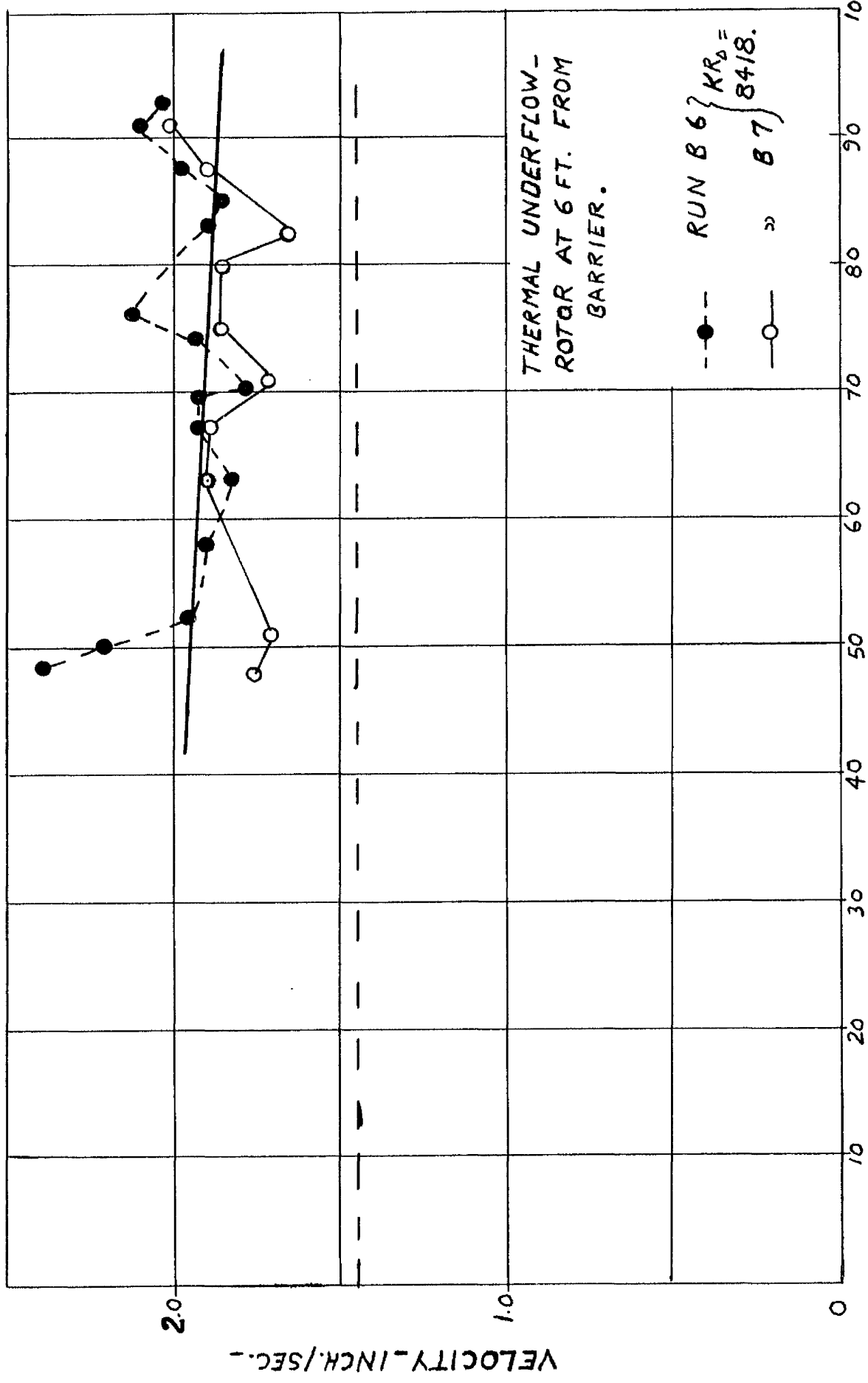


FIG. 6.4.17. VELOCITY VARIATION OF WATER BEHIND THE FRONT

FIG. 6.4.18 - VELOCITY VARIATION OF WATER BEHIND THE FRONT.



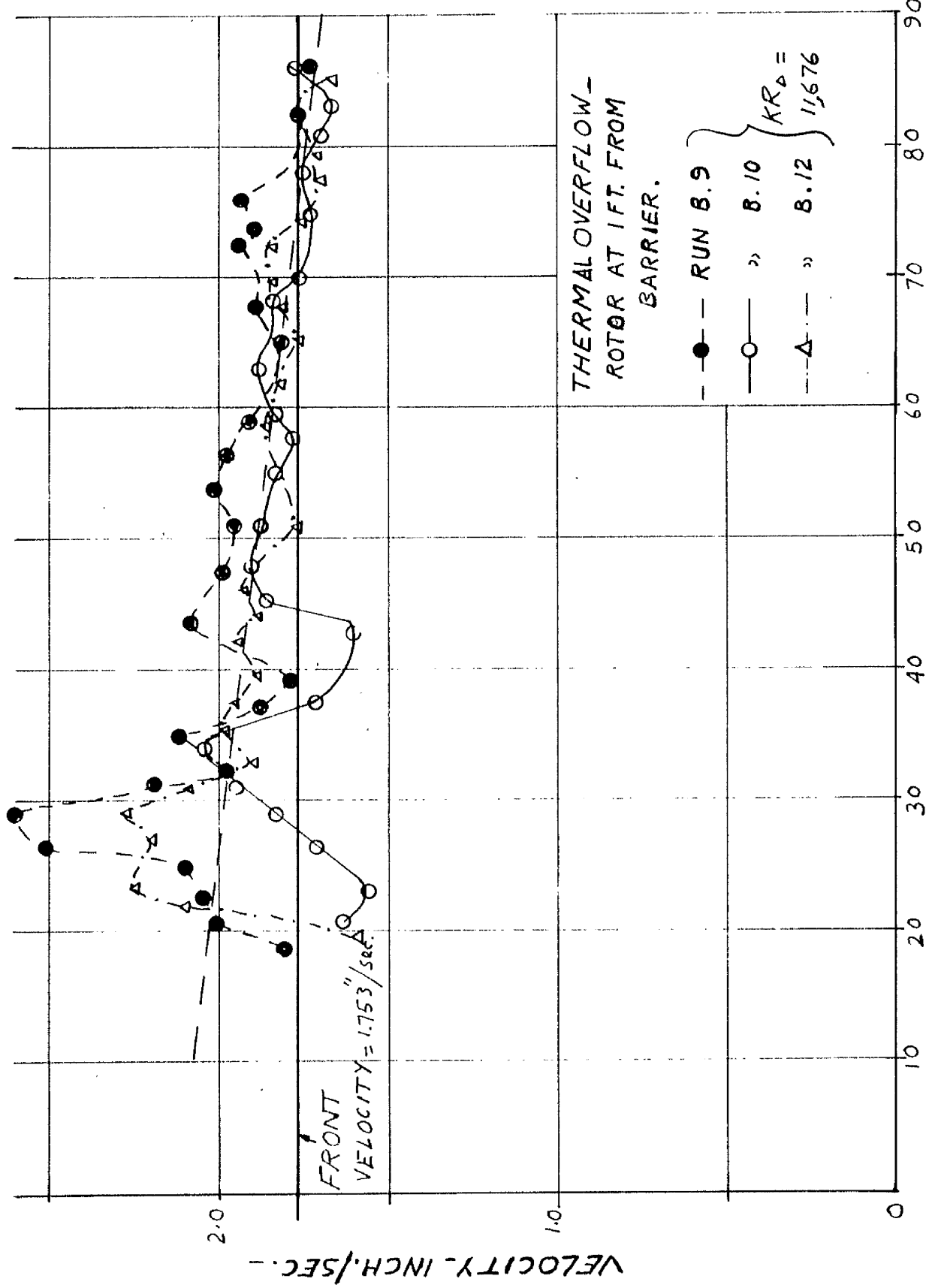


FIG. 6.419 - VELOCITY VARIATION OF WATER BEHIND THE FRONT.

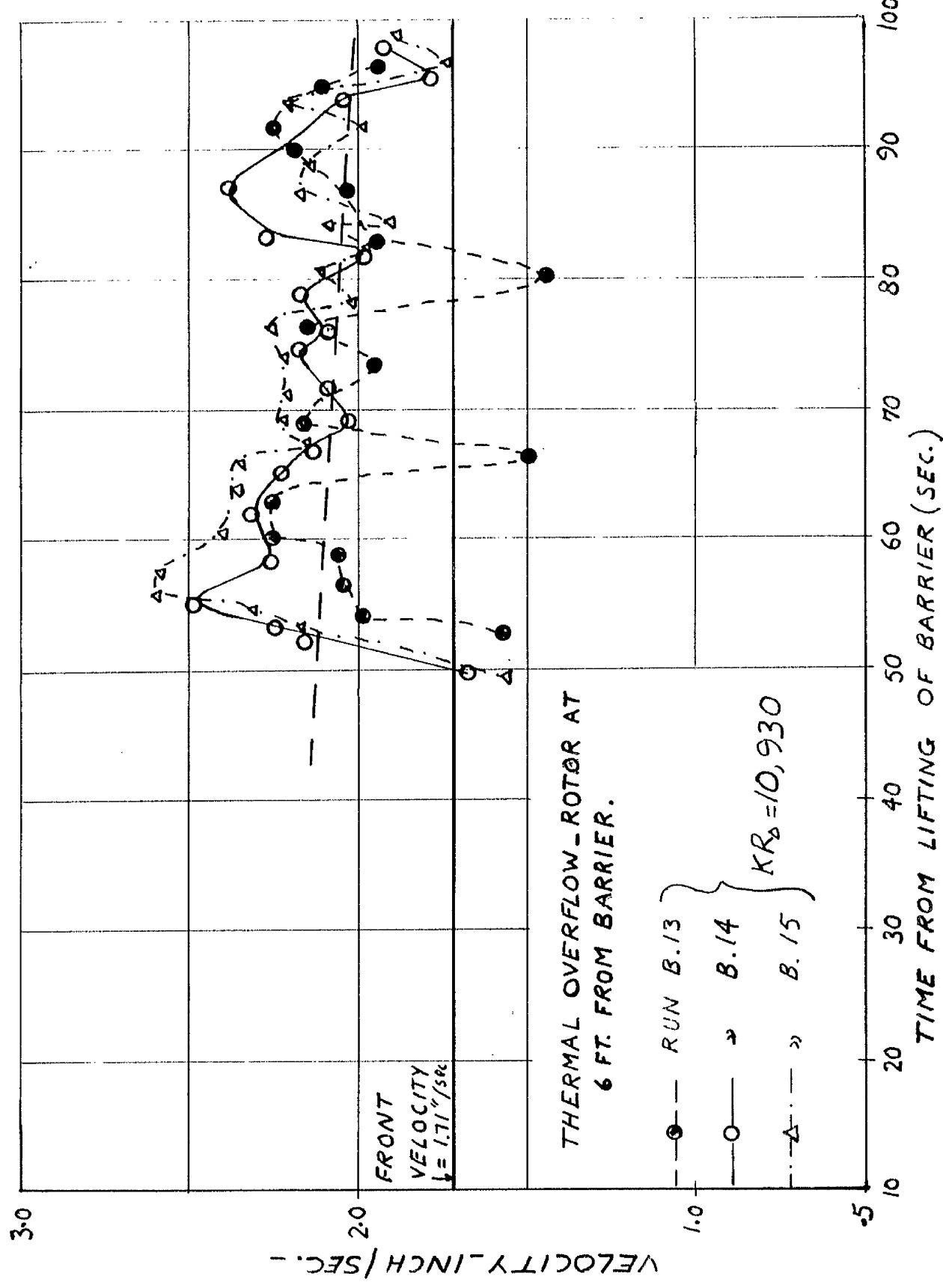


FIG. 6.42a. VELOCITY VARIATION OF WATER BEHIND THE FRONT.

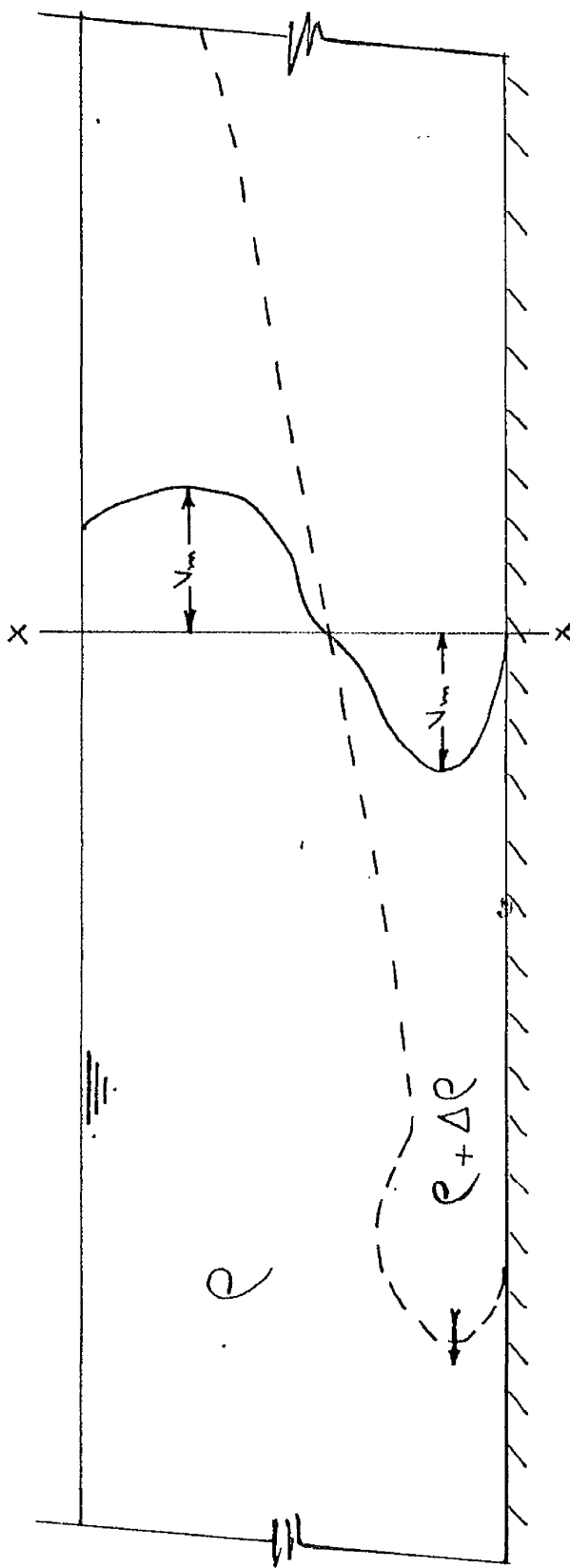


FIG. 6.4.21 - IMPRESSION OF VELOCITY GRADIENT  
AT A SECTION.

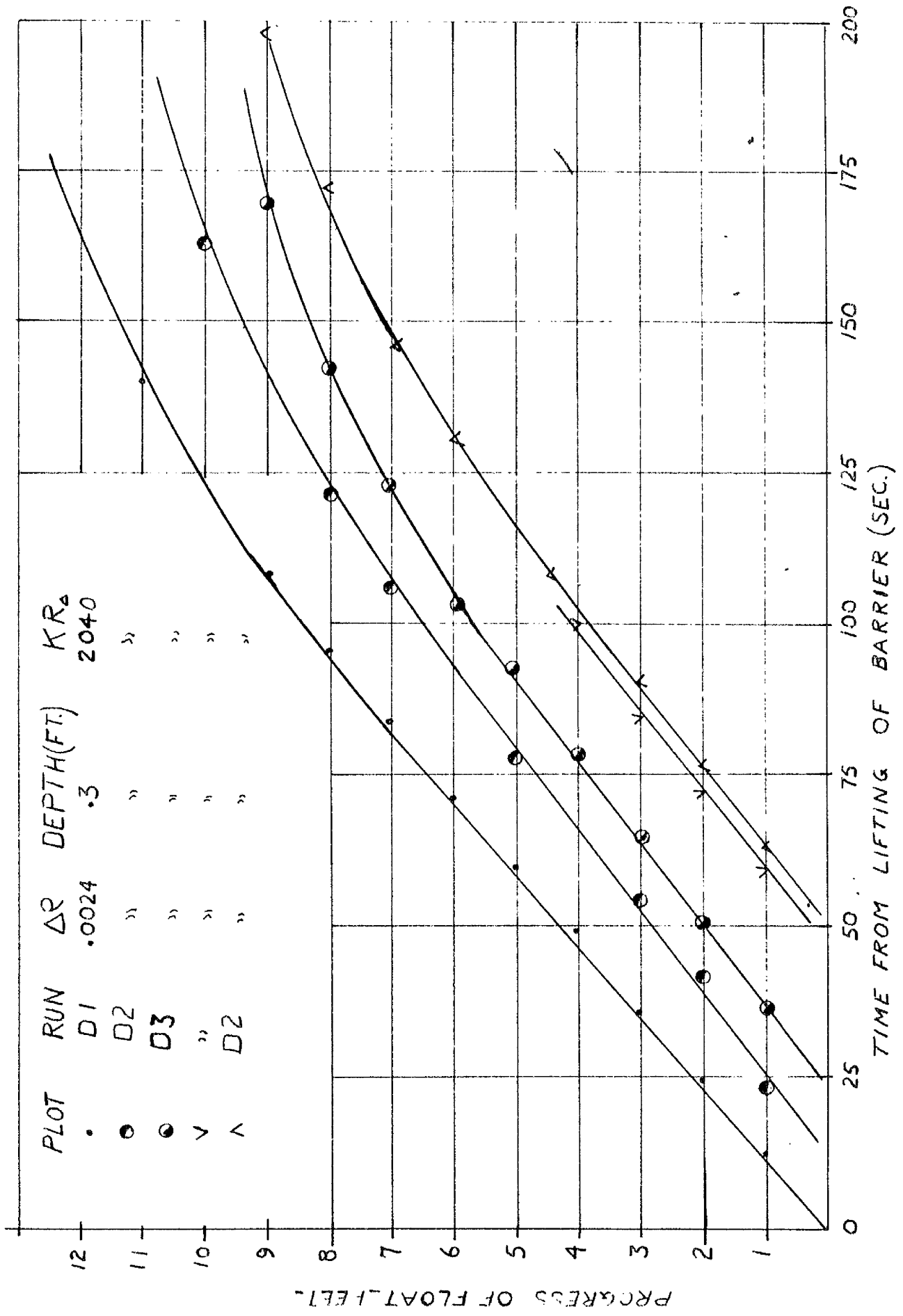


FIG. 6.4.22 - RATE OF TRANSIT OF FLOATS.

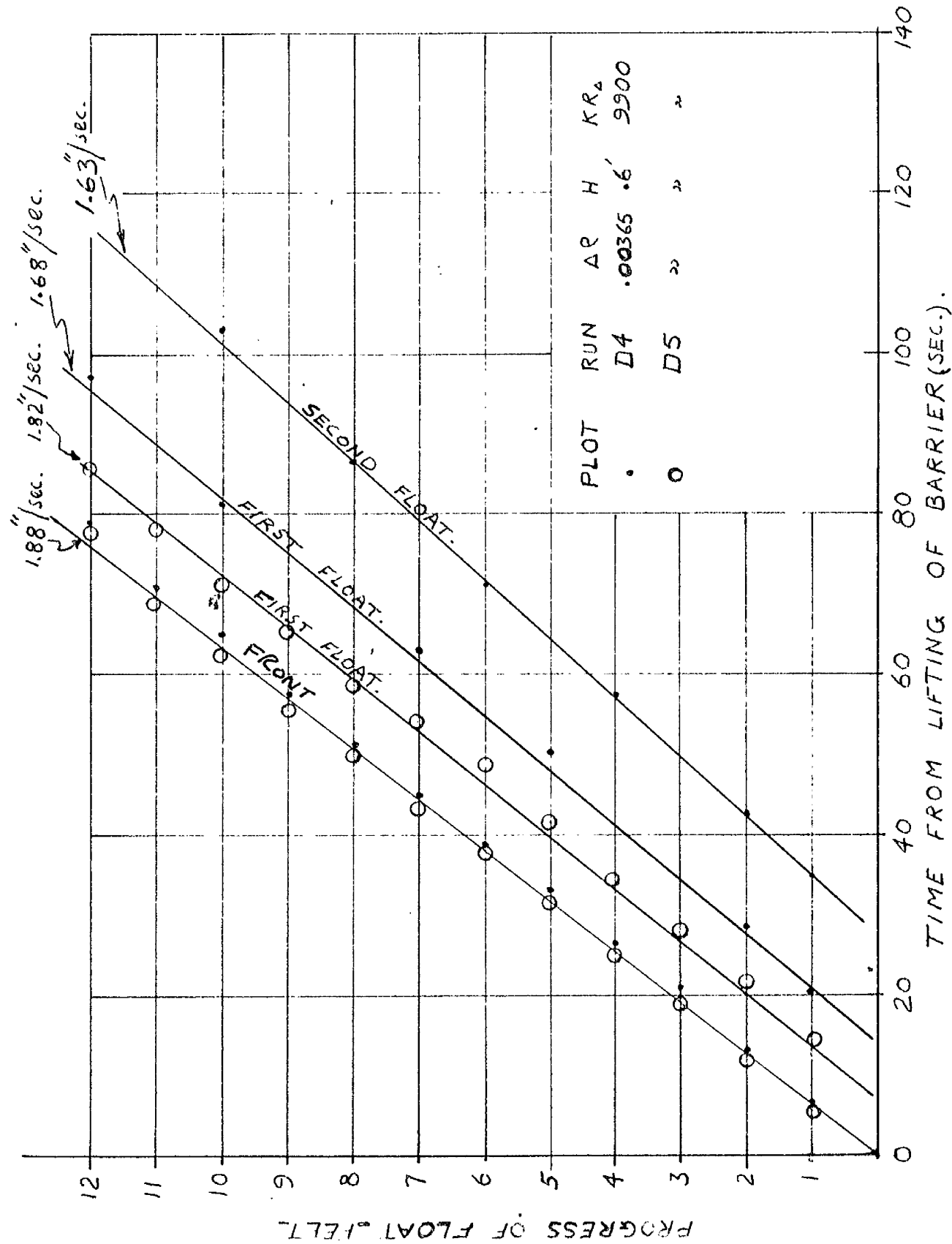


FIG. 6.4.23. RATE OF TRANSIT OF FLOATS.

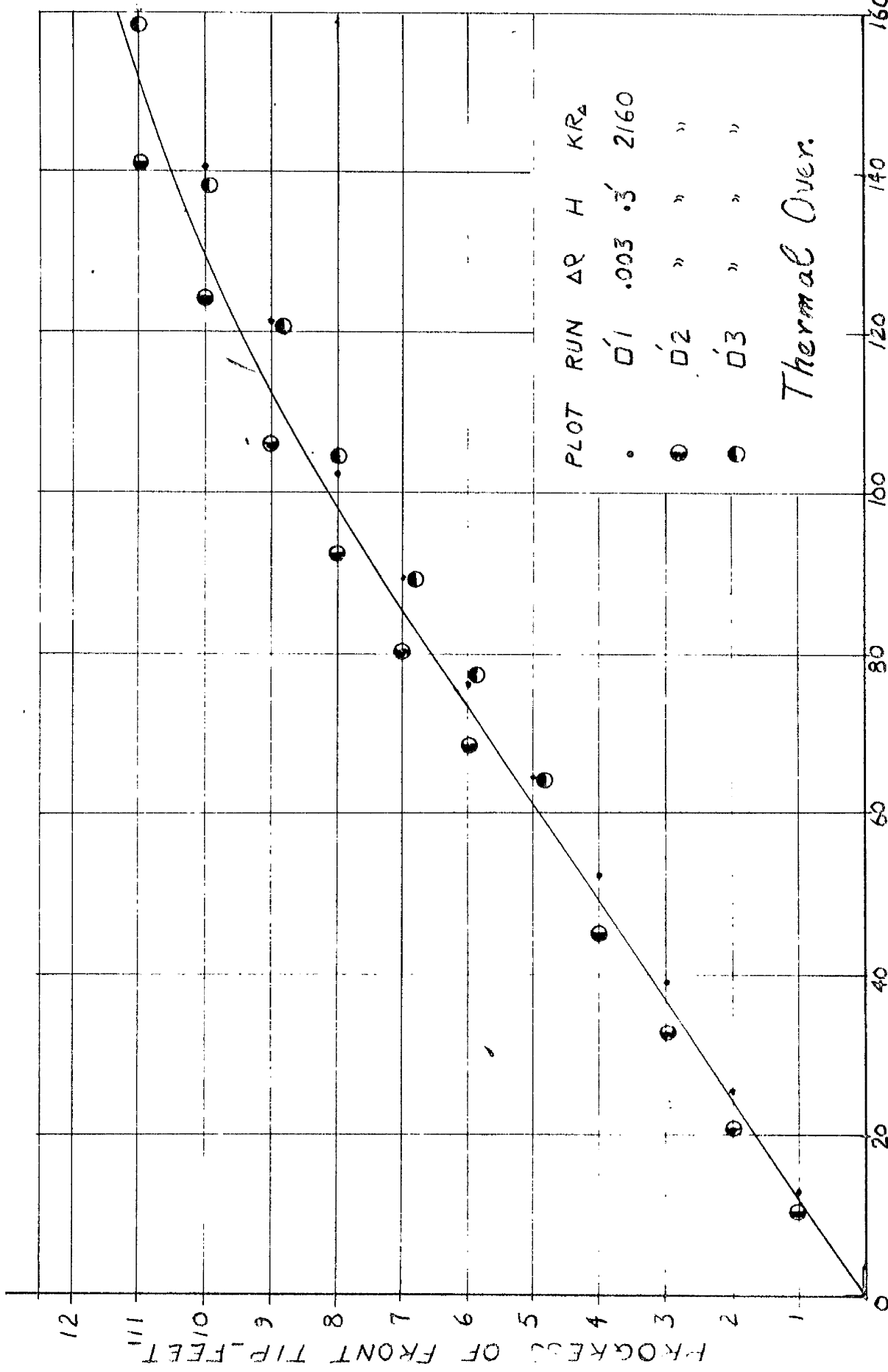


FIG. 6.4.24 RATE OF ADVANCE OF FRONT

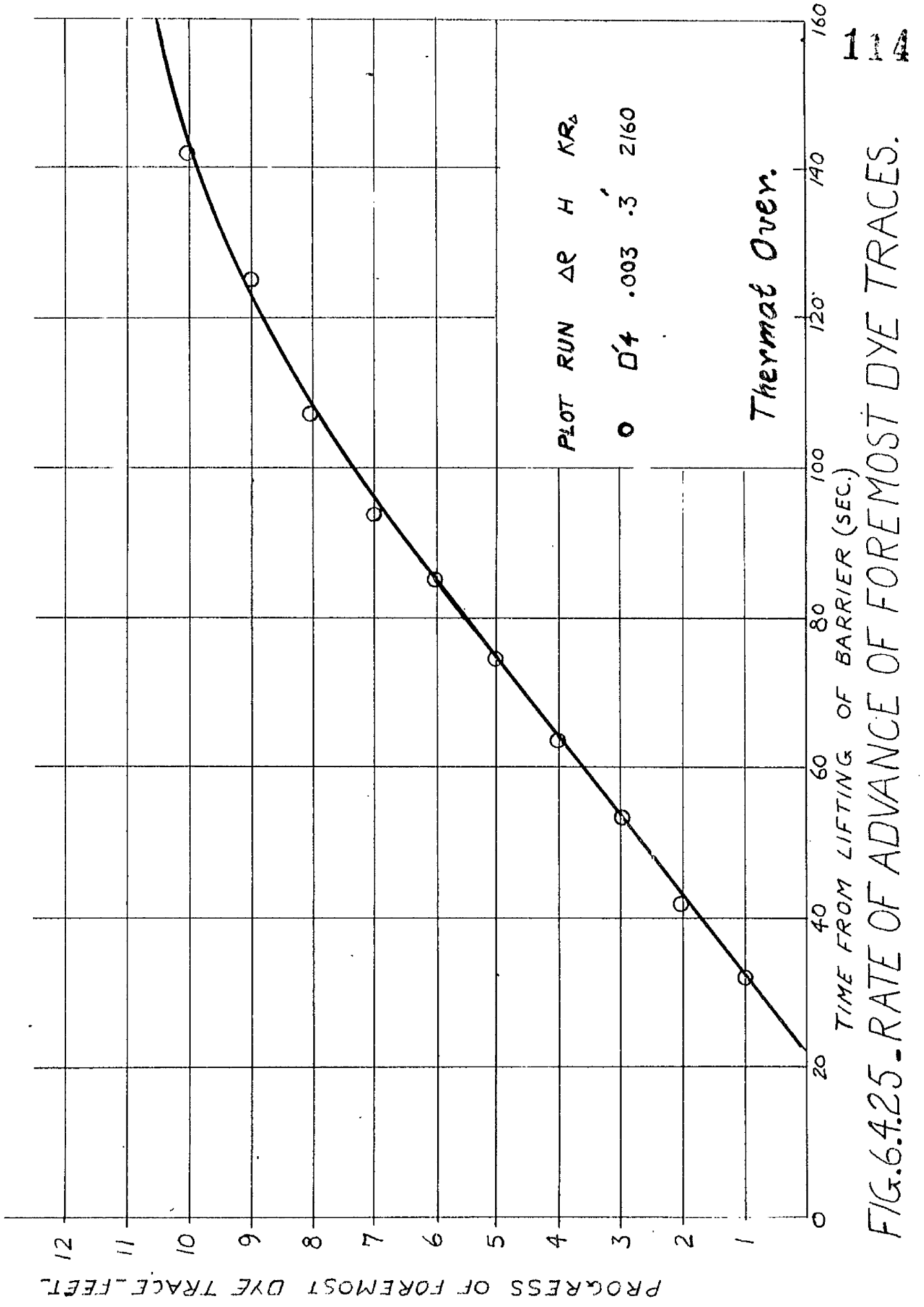
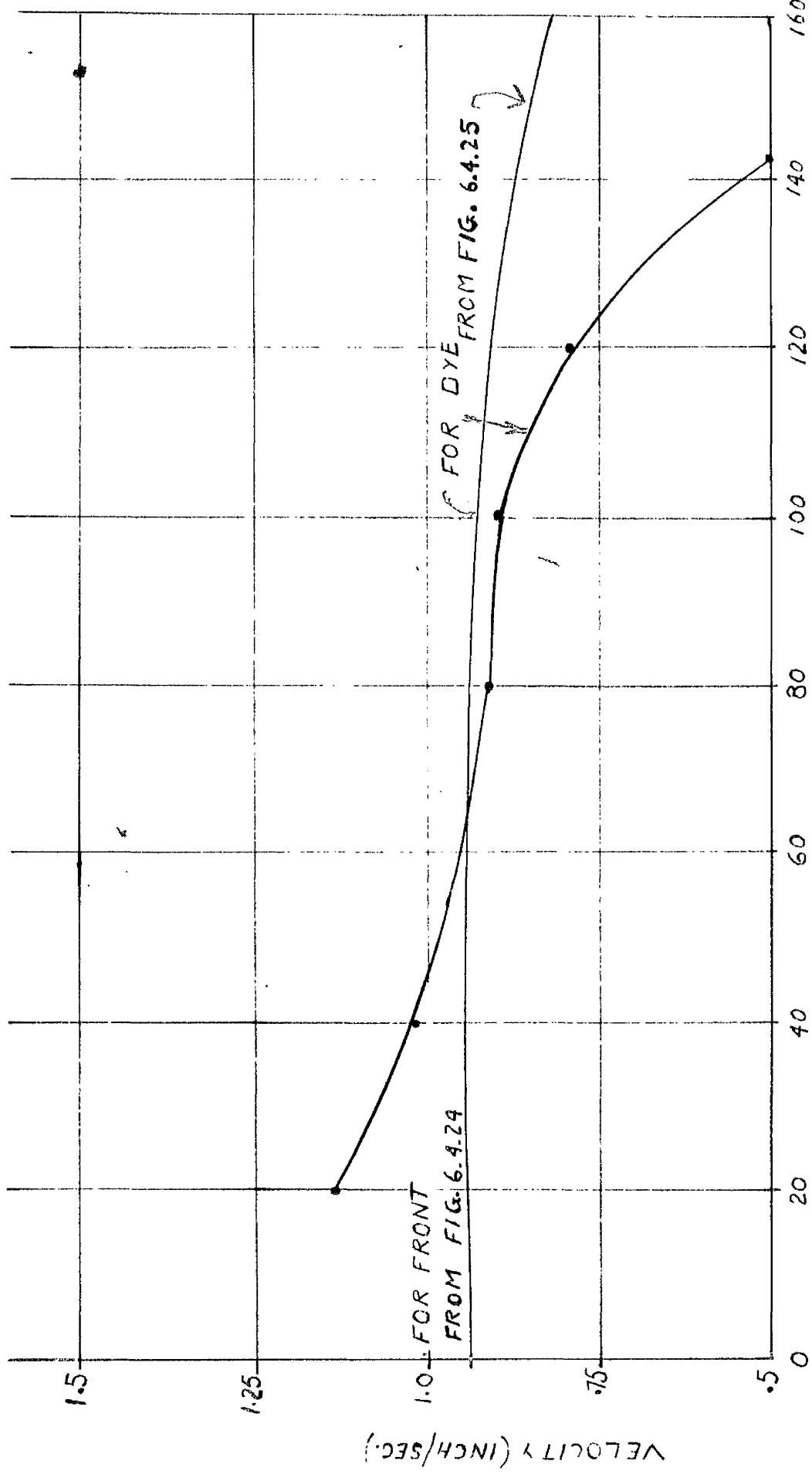


FIG.6.4.25. RATE OF ADVANCE OF FOREMOST DYE TRACES.



VELOCITY (INCH/SEC.)

FIG. 6.4.26. COMPARISONS BETWEEN VARIATIONS OF VELOCITY OF FRONT & FOREMOST DYE TRACES.

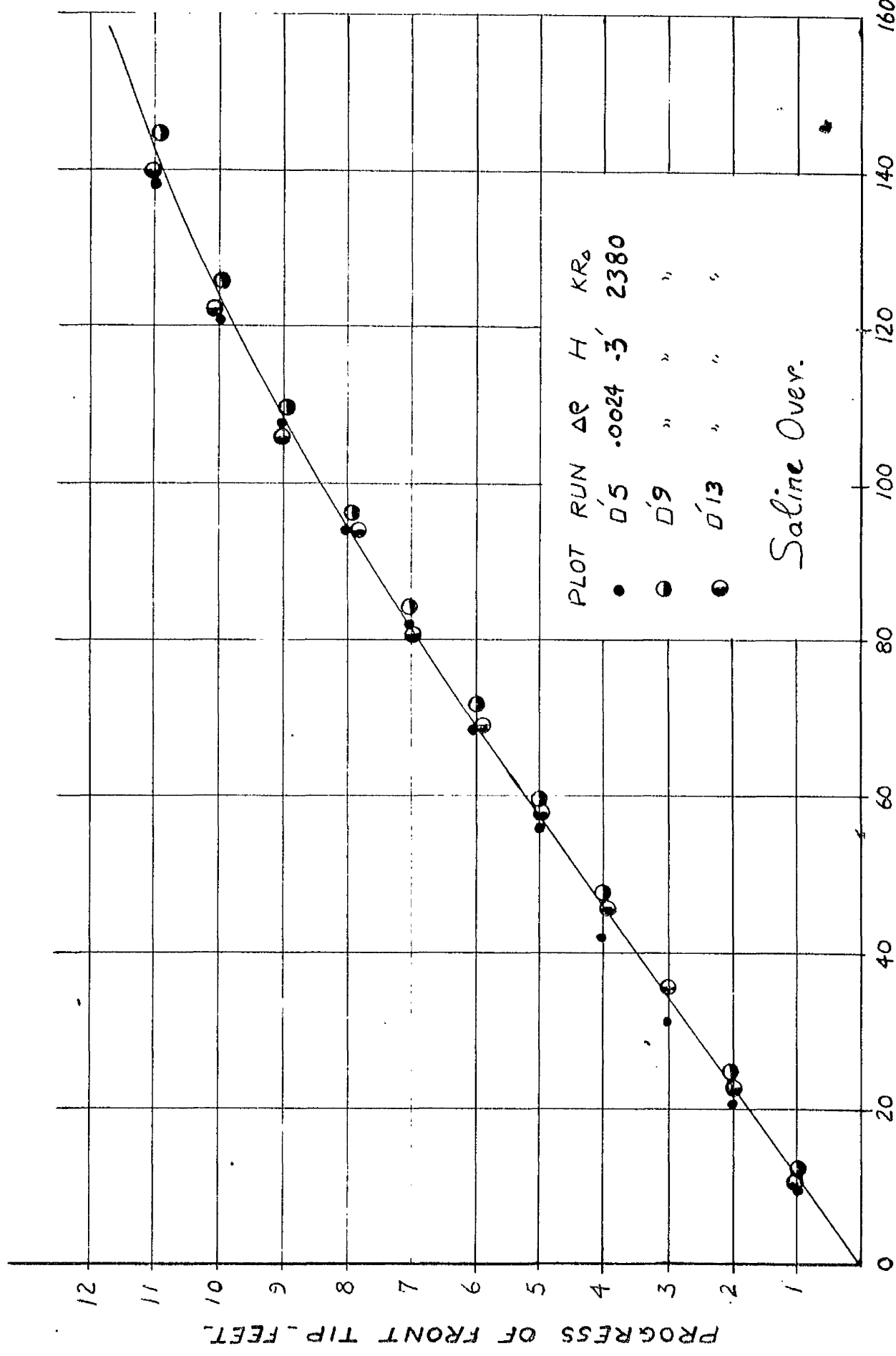


FIG 6.4.27 RATE OF ADVANCE OF FRONT.

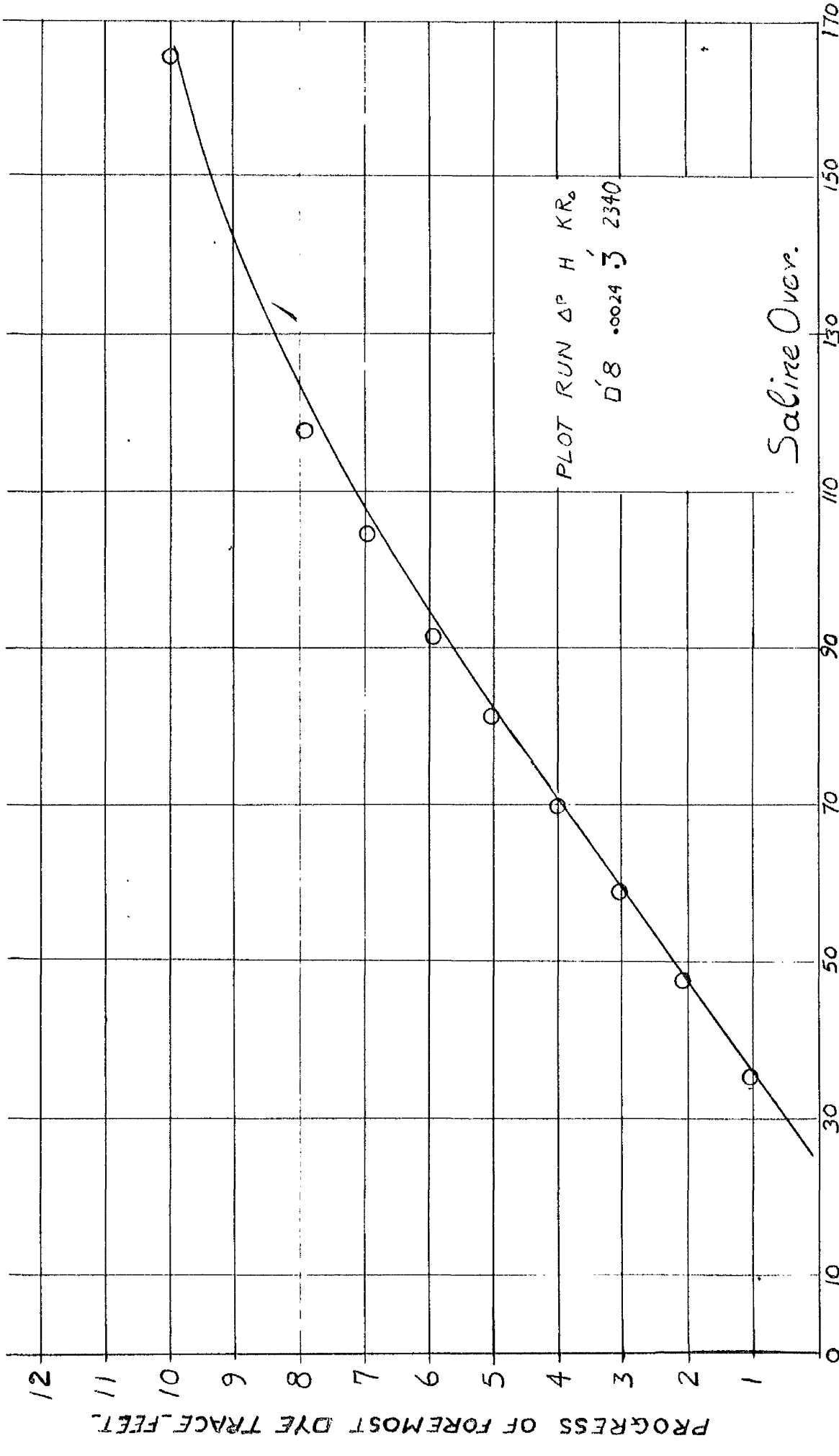


FIG. 6.4.28 - RATE OF ADVANCE OF FOREMOST DYE TRACES.

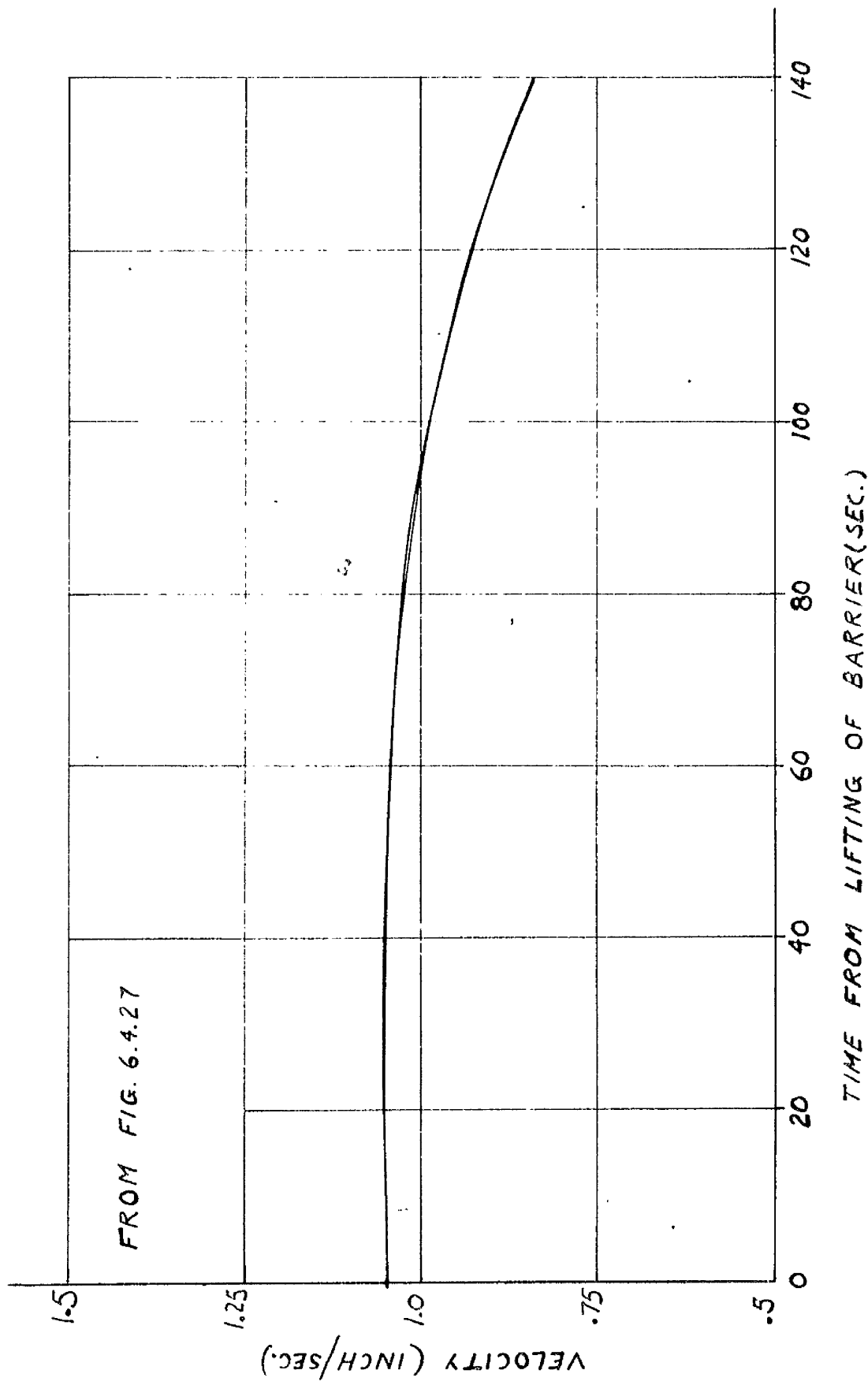


FIG. 6.4.29 - VARIATIONS OF OVERFLOW FRONT VELOCITY.

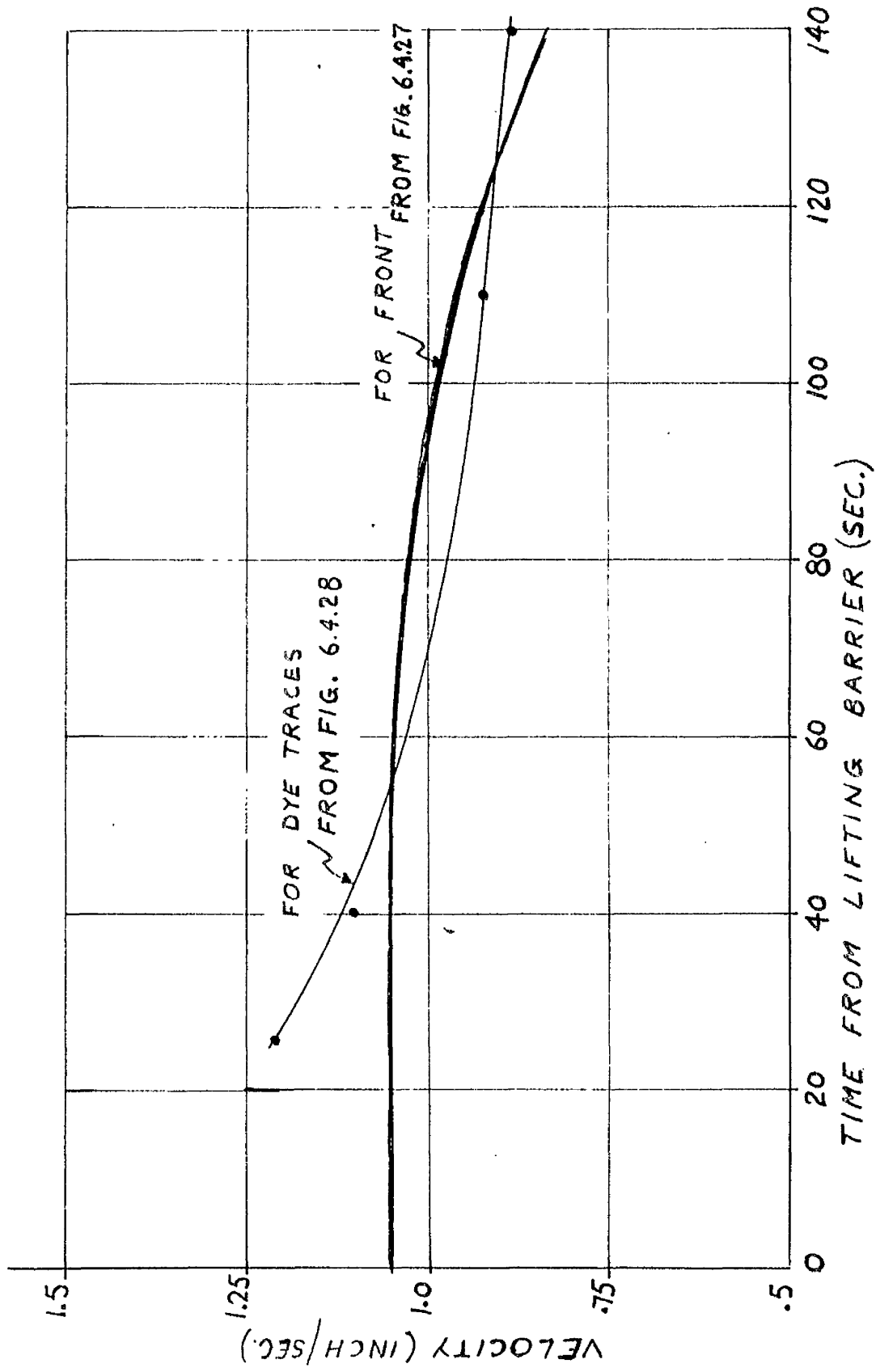


FIG. 6.4.30 COMPARISONS BETWEEN VARIATIONS OF VELOCITY OF FRONT & FOREMOST DYE TRACES.

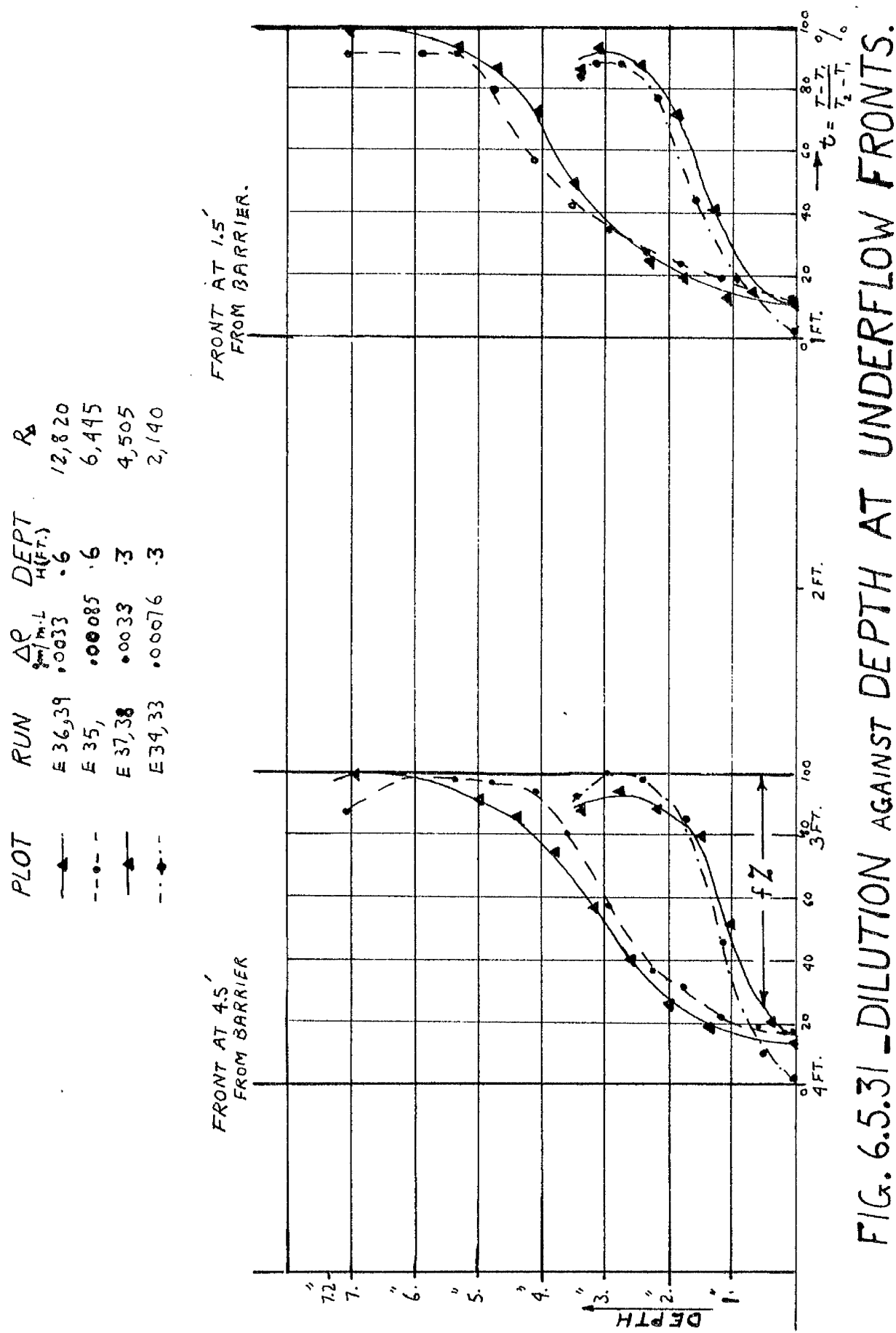


FIG. 6.5.31 - DILUTION AGAINST DEPTH AT UNDERFLOW FRONTS.

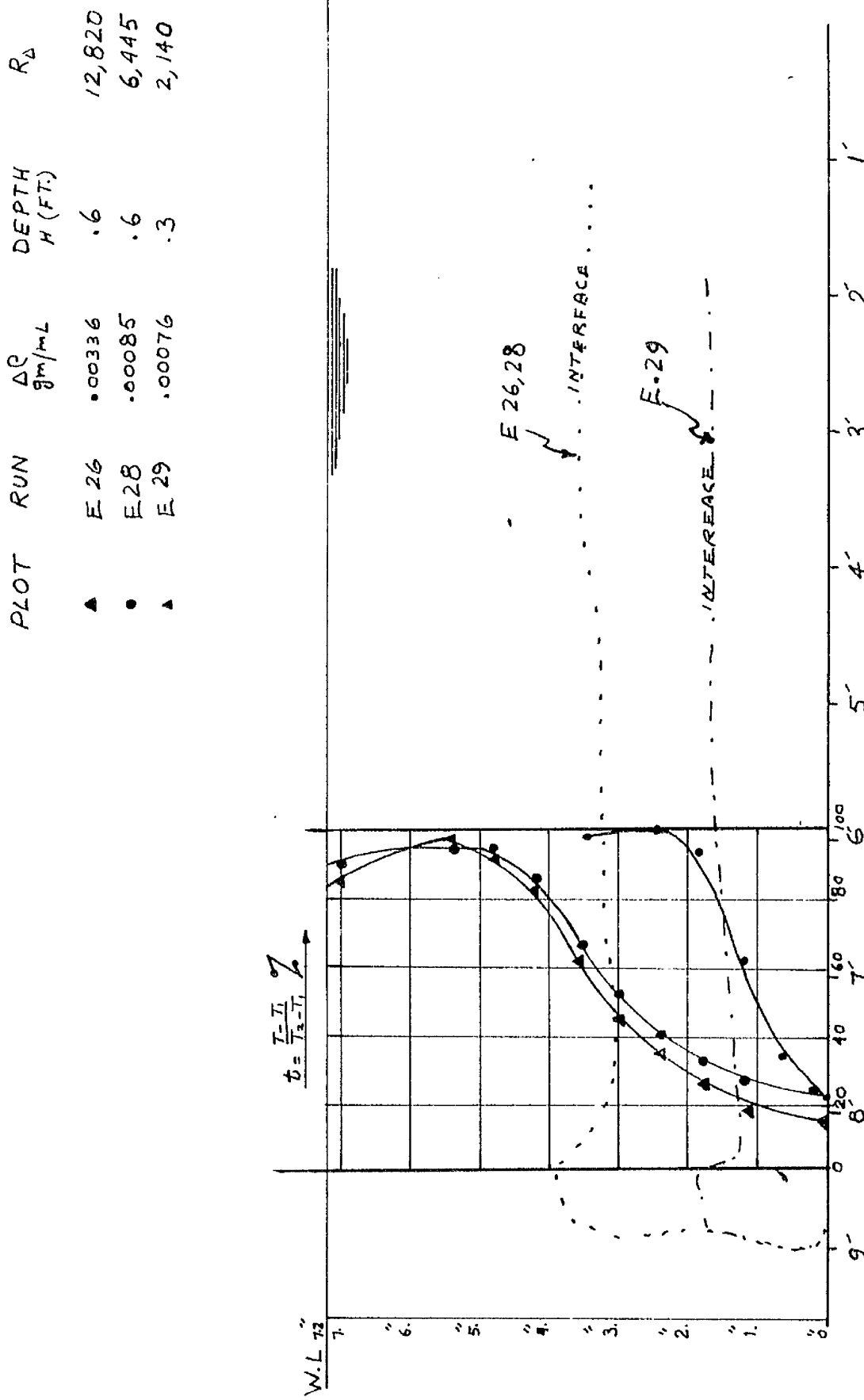


FIG. 6.5.32 - DILUTION AGAINST DEPTH AT UNDERFLOW FRONT

PLOT	RUN	$\frac{\Delta \rho}{\rho_m/\rho_L}$	DEPTH $H(F_R)$	$R_d$
○	E31	.01179	.6'	24,080
●	E30	.01189	"	"

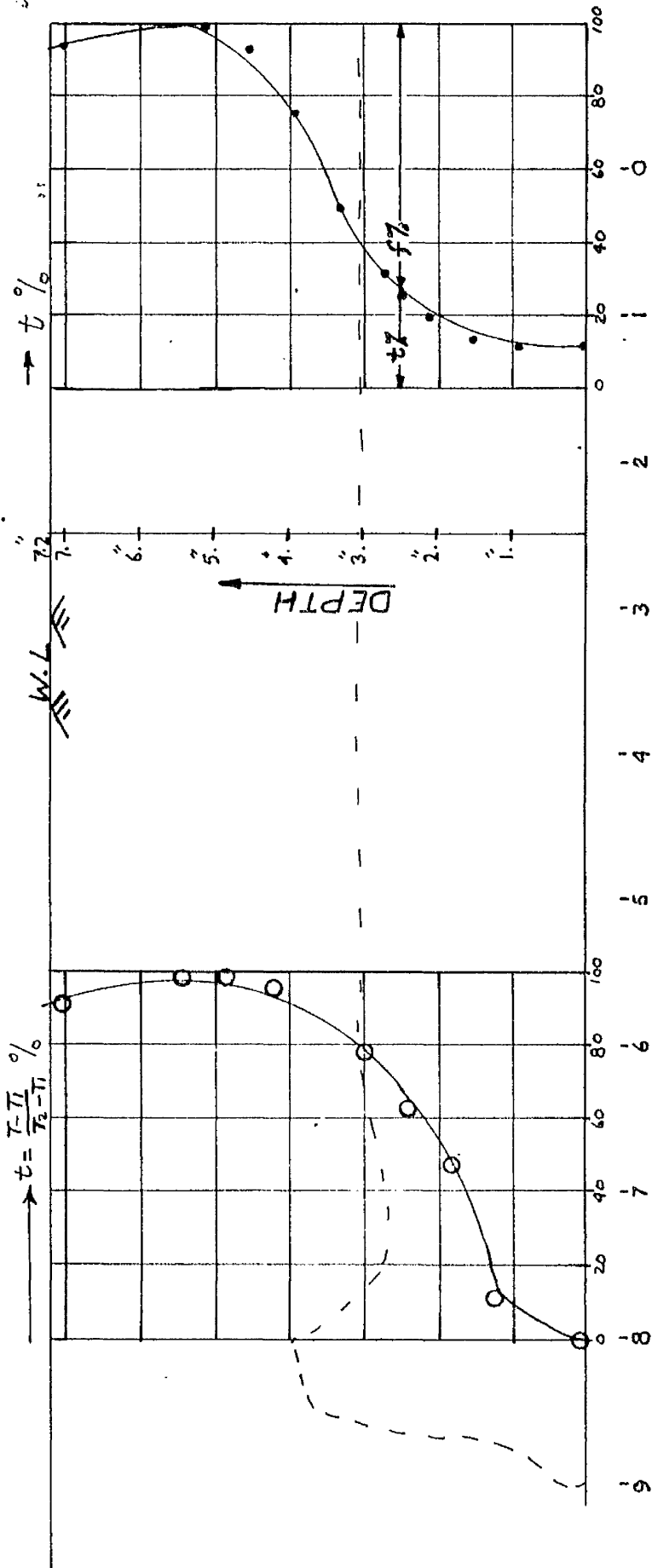


FIG. 6.5.33. DILUTION AGAINST DEPTH AT UNDERFLOW FRONT & AT AN EXTENDED PART OF IT.

$$\Delta \rho = .00085 \text{ gm/m.L}$$

$$H = .6 \text{ ft.}$$

$$R_d = 6445$$

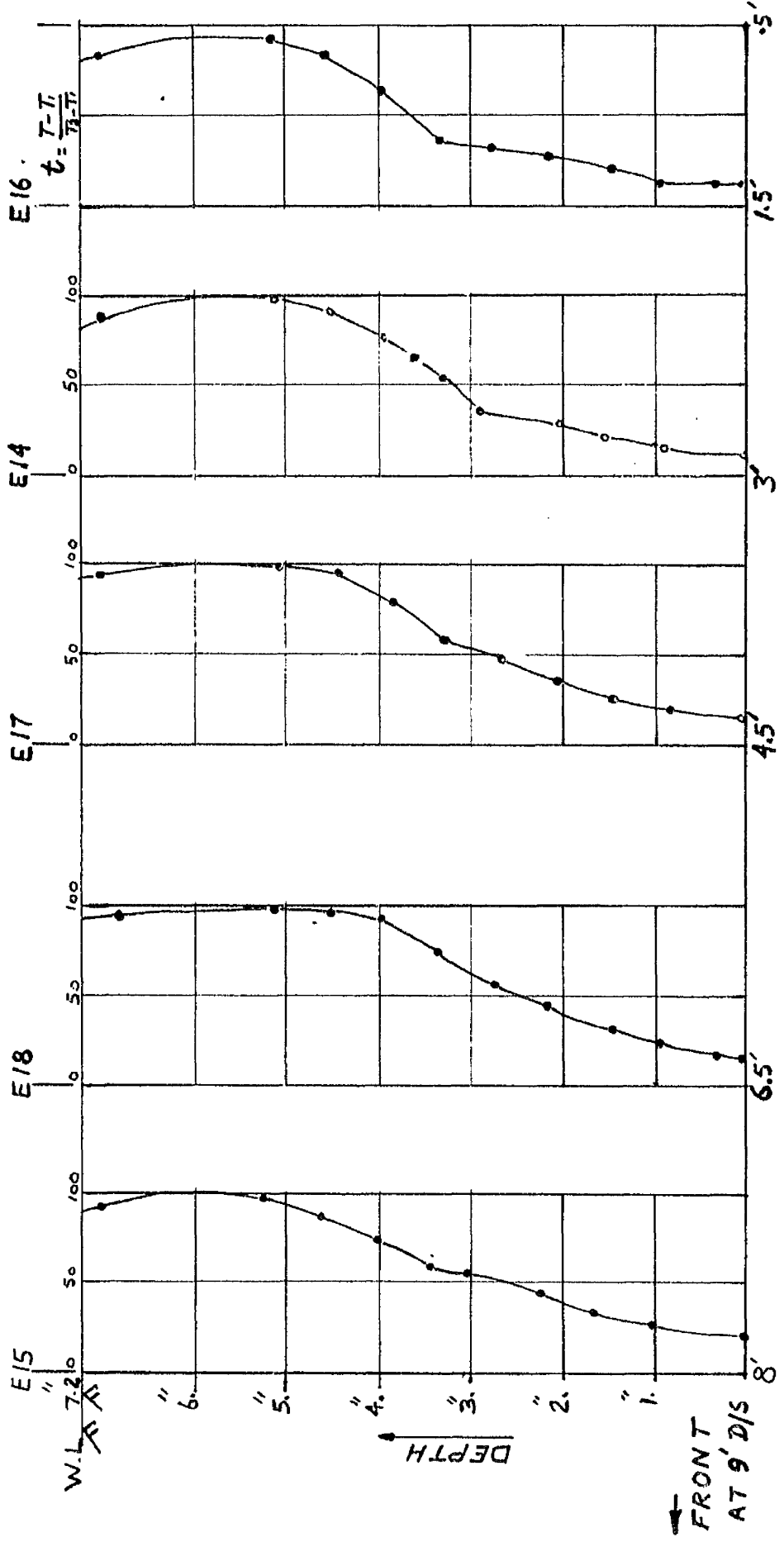


FIG. 6.5.34 - DILUTION AGAINST DEPTH FOR SAMPLES ALONG AN EXTENDED UNDERFLOW.

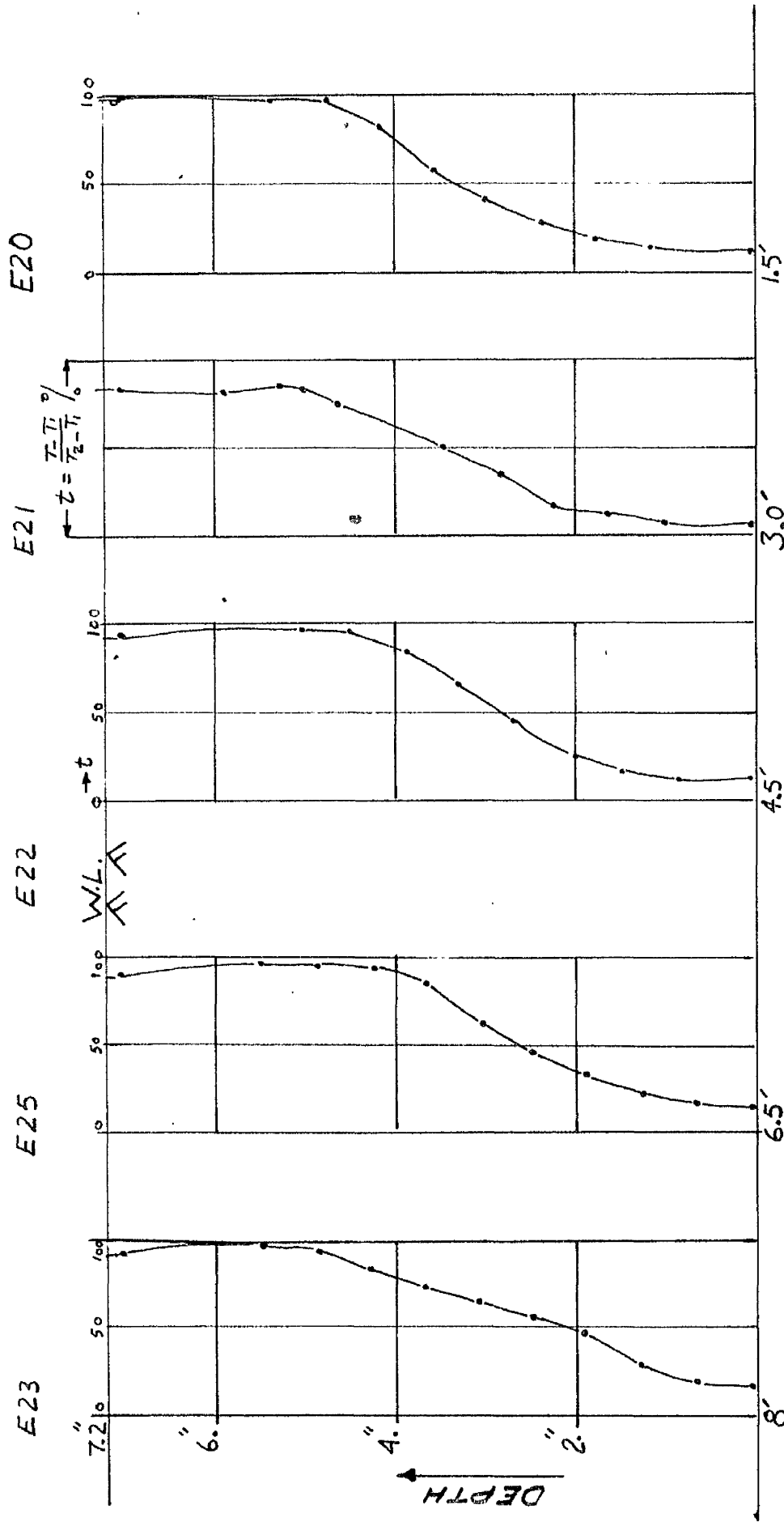


FIG. 6.5.35 - DILUTION AGAINST DEPTH FOR SAMPLES ALONG  
AN EXTENDED OVERFLOW.

$$\begin{aligned}\Delta C &= .00076 \text{ gm/mL} \\ H &= .3 \text{ ft.} \\ R_a &= 2140\end{aligned}$$

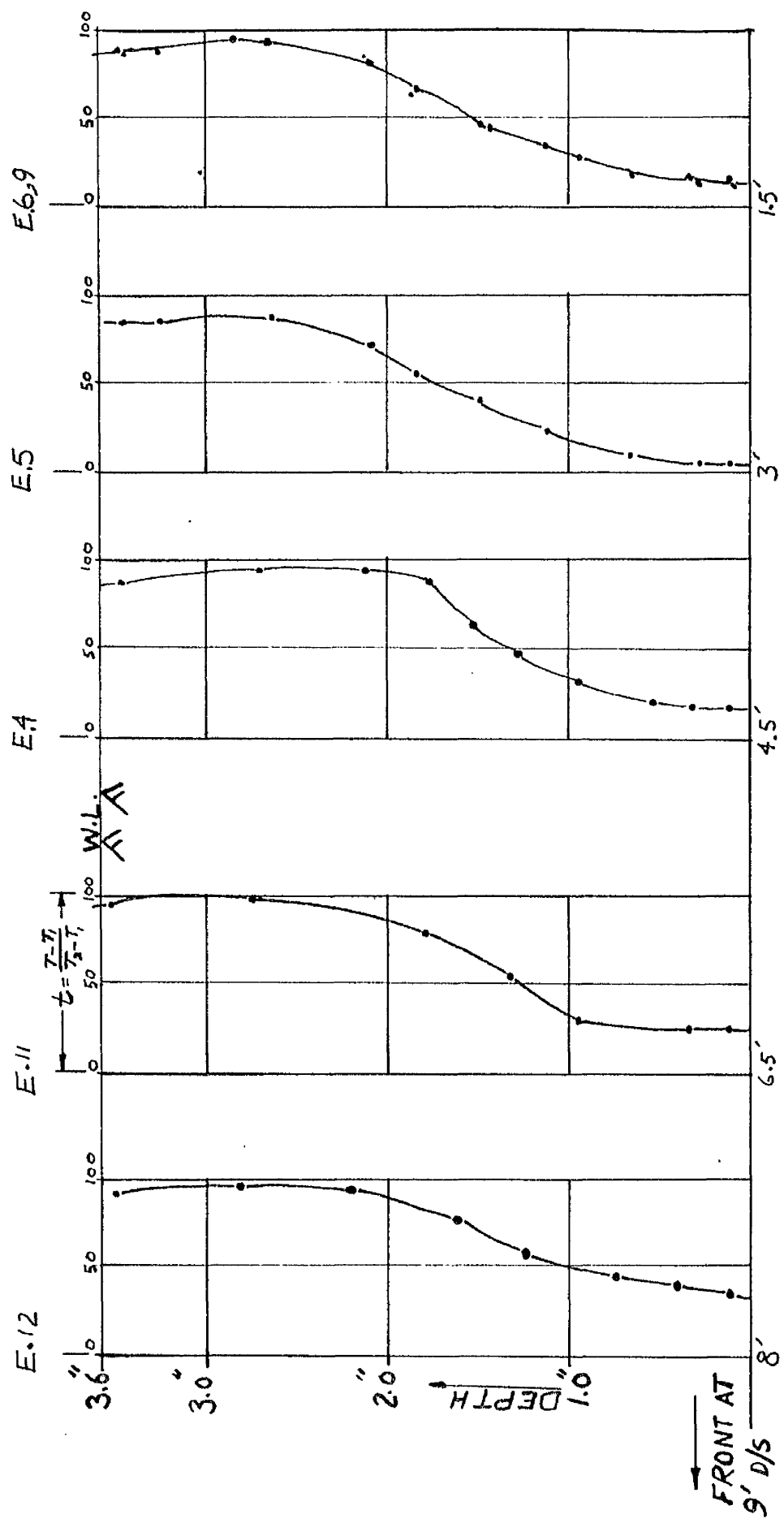
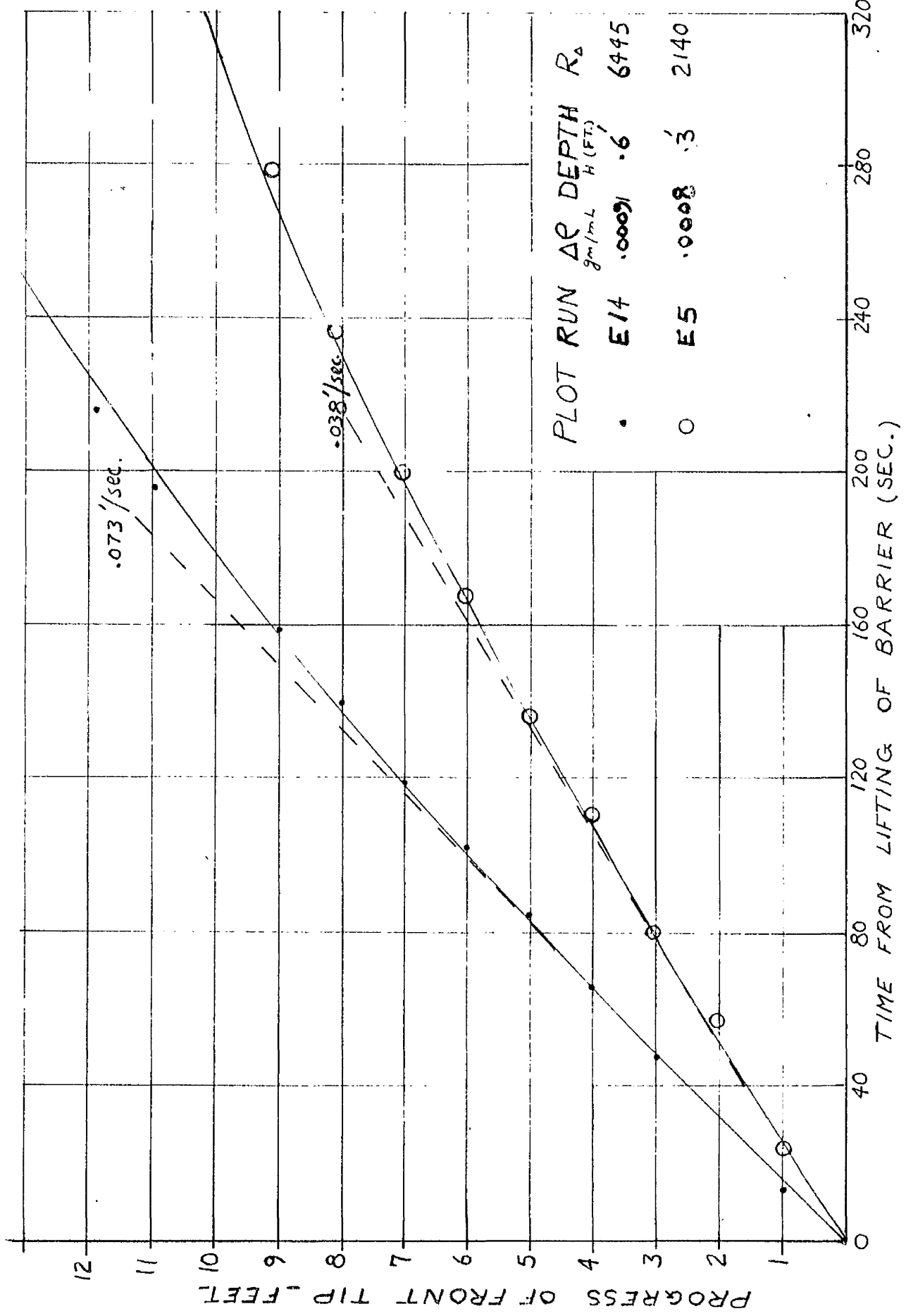


FIG. 6.5.36 - DILUTION AGAINST DEPTH FOR SAMPLES ALONG AN EXTENDED UNDERFLOW.

FIG. 6.5.37 - RATE OF ADVANCE OF FRONT.



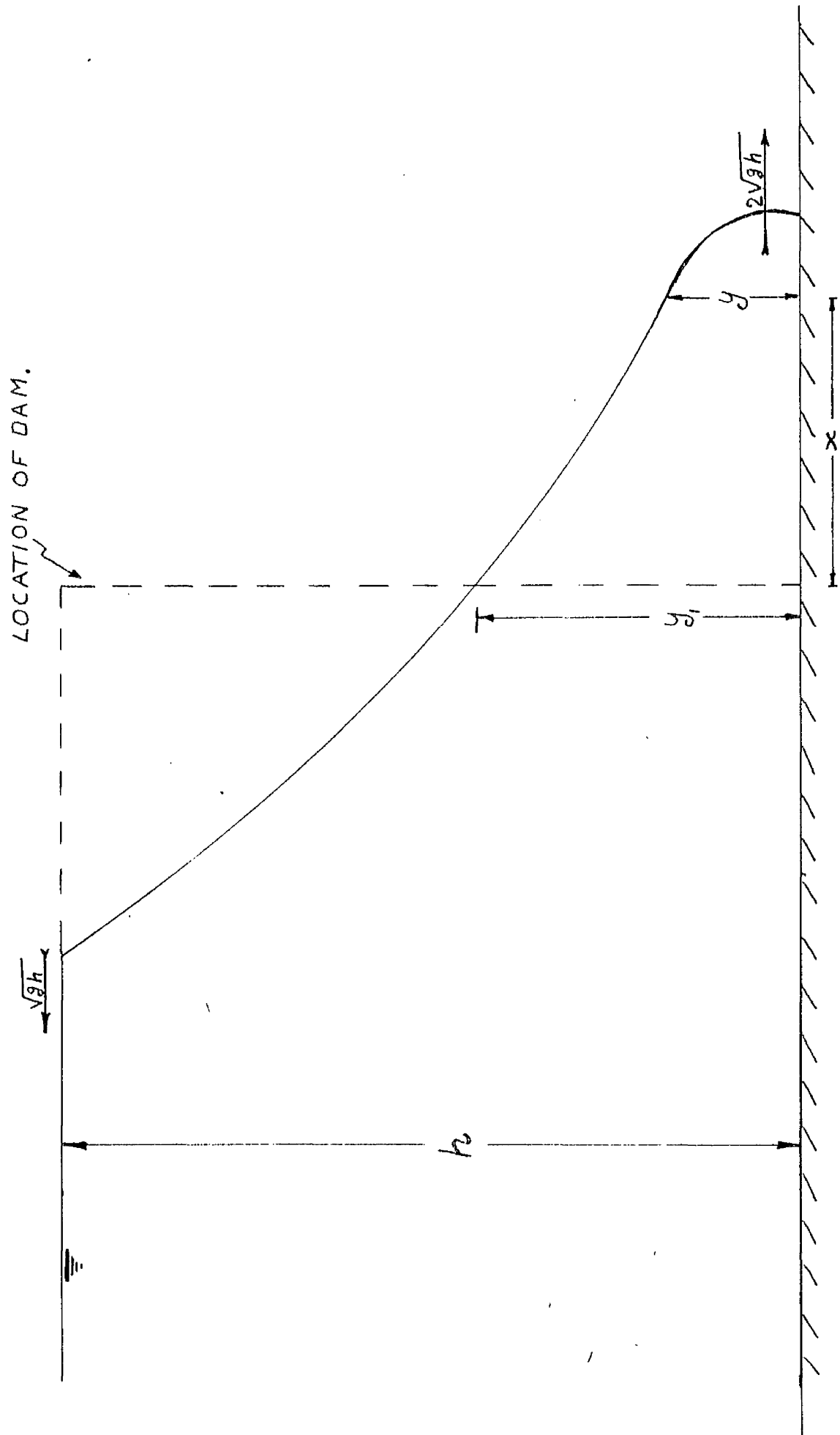


FIG. 7.1.1. THE ST. VENANT WAVE PROFILE RESULTING FROM SUDDEN DESTRUCTION OF A DAM.

FIG. 7.1.2 -- The outset of an ideal dam-burst.

FIG. 7.1.3 -- Developed stage of an ideal dam-burst.

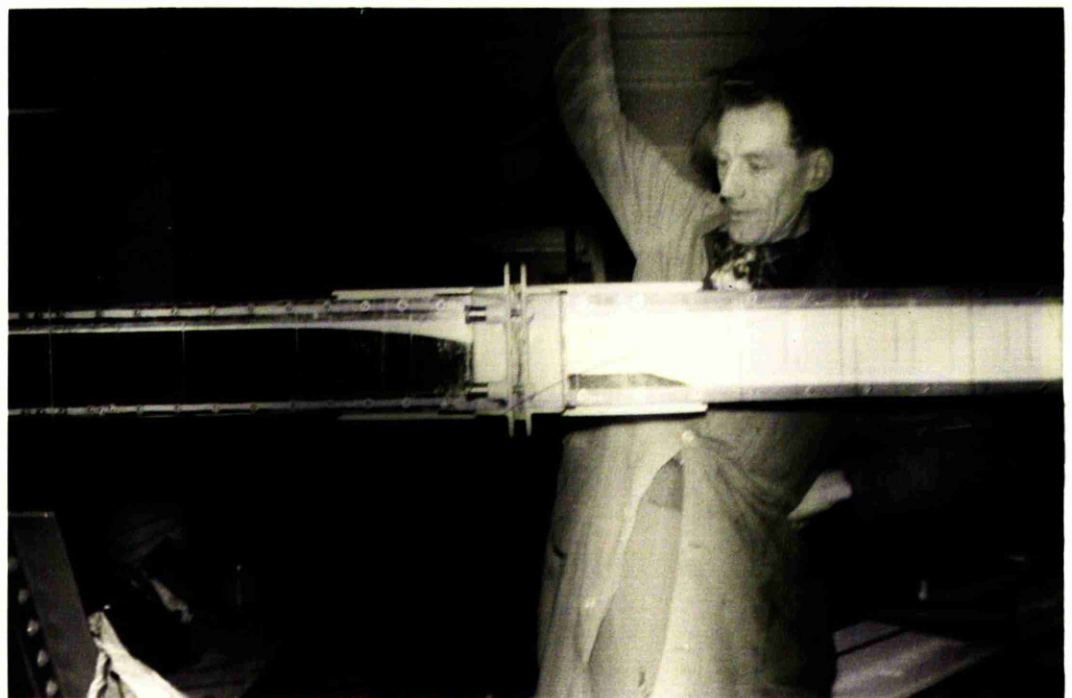
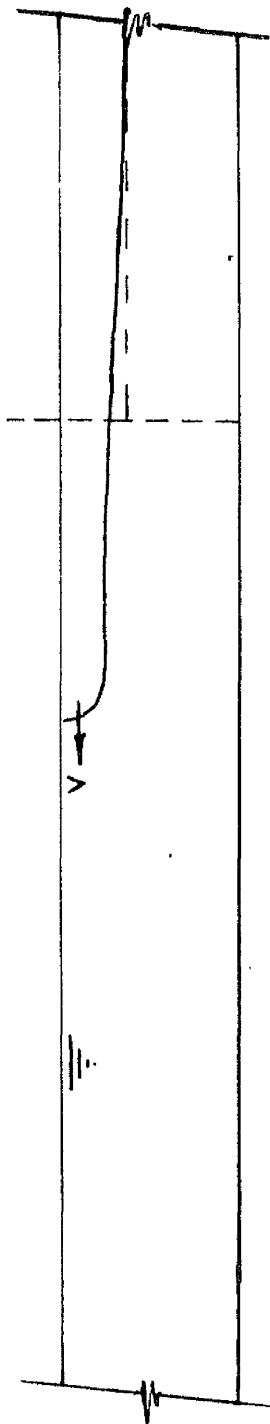


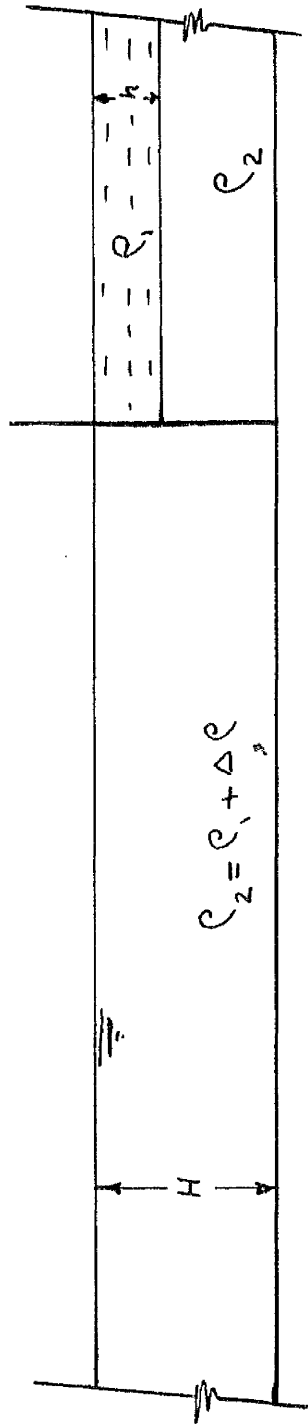
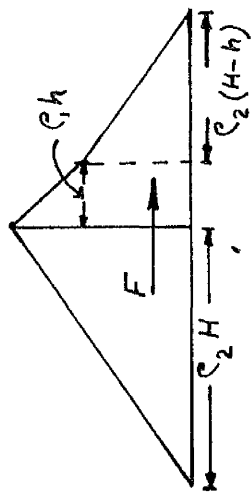
FIG. 7.2.4 - DAM-BURST ANALOGY\_OVERFLOW.

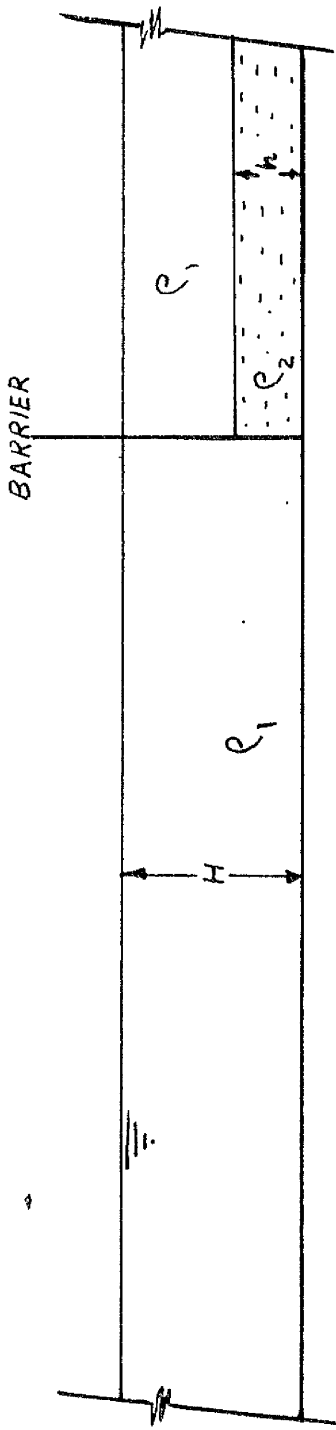
II. DEVELOPED UNDERFLOW.



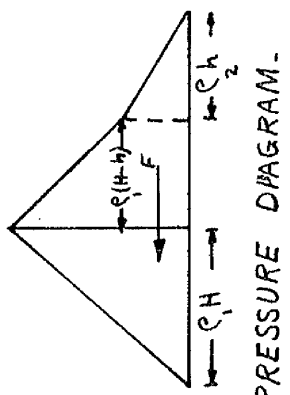
PRESSURE DIAGRAM.

I-STARTING CONDITIONS.

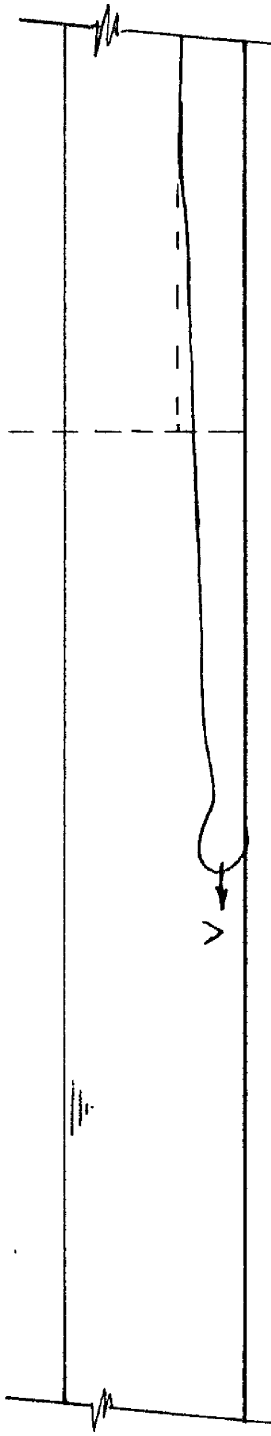




I. STARTING CONDITIONS.



PRESSURE DIAGRAM.

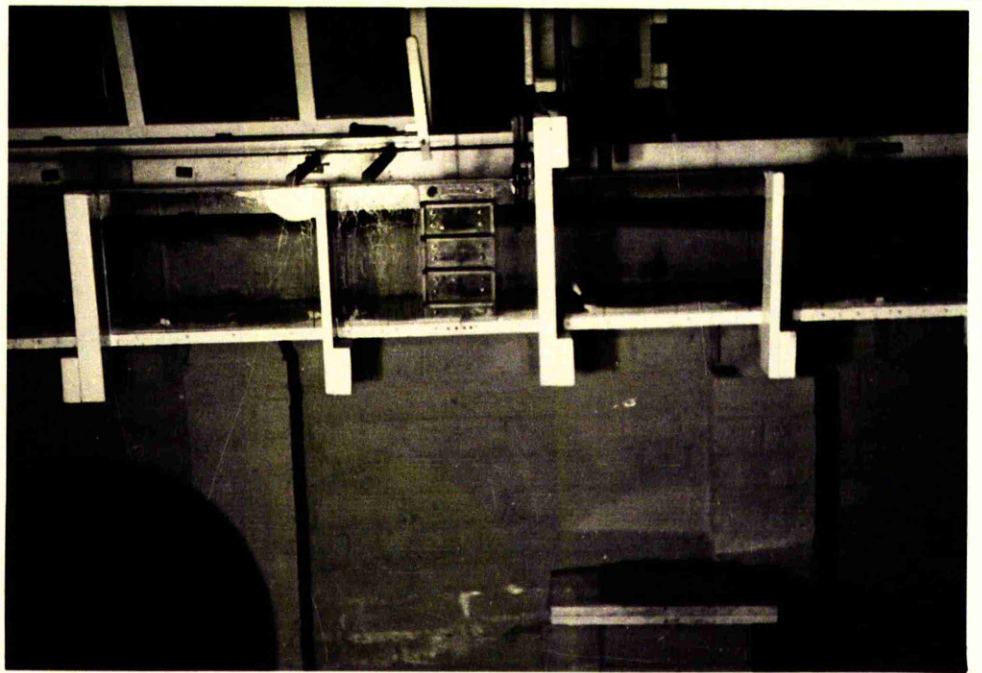
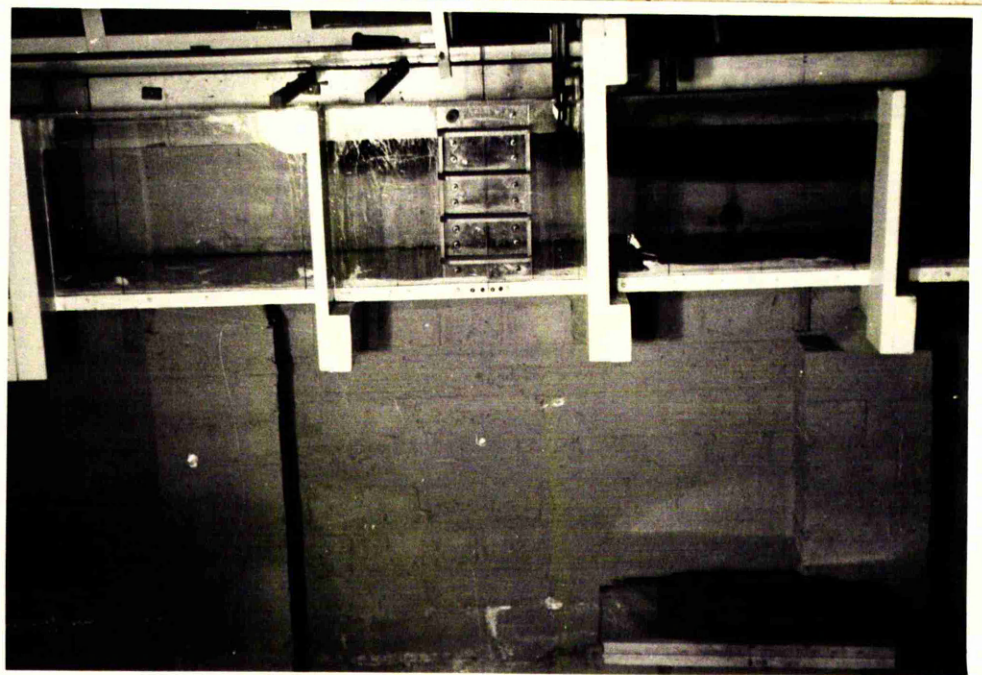


II. DEVELOPED UNDERFLOW.

FIG. 7.2.5 DAM-BURST ANALOGY - UNDERFLOW.

FIG. 7.2.6 - Dam-burst analogy overflow  
at the outset

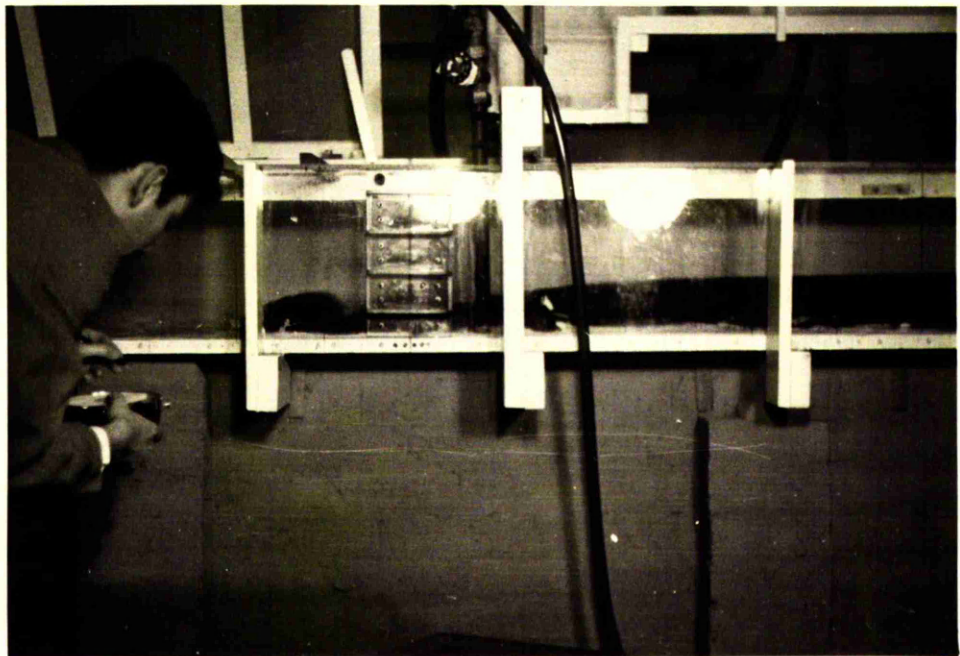
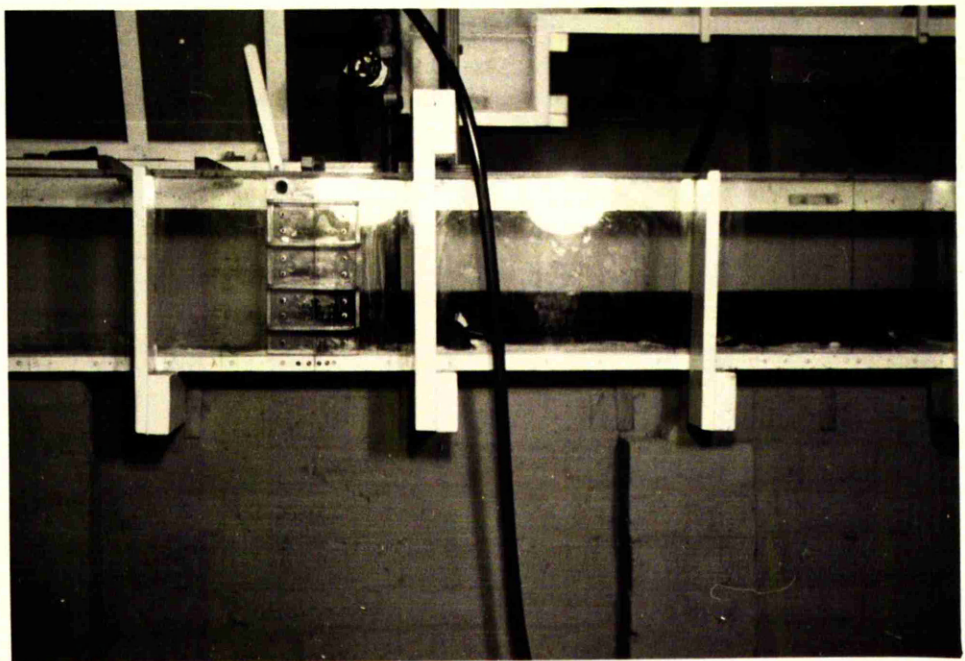
FIG. 7.2.7 - Dam-burst analogy overflow  
at a developed stage.



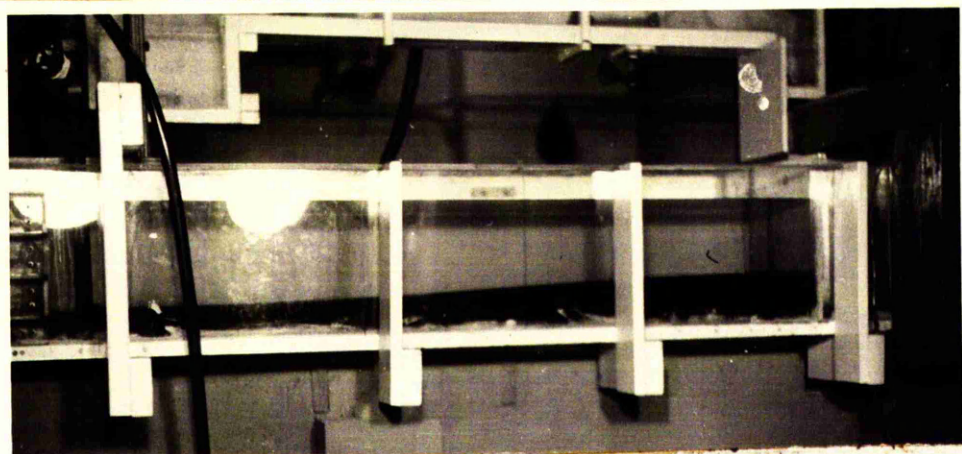
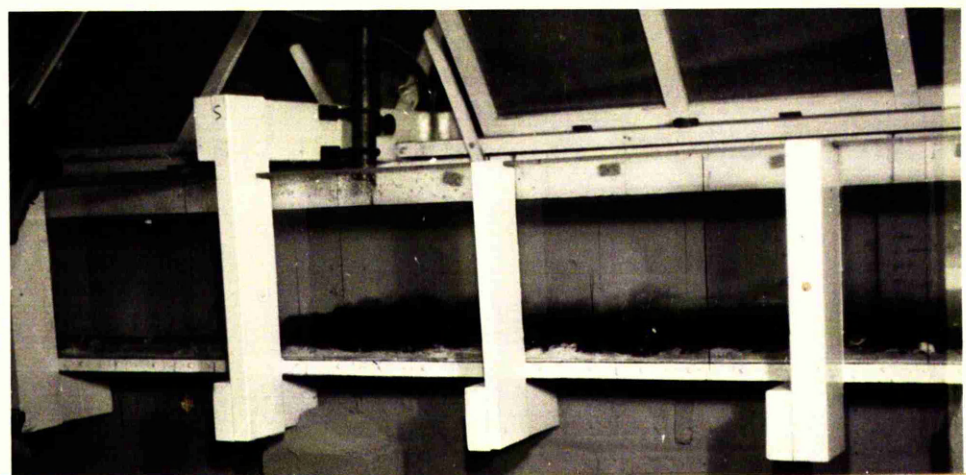
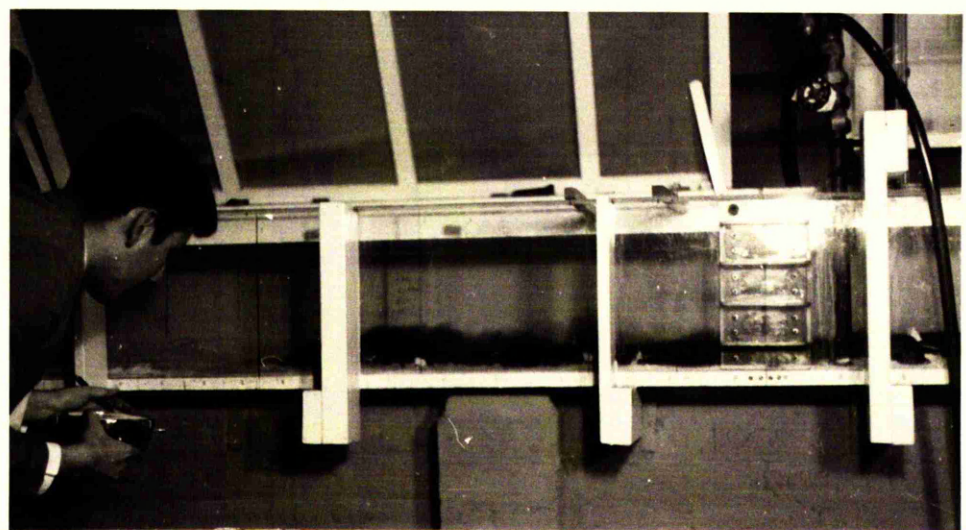
Dam-burst analogy underflow  
at various stages

a) At starting conditions

b) At initial stage



- c) At a developed stage.
- d) At a more developed stage.
- e) The form of interfacial layer at back regions being similar to that of the ideal dam-burst as given by the St.-Venant theory.



F/G.7.2.8-TYPICAL RATE OF ADVANCE OF DAM-BURST ANALOGY FRONTS.

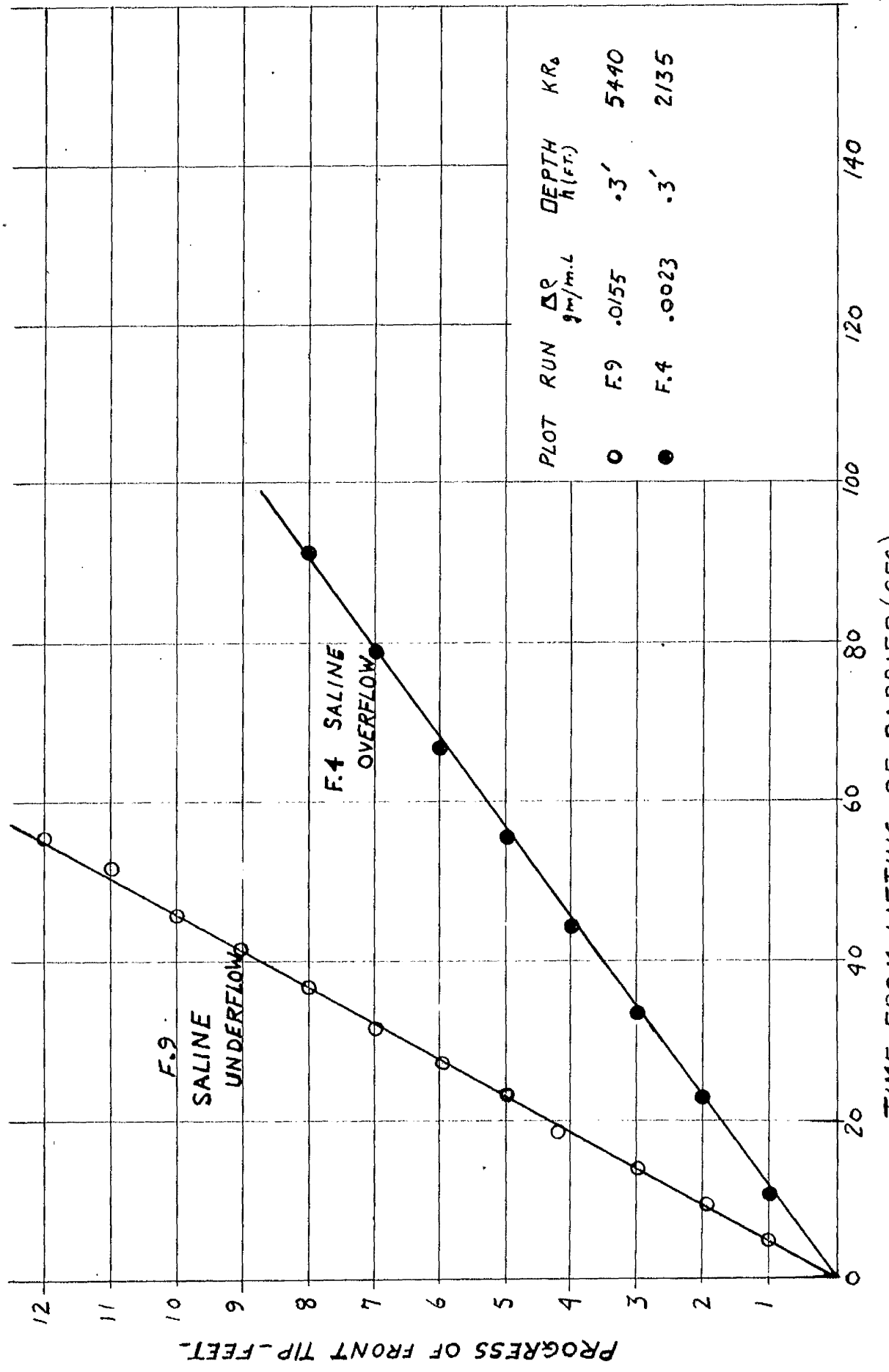
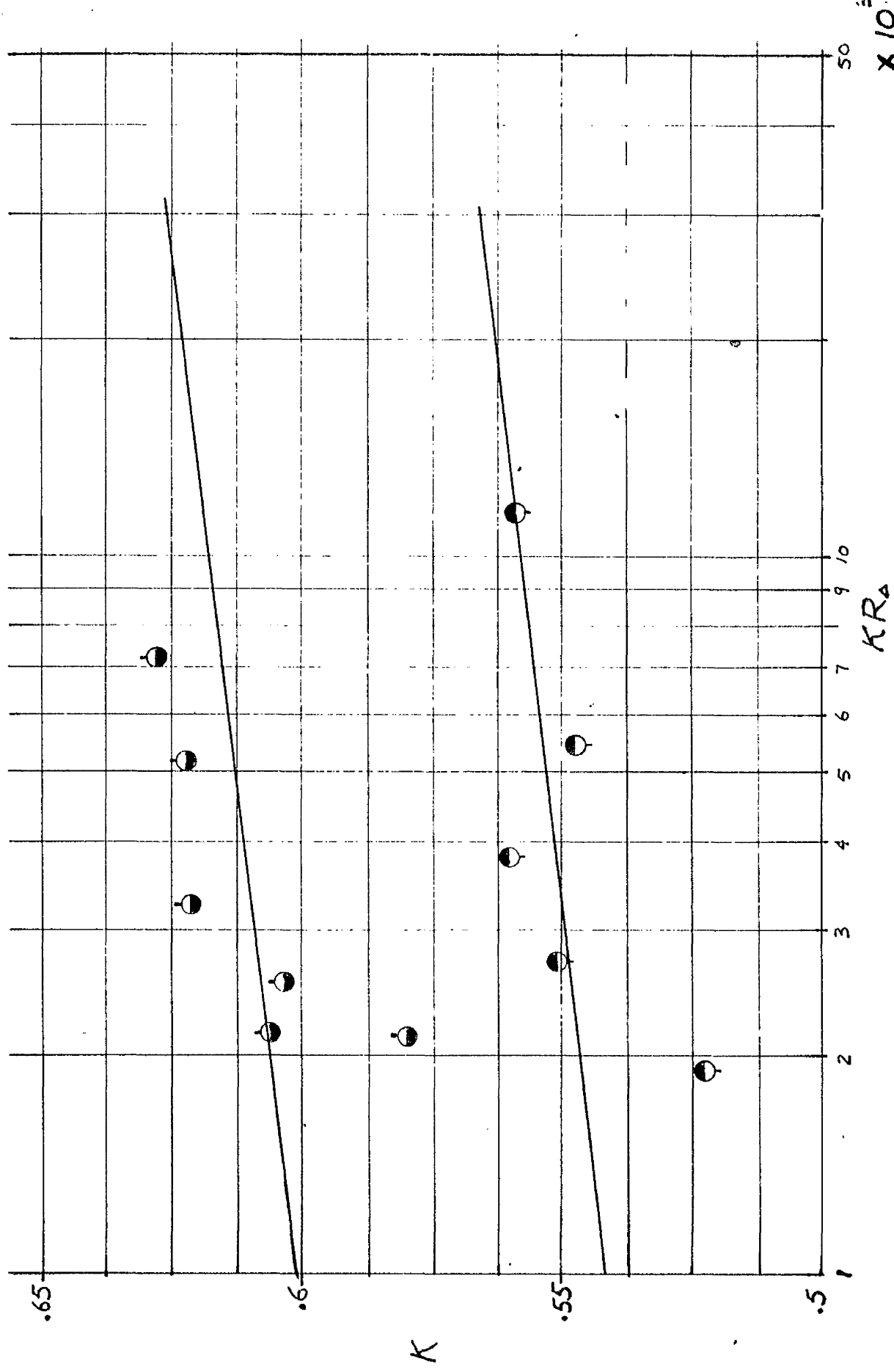


FIG. 72.9. DAM-BURST ANALOGY OVERFLOW\_UNDERFLOW COEFFICIENTS OF PROPORTIONALITY.



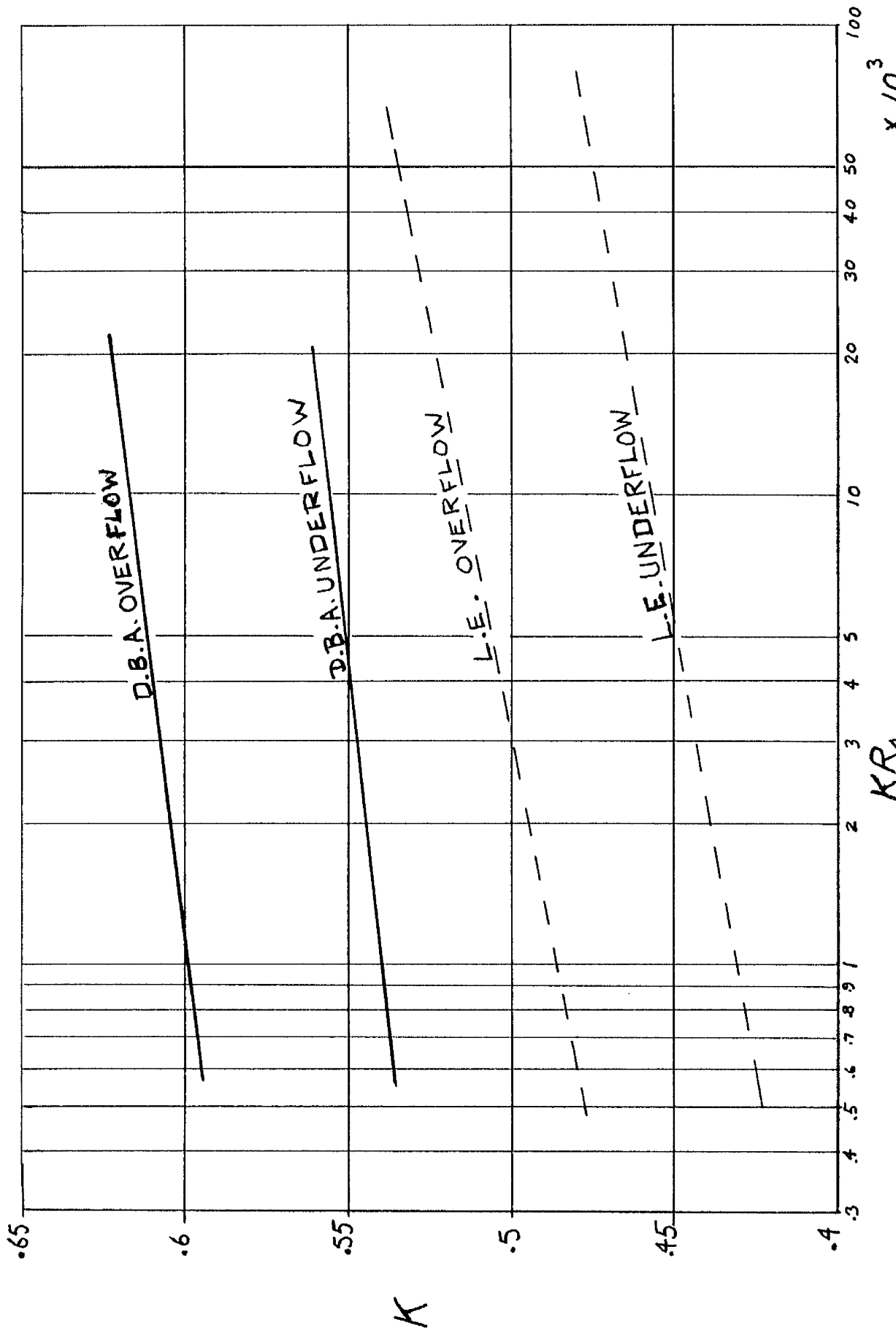
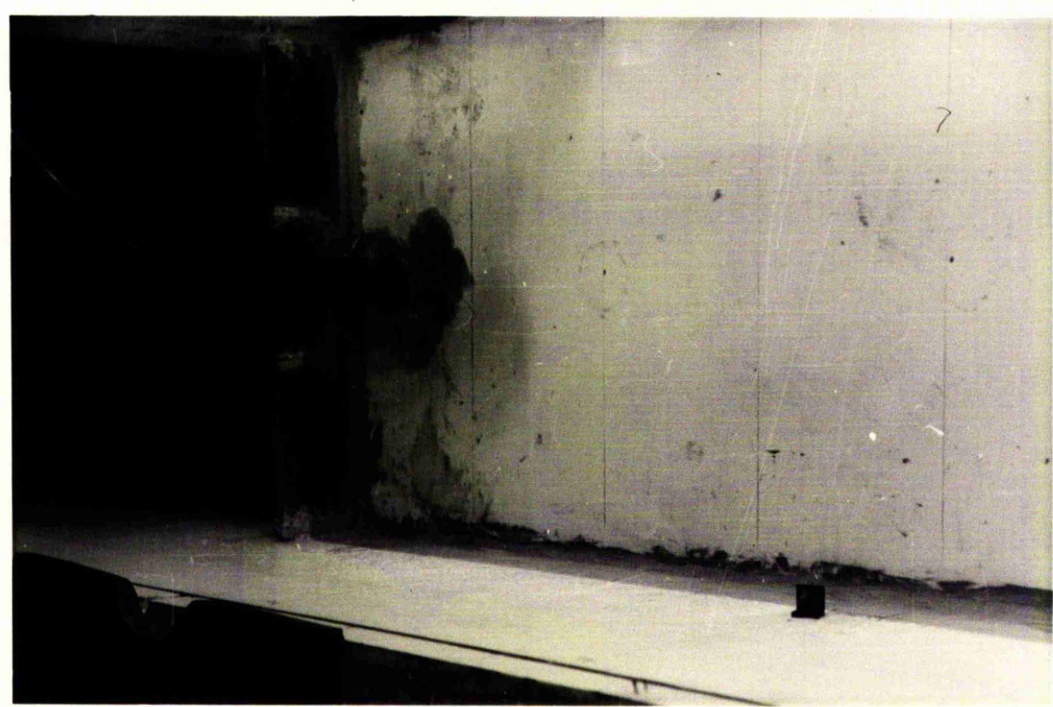
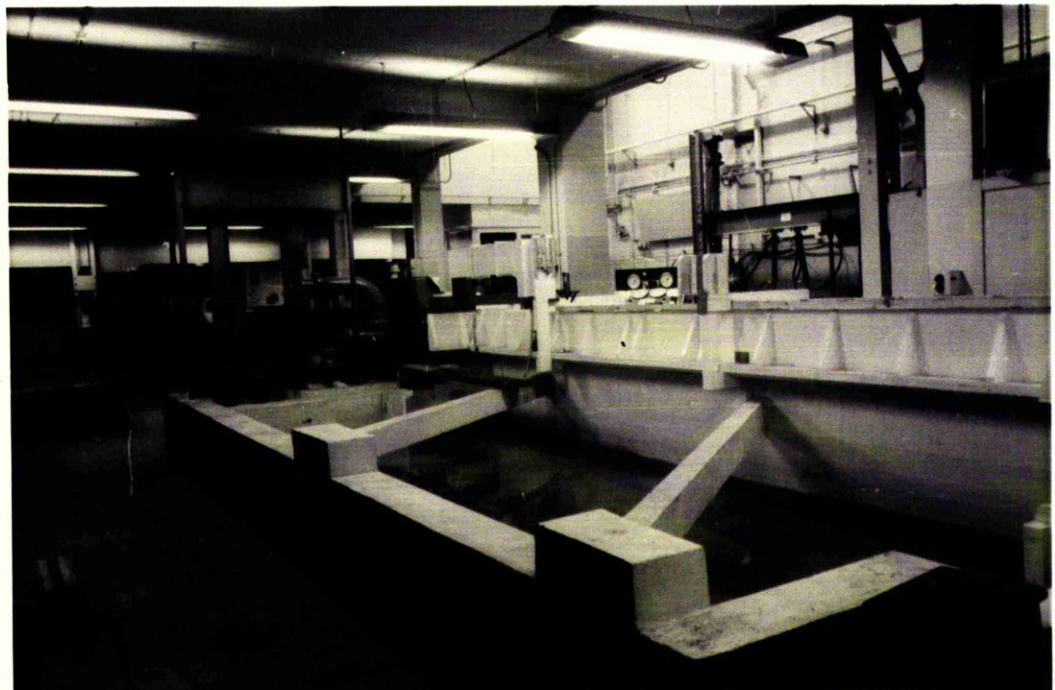


FIG. 7.2(a) COMPOSITE DIAGRAM OF COEFFICIENTS OF PROPORTIONALITY.

FIG. 8.1 - General view of  
tank and rear flume.

FIG. 8.5 - An early stage of spreading  
of outfall heated water.



↑ TO FRESH WATER TANK.

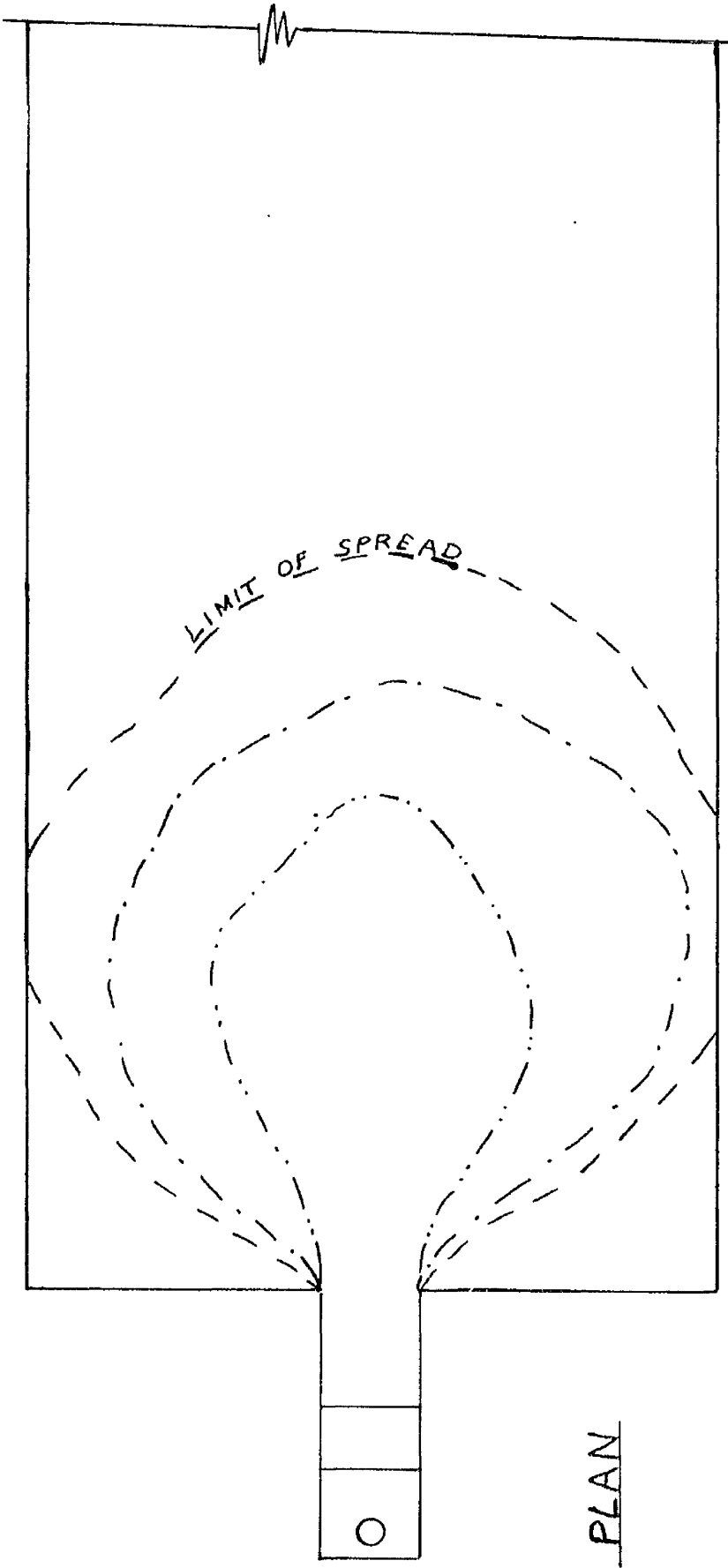
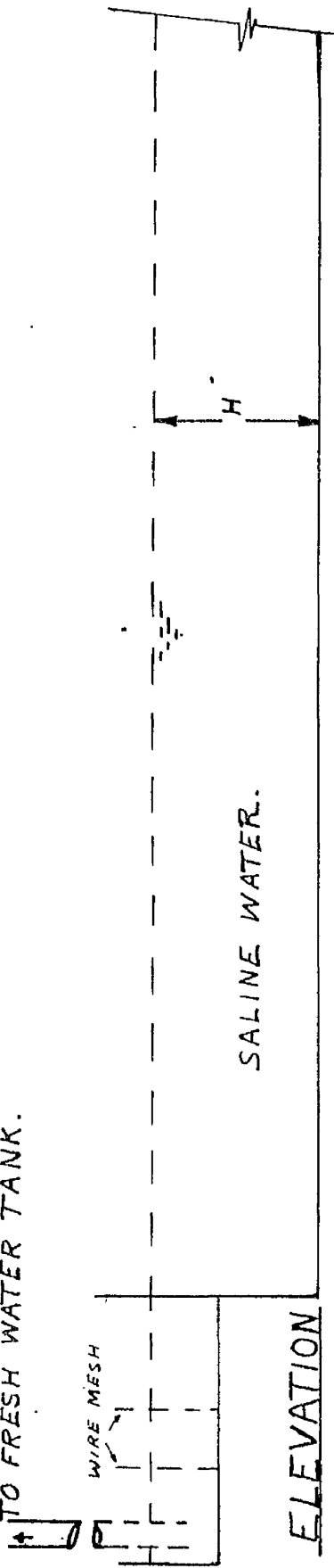


FIG. 8.1A - SIMPLIFIED OUTFALL.

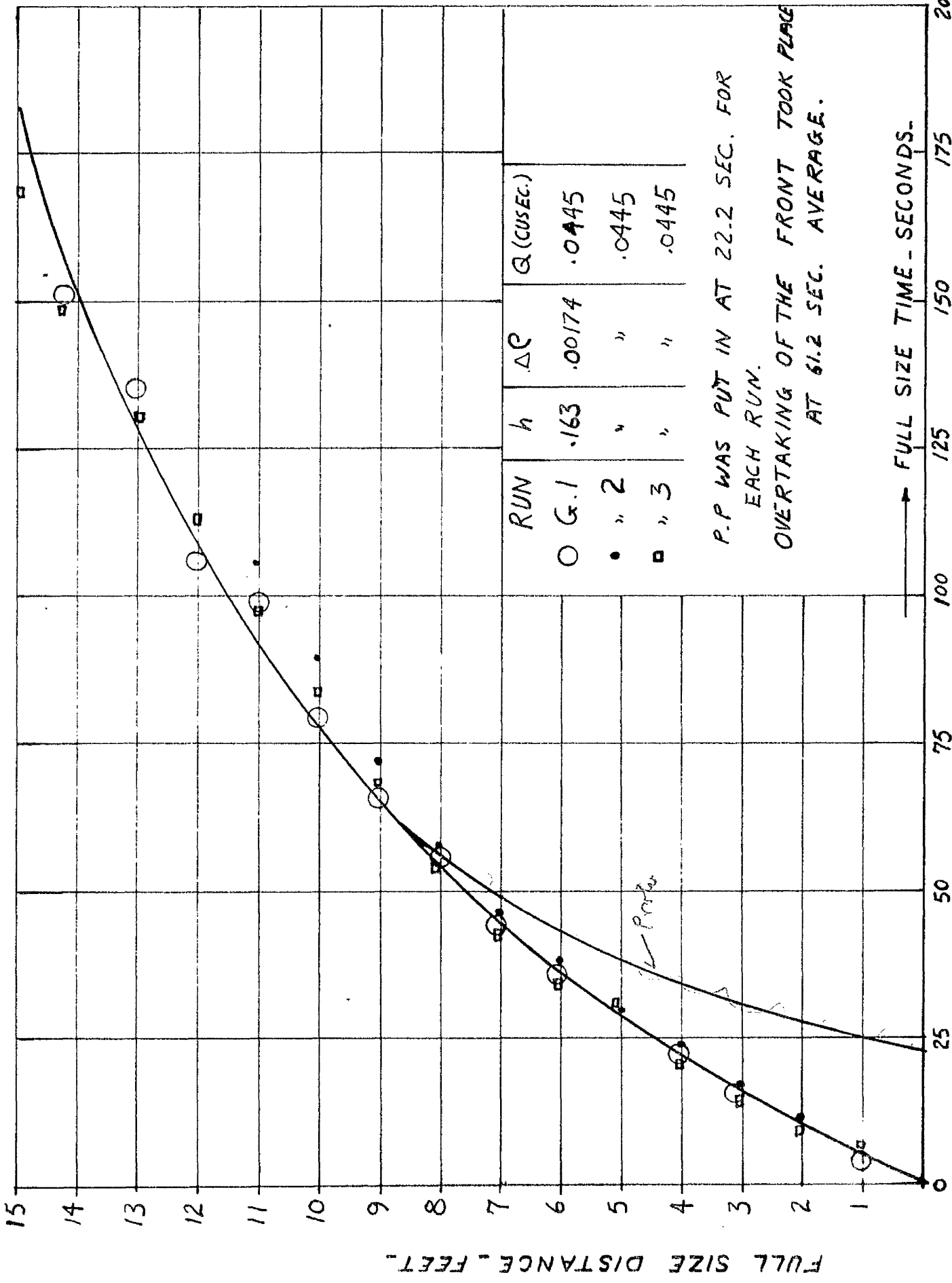


FIG. 8.2. MODEL/PROT. SIMILARITY IN BASIC OUTFALL STUDIES THROUGH VELOCITIES.

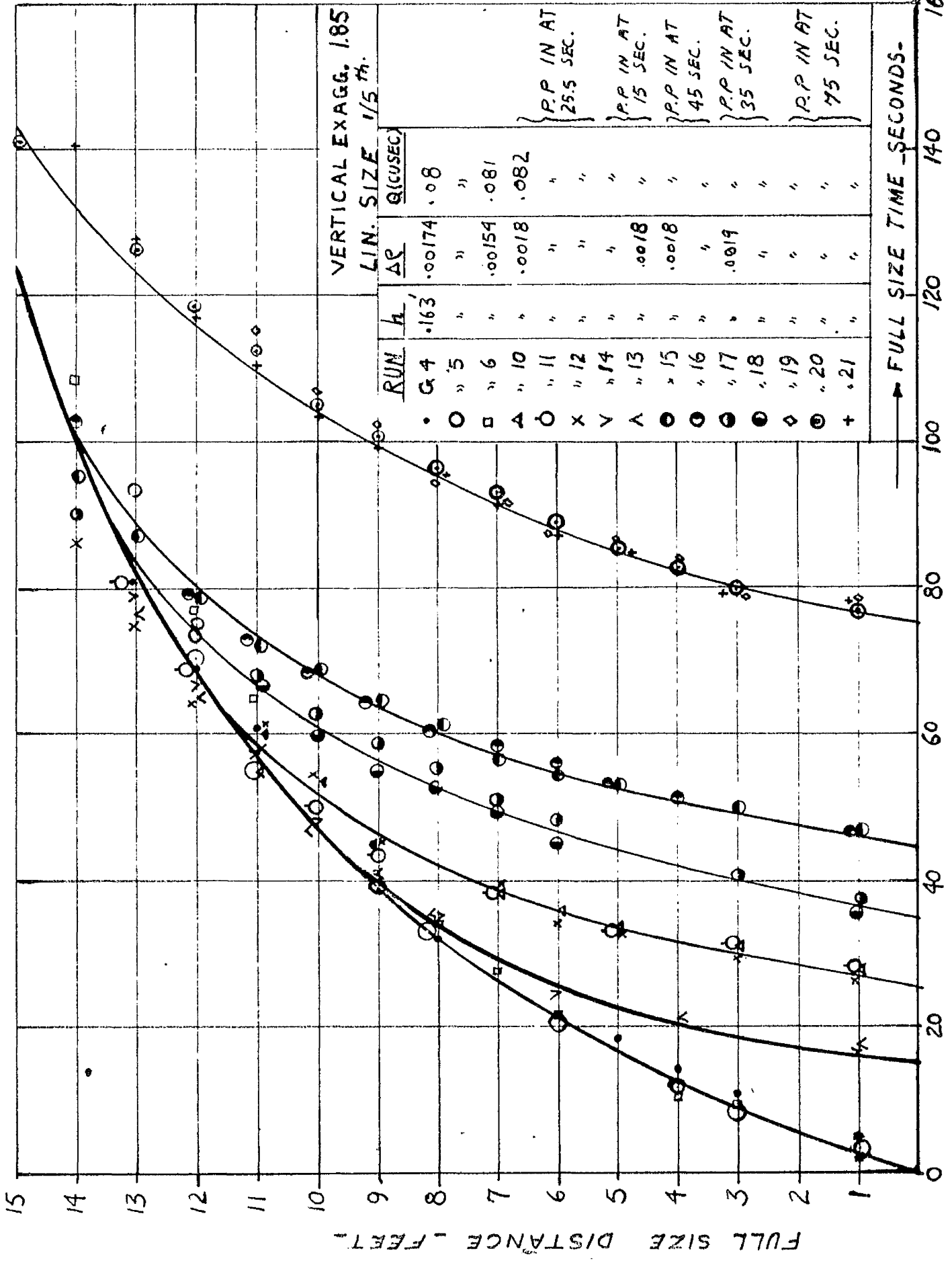


FIG. 8.3 MODEL/PROT. SIMILARITY IN BASIC OUTFALL STUDIES. THROUGH VELOCITIES.

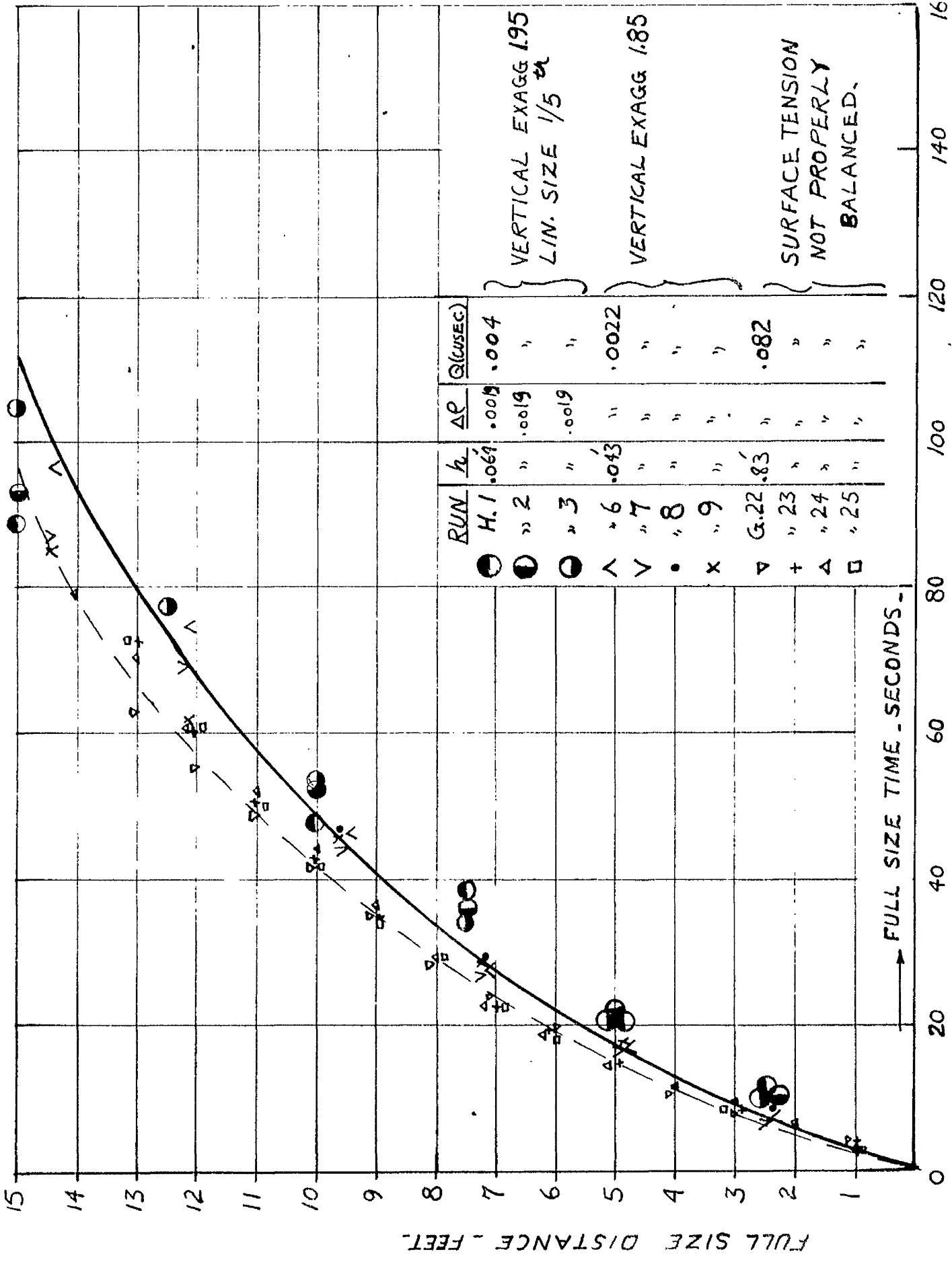
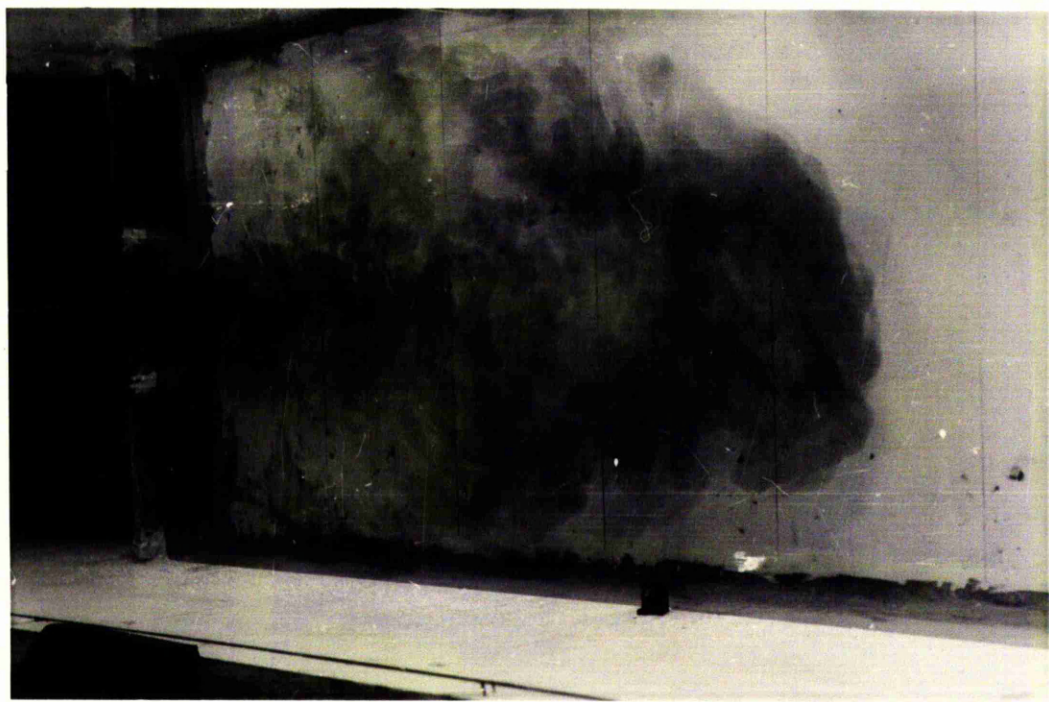
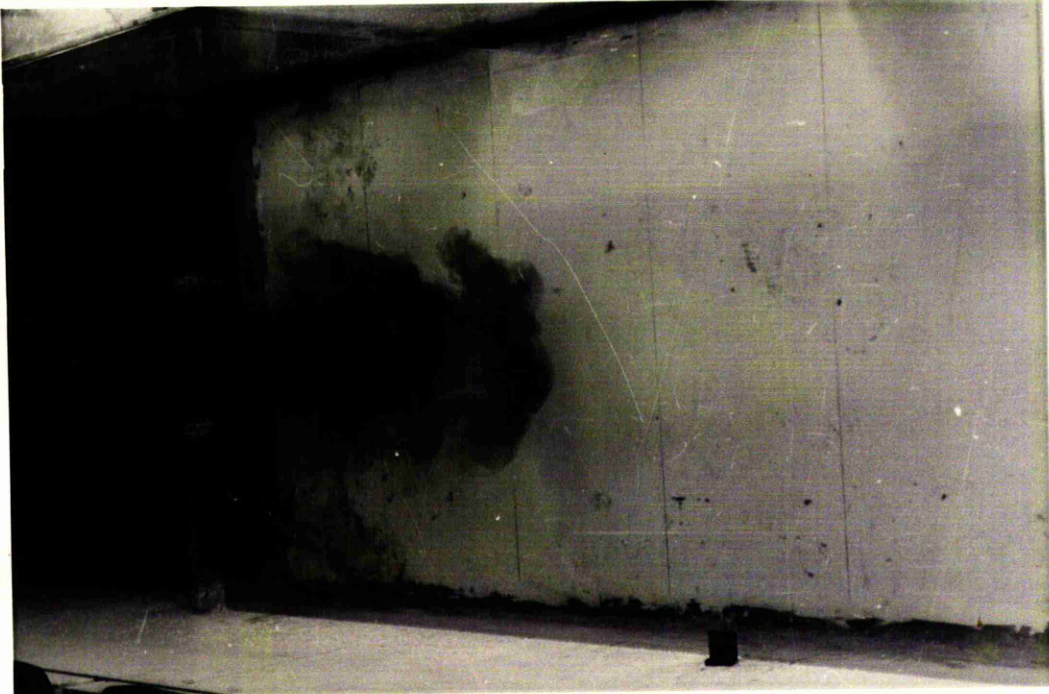


FIG. 8.4-MODEL/PROT. SIMILARITY IN BASIC OUTFALL STUDIES.

FIG. 8.6 - A more developed stage  
of spreading of outfall heated water.

FIG. 8.7 - Fully developed stage of  
spreading of outfall heated water.



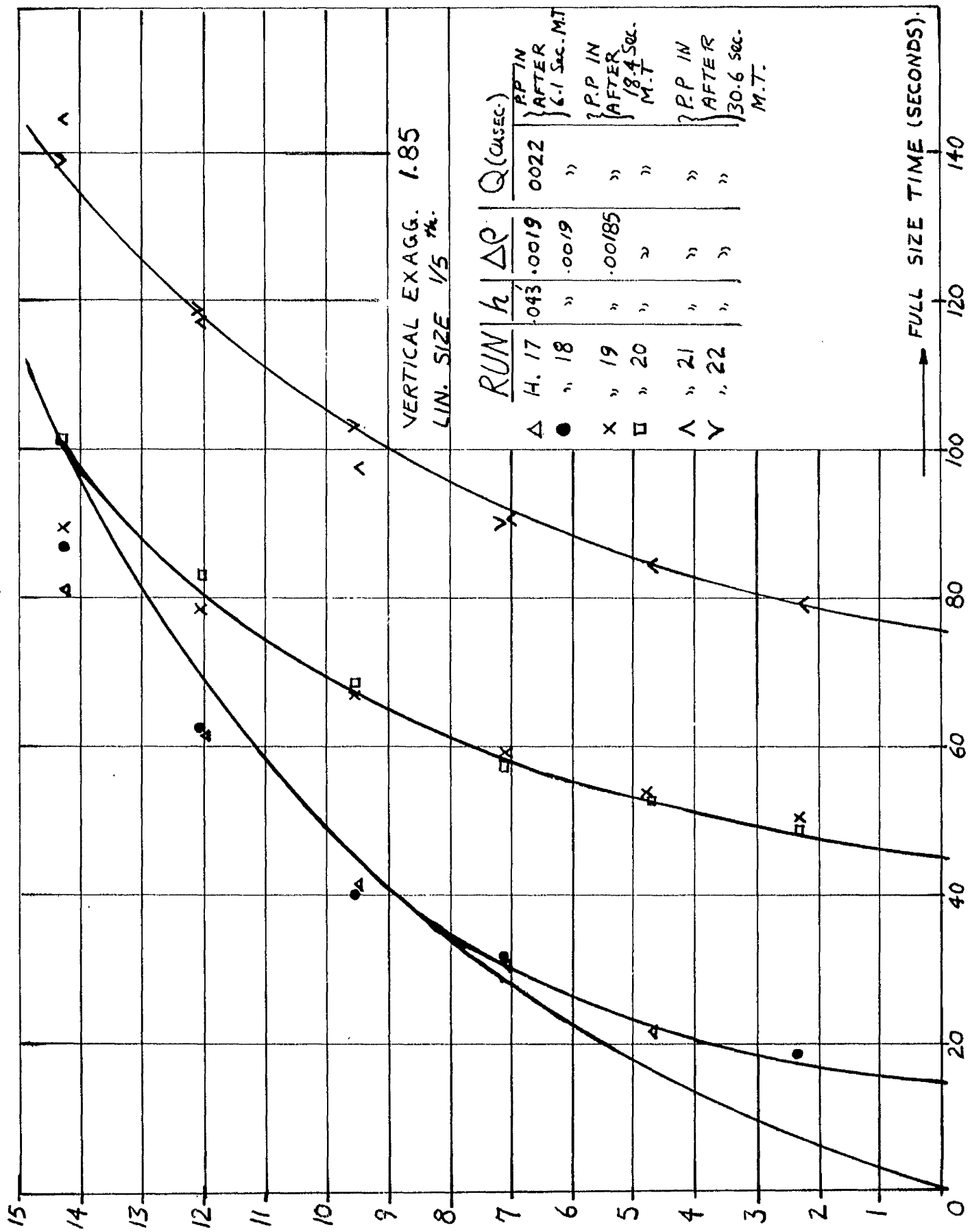


FIG. 8.8. MODEL/PROT. SIMILARITY IN BASIC OUTFALL STUDIES THROUGH VELOCITIES 8.8

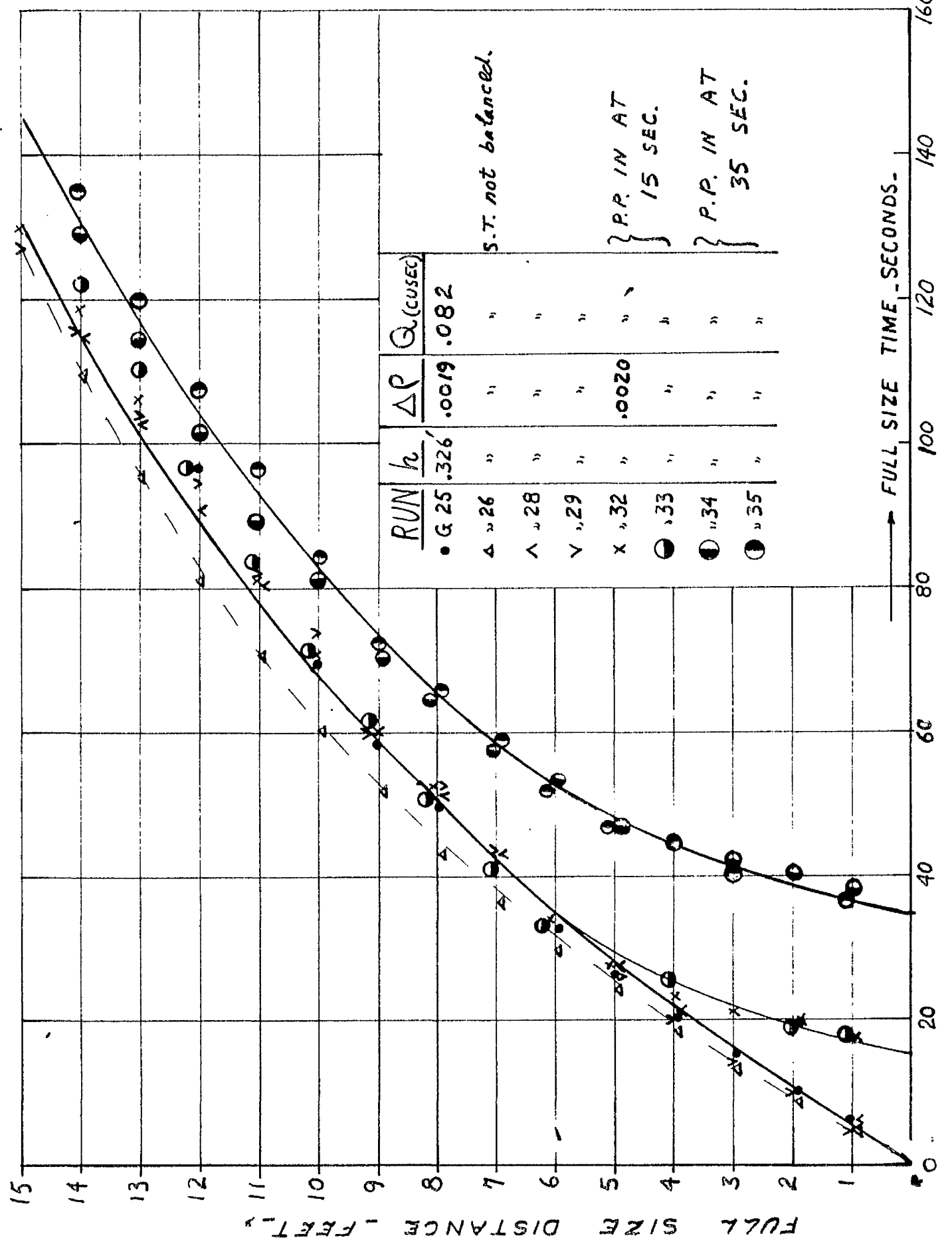


FIG. 8.9 - MODEL/PROT. SIMILARITY IN BASIC OUTFALL STUDIES THROUGH VELOCITIES.

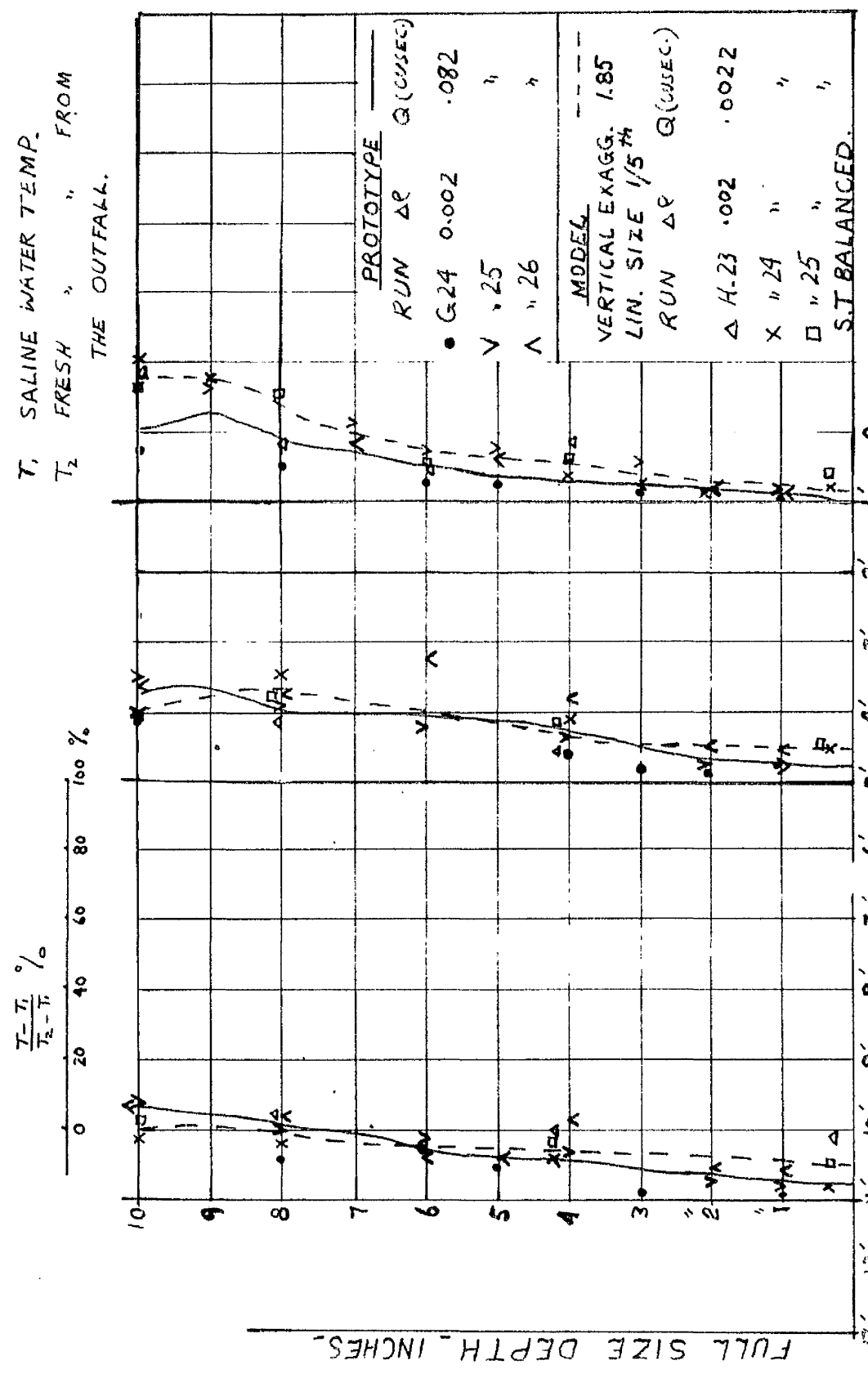


FIG. 8.10 MODEL/PROT. SIMILARITY IN BASIC OUTFALL STUDIES THROUGH VERTICAL THERMAL STRATIFICATION.

	page
12.	TEST RECORDINGS
12.1.	Recordings of front observation. 147
12.2.	Recordings of Observational study. 151
12.3.	Recordings of miniature flowmeter. calibration. 155
12.4.	Recordings of velocity variations of water behind the front. 156
12.5.	Recordings of floats observation. 166
12.6.	Recordings of dye traces observation. 167
12.7.	Recordings of small scale dilution study. 168
12.8.	Recordings of dam-burst analogy. 173
12.9.	Recordings of simplified outfall study. 174

Explanation of the front recording table.

D - date

T - type of flow ( $T_{u_1}$ : thermal underflow;  $T_{o_1}$ : thermal overflow;  $S_u$  and  $S_o$  are saline underflow and overflow respectively.)

H - depth of water in the flume.

$T_1$  - cold water temperature.

$T_2$  - hot water temperature.

P.L - rotor's position from the main barrier.

P.H - location of rotor with respect to either water surface or flume's bottom for overflow and underflow respectively.

Numbers 1, 2, ... 12 indicate distance travelled by the front.

16-26, 36-46, ... indicate time in sec. from the initial time (zero sec.) when the barrier was lifted. Here the miniature flowmeter was operated on "pulses/10 sec." which was discarded and instead "run pulses".

NO.	A1	A2	A3	"4	"5	"6	"7	"8	"9	"10
D		3-2-61	3-2	3-2	3-2	6-2	6-2	6-2	7-2	
T		Th.O.	"	"	"	"	Th.O.	"	"	
H		0.8"	"	"	"	"	"	"	"	
t <sub>1</sub>	1	60.4	61.3	60.9	61	61	65.5	60.3.	63	
t <sub>2</sub>	2	84.5	85.2	84.5	85	85	85.5	84.5	84.5	
P.L	7	<sup>1</sup> from Barrier		"	"	"	"	"	"	
P.H	1	2.5"	2.5	2.5	1.5"	1.5	1.5"	"	"	
1	9	9	10	10	-	11	9	9.5		
2	17	17.5	19	19	18	18	17	17.5		
3	25	24.5	24	24.5	24	27	25	25		
4	32.5	31	32	33	33	35	33	32		
5	39.5	39	40	40	39	43	40	40		
6	47	47	47	49	48	50	47	48.5		
7	55	54.5	55	57	55	58	54.5	55		
8	64	63	64	65	63	66	62.5	61.5		
9	72	71	72.5	74.5	71	75	68	69.5		
10	80	79	80	82	79.5	82	75.5	76		
11	89	86.5	87	89	86.5	91	84	83		
12	96	93.5	94	96	95	98	90	92		
16-26		43	36	45	50	51	39	48	41	
36-46		40	34	33	36	40	40	44	42	
56-66		42	29	34	33	38	35	42	41	
76-86		39	34	36	30	30	38	39	37	
96-106		-	14	-	16	16	19	16	22	



Run	$\Delta \rho$	H	$V_0$	$V_\Delta$	K	$N_m$	$KR_a$	Type
A9	.00276	.8	.1475	.2765	.532	$1.0 \times 10^{-5}$	11800	Tho
10	>	>	.1430	>	.5165	>	11425	>
11	.0031	>	.152	.2820	.538	$1.0 \times 10^{-5}$	12000	>
12	.0027	>	.140	.268	.522	$1.02 \times 10^{-5}$	10995	>
13	.00303	>	.1425	.279	.511	$1.01 \times 10^{-5}$	11295	>
14	.00293	>	.140	.275	.51	$1.03 \times 10^{-5}$	10880	>
15	.0031	>	.1435	.281	.511	$1.01 \times 10^{-5}$	11365	>
C.1	.0229	.3	.236	.47	.502	$1.055 \times 10^{-5}$	6710	S <sub>0</sub>
C.2	>	>	>	>	>	>	>	>
3	>	>	"	>	"	"	"	>
4	.0024	>	.074	.1521	.486	$1.129 \times 10^{-5}$	1957	>
5	>	>	.0796	>	.524	$1.129 \times 10^{-5}$	2120	>
6	.0008	>	.0418	.0856	.49	>	1112	>
7	.0225	.8	.389	.7615	.511	$1.069 \times 10^{-5}$	29250	>
8	>	>	.236	.4635	.51	>	6655	>
B3,4,5	.00314	.8	"	"	.445	-	9614	Th <sub>u</sub>
B16,18	.0032	>	"	"	.44	-	10640	>
B6,7	.00313	>	"	"	.426	-	8414	>
E24,21	.0034	.6	"	"	.435	-	5590	>
E30	.01186	.6	"	"	.427	-	10300	>
E11,5	.00086	.3	"	"	.431	-	675	>
14,16	.00085	.6	"	"	.458	-	2960	>

Observational results of partial colouring of water on one side of the barrier.

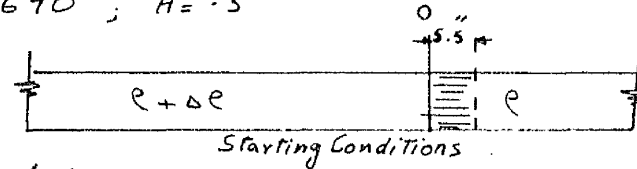
### 1) Saline Overflow

#### a) turbulent

$$\Delta R = -0.0229 \text{ gm/m.L} ; KR_d = 6690 ; H = 3'$$

#### RUN 0.1

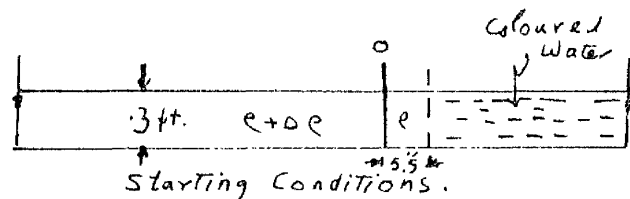
After arriving at stable



stratification with all movements vanished, it has been observed that the coloured layer started at -1 ft as thin and diluted, thickened and deepened in colour in flume's longer reach. It was estimated that the layer centred at 6'-6" where it was 1 inch thick and positioned at 3/4 inch under the surface. On the other hand, it was  $\frac{1}{4}$  inch thick at  $\frac{3}{4}$  inch under the surface near the far end barrier.

#### RUN 0.2

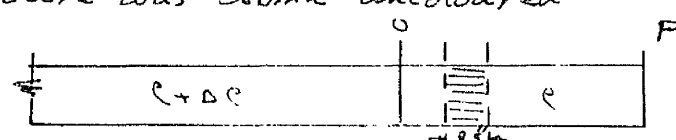
First 5.5 inch. of less dense water uncoloured, rest coloured.



Some overtaking at  $5\frac{1}{4}$  ft.. Before the front had hit the end barrier at 13 ft., there was some uncoloured water ( $\frac{1}{2}$  inch thick) at 7 ft - 9 inch.

#### RUN 0.3

First  $5\frac{1}{2}$  inch clear, next  $8\frac{1}{2}$  inch coloured, the following remainder clear.



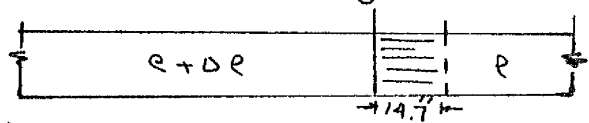
Overtaking at 4.4 ft. and a layer of about 0.6" of uncoloured water seen at 6'-6" just prior to the front reaching the end barrier.

After settling : there was a trace of coloured water at end F. The colouring thickened and deepened from 5 ft. centred at 8 ft and extended to the other end barrier.

Saline Overflow (more turbulent) -  $H = .8 \text{ ft}$ ;  $\Delta P = .02253 \text{ gm/m.L}$ ;  $KR_A = 29,450$  -

### RUN(O)4

First 14.7 inch coloured, rest uncoloured.



Severe eddying motion; clear water almost broken through the front, replacing the coloured water at the front quite markedly at 13 ft.

### RUN(O)5

$H = .3'$ . Water between 5.5 inch and 1'-5" was coloured. The state of affairs was similar to Run O.3.

Saline Overflow (more laminar) -  $\Delta P = .0024 \text{ gm/m.L}$ ;  $KR_A = 2050$

### RUN(O)6

First 5.5 inch coloured, leaving rest uncoloured.

Here, the tendency for overtaking seemed definitely less marked than in previous cases. After settling the coloured water stretched from 0 ft. to the far end barrier, but it was centred at 9 ft 6 inch. and it was thicker at between 9' - 13 inch.

### RUN(O)7

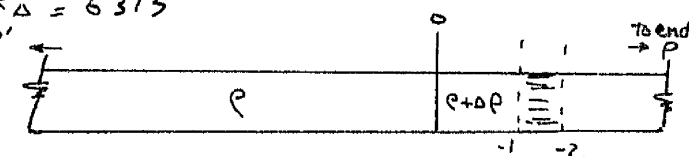
Colouring same as (O)6. Overtaking observed at 2.75 ft.

After settling : water near the far end barrier was coloured throughout the whole of the overflow depth, whereas in the proximities of the main barrier the coloured water was seen as a thin layer lying near the interface.

Saline Underflow -  $\Delta P = .0243$ ;  $KR_A = 6315$

### RUN(O)8

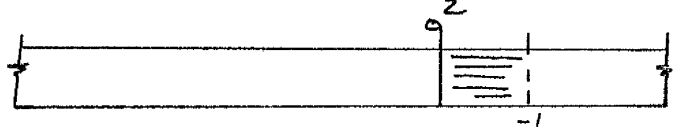
The uncoloured "bands" of water coming from behind were, once again, seen to move faster than the tips. This was seen to move at about  $\frac{1}{2}$  inch above the bottom of the flume.



### RUN(O)9

Overtaking was seen at 6.75 ft.

After settling : The coloured water stationed near the flume's bed, varying in thickness (1.1 inch near the barrier P' and 1" near end P).



Saline underflow (more laminar) -  $H = .3'$ ;  $\Delta \rho = .0022 \text{ gm/m.L}$ ;  $KR_d = 1560$

Run (O) 10 :

First 1 foot coloured, rest uncoloured.

The uncoloured water seems to overtake the coloured, but the exact position of overtaking was difficult to determine.

After settling : most of coloured water was shifted to the other end. The distribution was (i) slight trace of coloured water stretched between -1 ft. to 9 ft and resting on a layer of uncoloured water at the flume's bed. (ii) from 9 ft - 13 ft, the coloured water approximately occupied the underflow depth ( $\approx 1.2$  inches).

Run (O) 11

Second foot coloured, rest uncoloured.

Overtaking did not take place within the range available in the longer reach.

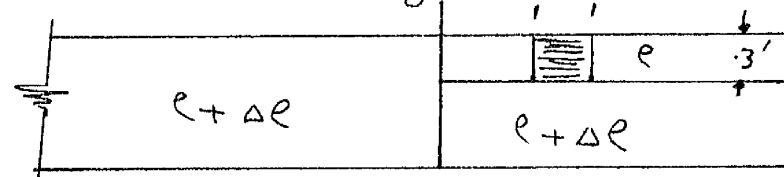
After settling : most of the coloured water was seen near the far end barrier. Between 6 ft - 13 ft the coloured layer depth was .75 inch. From -2 ft to 6 ft. the layer was thinner and lying not very far from the flume's bed.

" Observational results of the dam-burst analogy."

Saline overflow -  $\Delta \rho = .00229$ ;  $h = .3 \text{ ft}$ ;  $KR_d = 7200$  - i.e. -2-3"

Run (O) 1

Coloured water appeared to move faster than the front. During later stages, overtaking took



Starting conditions.

place at 8 ft from the main barrier position (0 point)

After settling : most of coloured was seen at the far end barrier.

N.B As the process of filling the flume (explained in chapter 7) involves a considerable amount of mixing, it was found difficult to test for differential movements of water in a more laminar case.

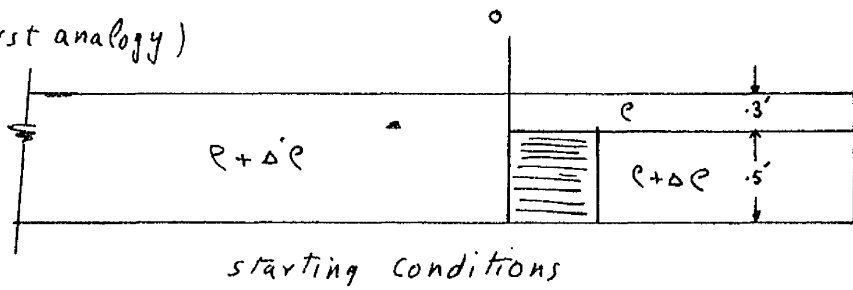
### Saline Underflow (Dam-burst analogy)

$$\Delta \rho = 0.0229$$

$$H = 0.5 \text{ ft}$$

$$KR_o = 15,640$$

Run (2)

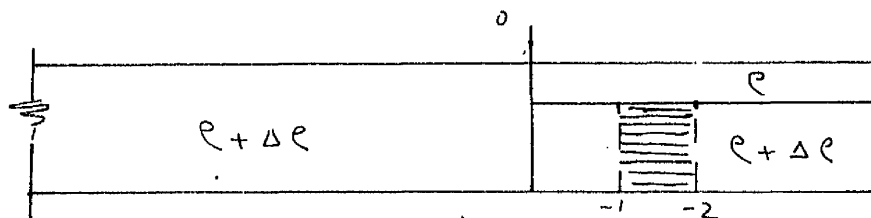


starting conditions

Coloured water very much left behind with swift upper zone of clear water. Considerable mixing took place whilst filling. Still some coloured water seen at the front "roller" at 12 ft. Overtaking appeared to take place at 10 ft - 8 inch.

Run (3)

Coloured water reached the surge



at 9 ft - 6 inch. Thereafter

starting conditions

much of it was dragged by the overflow current, and thus it was left behind. Indeed, the aforementioned was observed in all partially coloured exchange flows. After settling: much of coloured water was seen near the far end barrier.

## CALIBRATION OF MINIATURE CURRENT.

## FLOWMETER.

RUN	Average Pulses per 10 sec.	Distance Inch.	Average Time sec.	Average linear velocity Inch/sec.
1	95.6	60	18.9	3.18
2	47.33	"	30	2.0
3	69.6	"	23.23	2.68
4	61.7	"	23.63	2.535
5	112.8	"	16	3.745
6	42	"	31.6	1.9
7	34.1	"	35.25	1.7
8	35.9	"	37	1.62
9	24.8	"	40	1.5
10	21.7	"	46.1	1.3
11	19	"	54	1.11
12	18.5	"	57	1.05
13	12.3	"	66.7	.9

RUN B(48) Cont.

Run B.3

No	T		t	No	T		t	No	T		t
	S	E			S	E			S	E	
12	31.45	33.6	2.15	1	11.5	13.25	1.75	28	76	78.5	2.5
13	33.6	35.8	2.2	2	13.25	14.8	1.55	29	78.5	82	3.5
14	35.8	38.8	3.0	3	14.8	17	2.2	30	82	.85	3
15	38.8	40.75	1.95	4	17	19.3	2.3	31	85	90	2
16	40.75	43.4	2.65	5	19.3	20.7	1.4	32	90	93.3	3.3
17	43.4	45.5	2.1	6	20.7	22.4	1.7	1	8	12.5	4.5
18	45.5	48.5	3.0	7	22.4	24.9	2.5	2	12.5	14.6	2.1
19	48.5	51	2.5	8	24.9	27	2.1	3	14.6	17.8	3.2
20	51	53.1	2.1	9	27	29	2.0	4	17.8	21.2	3.4
21	53.1	55.7	2.6	10	29	31	2.0	5	21.2	23.5	2.3
22	55.7	59.1	3.4	11	31	33.5	2.5	6	23.5	26.2	2.7
23	59.1	61.75	2.65	12	33.5	36	2.5	7	26.2	28.8	2.6
24	61.75	65.55	3.8	13	36	38.5	2.5	8	28.8	32.0	3.2
25	65.55	68.0	2.45	14	38.5	41.25	2.75	9	32.0	35.0	3.0
26	68.0	70.5	2.5	15	41.25	43.3	2.05	10	35.0	37.2	2.2
27	70.5	73.2	2.7	16	43.3	45.5	2.2	11	37.2	39	1.83
28	73.2	76.1	2.9	17	45.5	48	2.5	12	39	41.5	3.5
29	76.1	79	2.9	18	48	50.7	2.7	13	41.5	44	2.5
30	79	82.2	3.2	19	50.7	53.3	2.6	14	44	46.5	2.5
31	82.2	86.0	3.8	20	53.3	56	2.7	15	46.5	48.8	2.3
				21	56	59	3.0	16	48.8	51.3	2.5
				22	59	61.8	2.8	17	51.3	53.5	2.2
				23	61.8	64.3	2.5	18	53.5	56.6	3.1
				24	64.3	67.5	3.2	19	56.6	59.3	2.7
				25	67.5	70	2.5	20	59.3	62.0	2.7
				26	70	72.8	2.8	21	62.0	65.2	3.2
				27	72.8	76.0	3.2	22	65.2	67.7	2.5

## RUN B(4) (mt)

No	T		t	No.	T		t
	S	E			S	E	
23	67.7	70.1	2.4	17	64.8	68.5	3.7
24	70.1	73.3	3.2	18	68.5	72.5	4.0
25	73.3	76.0	2.7	19	72.5	76.2	3.7
26	76.0	79.4	3.4	20	76.2	80.3	4.1
27	79.4	83.6	4.2	21	80.3	86.1	5.8
28	83.6	89.5	5.9	22	86.1	92	5.9
					RUN B(6)		
29	89.5	95	5.5	1	47.0	48.8	1.8
30	95	101	6	2	48.8	50.3	1.5
31	101	108	7	3	50.3	52.3	2.0
					RUN B(5)		
1	11	15.5	4.5	4	52.3	54.5	2.2
2	15.5	18.8	3.3	5	54.5	61	—
3	18.8	21	2.2	6	61	63.2	2.2
4	21	24.1	2.1	7	63.2	65.7	2.5
5	24.1	27	2.9	8	65.7	67.6	1.9
6	27	29.8	2.8	9	67.6	69.8	2.2
7	29.8	33	3.2	10	69.8	72	2.4
8	33	36.2	3.2	11	72	74.4	2.4
9	36.2	39.5	3.3	12	74.4	76.3	1.9
10	39.5	42.3	2.8	13	76.3	78	1.7
11	42.3	46.2	3.1	14	78	80	2.0
12	46.2	49.7	3.5	15	80	82.2	2.2
13	49.7	53.4	3.7	16	82.2	84.5	2.3
14	53.4	57.2	3.8	17	84.5	86.8	2.3
15	57.2	60.8	3.6	18	86.8	88.9	2.1
16	60.8	64.8	4.0	19	88.9	90.7	1.8
				20	90.7	92.7	2.0

RUN B.9

No.	T		t sec.	No.	T		t sec.	No.	T		t sec.
	S	E			S	E			S	E	
1	16	18.45	2.45	28	71.7	73.9	2.2	17	57.0	59.45	2.45
2	18.45	20.8	2.35	29	73.9	76.2	2.3	18	59.45	61.7	2.25
3	20.8	22.6	1.8	30	76.2	78.4	2.2	19	61.7	64.2	2.5
4	22.6	24.85	2.25	31	78.4	81.1	2.7	20	64.2	66.2	2.0
5	24.85	26.5	1.65	32	81.1	83.6	2.5	21	66.2	68.5	2.3
6	26.5	27.85	1.35	33	83.6	85.8	2.2	22	68.5	71.0	2.5
7	27.85	29.30	1.45	34	85.8	89.2	2.4	23	71.0	73.5	2.5
8	29.30	30.8	1.5	35	89.2	91.5	2.3	24	73.5	75.5	2.0
9	30.8	32.9	2.10	36	91.5	94.0	2.5	25	75.5	78.1	2.6
10	32.9	35.0	2.10	37	94.0	98.2	4.2	26	78.1	80.6	2.5
11	35.0	36.7	1.7	<u>RUN B. 10</u>				27	80.6	83.4	2.8
12	36.7	39.5	2.8	1	17.2	20	2.8	28	83.4	86.1	2.7
13	39.5	41.6	2.1	2	20.0	22.9	2.9	29	86.1	88.5	2.4
14	41.6	43.6	2.0	3	22.9	26.1	3.2	30	88.5	91.7	3.2
15	43.6	45.5	1.9	4	26.1	28.5	2.4	31	91.7	95.8	4.1
16	45.5	47.3	1.8	5	28.5	30.8	2.3	32	95.8	101.5	5.7
17	47.3	49.6	2.3	6	30.8	32.8	2.0	<u>RUN B. 12</u>			
18	49.6	51.8	2.2	7	32.8	34.8	2.0	1	16	20	4
19	51.8	53.8	2.0	8	34.8	36.8	2.0	2	20	22.2	2.2
20	53.8	55.9	2.1	9	36.8	39.5	2.7	3	22.2	23.8	1.6
21	55.9	58.0	2.1	10	39.5	42.7	3.2	4	23.8	25.7	1.9
22	58.0	60.2	2.2	11	42.7	45.5	2.8	5	25.7	27.5	1.8
23	60.2	62.5	2.3	12	45.5	47.5	2.0	6	27.5	29.2	1.7
24	62.5	65.0	2.5	13	47.5	50.0	2.5	7	29.2	30.9	1.7
25	65.0	67.2	2.2	14	50.0	52.3	2.3	8	30.9	33.1	2.2
26	67.2	69.5	2.3	15	52.3	54.5	2.2	9	33.1	35.3	2.2
27	69.5	71.7	2.2	16	54.5	57.0	2.5	10	35.3	37.3	2.0

RUN B.(13)

RUN B.(14)

No.	T		t sec.	No.	T		t sec.	No.	T		t sec.
	S	E			S	E			S	E	
<u>RUN B.12 (Cont.)</u>											
11	37.3	39.5	2.2	2	51.1	53.1	2.0	2	50.0	52.0	2.0
12	39.5	41.8	2.3	3	53.1	55.2	2.1	3	52.0	53.7	1.7
13	41.8	43.8	2.0	4	55.2	57.2	2.0	4	53.7	55.5	1.8
14	43.8	46.2	2.4	5	57.2	59.1	1.9	5	55.5	56.6	1.1
15	46.2	48.2	2.0	6	59.1	61.1	2.0	6	56.6	58.7	2.1
16	48.2	50.6	2.4	7	61.1	62.5	1.9	7	58.7	60.4	1.7
17	50.6	53.2	2.6	8	62.5	64.1	1.6	8	60.4	61.8	1.2
18	53.2	55.5	2.3	9	64.1	66.1	2.0	9	61.8	63.5	1.7
19	55.5	57.7	2.2	10	66.1	67.6	1.5	10	63.5	65.0	1.5
20	57.7	60.0	2.3	11	67.6	69.5	1.9	11	65.0	67.0	2.0
21	60.0	62.5	2.5	12	69.5	71.2	1.7	12	67.0	68.7	1.7
22	62.5	65.2	2.7	13	71.2	73.2	2.0	13	68.7	70.3	2.3
23	65.2	67.5	2.3	14	73.2	75.5	2.3	14	70.3	72.2	1.9
24	67.5	69.8	2.3	15	75.5	77.5	2.0	15	72.2	73.7	1.5
25	69.8	72.2	2.4	16	77.5	79.2	1.7	16	73.7	75.85	2.15
26	72.2	74.5	2.3	17	79.2	80.9	1.7	17	75.85	77.5	1.65
27	74.5	77.3	2.8	18	80.9	82.6	1.7	18	77.5	79.3	1.80
28	77.3	79.8	2.5	19	82.6	84.9	2.3	19	79.3	81.5	2.2
29	79.8	82.6	2.8	20	84.9	87.0	2.1	20	81.5	83.45	1.95
30	82.6	84.85	2.25	21	87.0	88.8	1.8	21	83.45	85.8	1.35
31	84.85	87.8	2.95	22	88.8	90.6	1.8	22	85.8	87.4	1.6
32	87.8	91.3	3.5	23	90.6	92.4	1.8	23	87.4	89.3	1.9
33	91.3	94.4	3.1	24	92.4	94.1	1.7	24	89.3	91.2	1.9
34	94.4	97.5	3.1	25	94.1	96.2	2.1	25	91.2	93.1	1.9
35	97.5	102.2	4.7	26	96.2	98.45	2.25	26	93.1	94.8	1.7
-	-	-	-	27	98.45	100.7	2.25	27	94.8	97.5	2.7

## RUN B. 14(Cont.)

No.	T		t	No.	T		t	No.	T		t
	S	E			S	E			S	E	
28	97.5	99.5	2.0	25	89.4	92.1	2.7	22	56.5	59	2.5
29	99.5	101.2	1.7	26	92.1	93.5	1.4	23	59	61.9	2.9
<u>RUN B. (15)</u>				27	93.5	95.75	2.25	24	61.9	64.7	2.8
1	44.6	49.0	4.4	28	95.75	98.0	2.85	25	64.7	67.3	2.6
2	49.0	51.3	2.3	29	98.0	100.2	1.60	26	67.3	70.4	3.1
3	51.3	52.9	1.6	<u>RUN B. (16)</u>				27	70.4	72.8	2.4
4	52.9	54.9	2.0	1	11.8	14	2.2	28	72.8	75.8	3.0
5	54.9	56.2	1.3	2	14	16.2	2.2	29	75.8	78.5	2.7
6	56.2	57.7	1.5	3	16.2	18.1	1.9	30	78.5	81.3	2.8
7	57.7	59.1	1.4	4	18.1	19.8	1.7	31	81.3	84.9	3.6
8	59.1	60.6	1.5	5	19.8	21.25	1.45	<u>RUN B. (17)</u>			
9	60.6	62.2	1.6	6	21.25	23	1.75	Instrument failed			
10	62.2	64.0	1.8	7	23	24.7	1.7	to operate, because			
11	64.0	65.4	1.4	8	24.7	26.45	1.75	of sudden Voltage			
12	65.4	67.2	1.8	9	26.45	28.2	1.75	drop due to unexplained			
13	67.2	69.1	1.9	10	28.2	30.2	2.0	loss of balance.			
14	69.1	70.7	1.6	11	30.2	32.5	2.3	1	10	11.9	1.9
15	70.7	72.5	1.8	12	32.5	34.7	2.2	2	11.9	13.5	1.6
16	72.5	74.5	2.0	13	34.7	36.6	1.9	3	13.5	15.7	2.2
17	74.5	76.0	1.5	14	36.6	38.8	2.2	4	15.7	17.2	1.5
18	76.0	77.9	1.9	15	38.8	41.5	2.7	5	17.2	19.1	1.9
19	77.9	80.0	2.1	16	41.5	43.75	2.25	6	19.1	20.8	1.7
20	80.0	81.8	1.8	17	43.75	46.2	2.45	7	20.8	22.5	1.7
21	81.8	84.2	2.4	18	46.2	48.5	2.3	8	22.5	25	2.5
22	84.2	85.7	1.5	19	48.5	51.4	2.9	9	25	26.8	1.8
23	85.7	87.4	1.7	20	51.4	54	2.6	10	26.8	29	2.2
24	87.4	89.9	2.0	21	54	56.5	2.5	11	29	31.45	2.45

RUN B(4)

RUN B(3)

RUN B(5)

T	t	P	V	T	t	P	V	T	t	P	V
11.8	3.3	30.25	1.51	13.5	1.65	60.5	2.32	16.8	3.3	30.25	1.51
14.5	2.7	37	1.68	15.0	1.90	52.6	2.11	21.3	2.15	46.6	1.94
18.0	3.3	30.25	1.51	17.0	2.25	44.5	1.90	22.1	2.5	40.0	1.76
20.4	2.8	35.7	1.65	19.0	1.85	59.1	2.15	27	2.82	35.46	1.65
23	2.5	4.0	1.76	21.0	1.55	64.5	2.42	29.5	3.1	32.25	1.57
26.3	2.64	37.8	1.70	22.0	1.90	52.6	2.11	33.0	3.32	30.15	1.51
28.5	2.9	34.95	1.62	25.0	2.3	43.5	1.86	36.2	3.25	30.8	1.54
32	3.1	32.25	1.57	27.0	2.05	48.75	2.0	39	3.03	33.0	1.58
41.7	3.0	33.3	1.58	29.0	2.0	50.0	2.03	42.5	3.3	30.25	1.51
43.6	2.5	40	1.76	31.0	2.25	44.5	1.89	46.5	3.78	26.67	1.40
46.5	2.4	41.6	1.83	34.0	2.5	40.0	1.76	50.0	3.6	27.8	1.44
51.2	2.32	43.2	1.86	38.0	2.6	38.45	1.73	53.6	3.75	26.65	1.40
53.3	2.65	37.8	1.70	41.0	2.4	41.65	1.80	57.5	3.7	27.0	1.41
56.2	2.9	34.5	1.61	43.0	2.1	47.6	1.96	61.0	3.78	26.67	1.40
59.0	2.7	37.1	1.69	45.0	2.3	43.5	1.86	65.0	3.82	26.2	1.38
62	2.95	33.9	1.60	48.0	2.6	38.45	1.73	68.5	3.87	25.85	1.36
65	2.85	35.1	1.66	50.6	2.65	37.8	1.70	72.5	3.87	25.85	1.36
67.5	2.45	40.8	1.79	53	2.65	37.8	1.70	76.2	3.9	25.62	1.358
70.5	2.8	35.75	1.63	55.6	2.8	35.7	1.65	81.0	5.0	20.0	1.21
73.5	2.93	34.2	1.61	59.5	2.85	35.1	1.64	86.0	5.85	17.2	—
75.5	3.0	33.4	1.61	62.0	2.60	38.45	1.73	—	—	—	—
79.3	3.8	26.3	1.38	64.0	2.8	35.7	1.65				
83.5	5.0	2.0	1.27	67.0	2.8	35.7	1.65				
89.5	5.65	17.7	—	69.0	2.65	37.75	1.70				
95.0	5.72	17.5	—	73.0	2.95	33.9	1.60				
—	—	—	—	76.0	2.8	35.7	1.65				
—	—	—	—	79.0	3.0	33.3	1.58				
—	—	—	—	82.0	3.2	31.25	1.54				
				87.5	3.15	31.75	1.56				

RUN B(6)

T	t	P	V	T	t	P	V	T	t	P	V
48.5	1.625	63.5	2.4	48.5	2.5	40	1.77	18.8	2.4	41.63	1.81
50.05	1.775	56.4	2.22	51	2.6	3845	1.72	20.7	2.05	4875	2.0
52.5	2.10	47.6	1.97	63.5	2.25	49.5	1.90	23.0	2.0	50	2.03
58	2.2	45.5	1.91	67.1	2.2	4545	1.92	25.0	1.92	52.1	2.1
63.5	2.35	42.55	1.83	71.2	2.5	40.0	1.77	26.5	1.48	67.5	2.51
67.0	2.18	46.0	1.93	75.0	2.3	43.5	1.86	29	1.42	70.4	2.60
69.5	2.15	46.55	1.94	79.8	2.3	43.5	1.86	31	1.8	55.6	2.18
70.25	2.4	41.65	1.80	82.5	2.75	36.4	1.67	32	2.1	47.6	1.97
74.3	2.15	46.55	1.94	85.0	2.5	40	1.77	35	1.87	53.5	2.12
76	1.8	55.5	2.13	87.5	2.25	44.5	1.90	37.2	2.26	44.2	1.89
80.5	2.0	50.0	2.03	91.0	2.0	50	2.03	39.5	2.45	40.8	1.78
83.0	2.25	44.5	1.90					43.6	1.94	51.55	2.08
85	2.3	43.5	1.87					47.6	2.1	47.6	1.98
87.5	2.10	47.6	1.97					51	2.12	47.2	1.96
91.0	1.9	52.6	2.11					54	2.05	48.75	2.01
93.0	2.0	50.0	2.03					56.2	2.1	47.6	1.98
								59.0	2.2	45.5	1.92
								62.5	2.37	42.2	1.82
								65.0	2.35	42.55	1.83
								67.5	2.26	44.25	1.89
								69.3	2.27	44.1	1.89
								72.0	2.2	45.5	1.93
								73.5	2.25	44.5	1.90
								76.0	2.2	45.5	1.93
								78.8	2.47	40.5	1.77
								82.5	2.5	40.0	1.76
								86.0	2.8	35.75	1.74

RUN B(10)				RUN B(12)				RUN B(13)			
T	t	N	V	T	t	N	V	T	t	N	V
20.5	2.85	35.1	1.64	20	2.9	34.45	1.61	52.7	3.0	33.35	1.58
23.4	3.05	32.8	1.57	22	1.9	52.6	2.11	54	2.06	48.55	2.0
26.3	2.8	35.7	1.70	23.5	1.7	58.8	2.26	56.5	2.0	50.0	2.03
28.8	2.35	42.51	1.84	27	1.8	55.6	2.20	59	1.96	51.0	2.06
31	2.13	47.0	1.95	29	1.7	58.8	2.28	61	1.7	58.8	2.26
33	2.0	50.0	2.03	31	1.9	52.6	2.10	63.2	1.7	58.8	2.26
35	2.0	50.0	2.03	33	2.2	45.5	1.91	66.2	1.72	28.5	1.50
38	2.62	38.2	1.72	35.3	2.08	48.2	2.0	67.6	1.71	28.6	1.51
43	2.95	33.9	1.60	37.5	2.1	47.6	1.97	69	1.81	55.4	2.17
45.5	2.3	43.5	1.87	39.6	2.25	44.5	1.90	71.2	1.9	52.6	2.11
47.7	2.23	44.8	1.91	42	2.12	47.2	1.96	73.5	2.15	46.5	1.95
51.2	2.3	43.5	1.87	43.6	2.2	45.5	1.9	76.2	1.98	50.5	2.16
55	2.35	42.51	1.84	46.8	2.17	46.2	1.94	80	1.7	58.8	1.45
57.5	2.47	40.5	1.78	51	2.47	40.5	1.78	83	2.1	47.6	1.97
59.5	2.35	42.51	1.84	55	2.35	42.6	1.85	86.5	2.0	50.0	2.03
63	2.27	44.2	1.90	59	2.3	43.5	1.87	90	1.8	55.6	2.20
66.3	2.14	46.7	1.85	65.3	2.46	40.6	1.78	91.5	1.75	57.2	2.25
68	2.4	41.6	1.81	67.8	2.3	43.5	1.87	94.7	1.9	52.6	2.11
70	2.5	40.0	1.77	69.5	2.35	42.6	1.85	96.5	2.16	46.3	1.95
75	2.55	39.22	1.73	72.5	2.33	42.9	1.86	—	—	—	—
78.2	2.53	39.55	1.76	74.9	2.54	39.4	1.75				
81	2.63	38.1	1.71	77.5	2.62	38.2	1.72				
83	2.75	36.4	1.67	79.5	2.61	38.3	1.72				
86.2	2.52	39.7	1.75	82.5	2.5	40.0	1.77				
—	—	—	—	86	2.71	36.9	1.68				

RUN B (14)

RUN B(15)

RUN B (16)

## RUN B (18)

T	t	P	V
14.5	2.2	45.5	1.91
18	1.85	54.0	2.16
21.8	1.6	62.5	2.38
23.4	1.72	58.1	2.27
25	1.71	58.5	2.28
26.5	1.74	57.5	2.25
29.5	2.0	50.0	2.09
33	2.23	49.8	1.9
35.6	2.05	48.78	2.0
37.5	2.26	44.2	1.89
43.7	2.34	42.75	1.84
46.0	2.38	42.0	1.82
49.8	2.57	38.95	1.74
51.3	2.72	36.4	1.66
53.7	2.52	39.7	1.75
56.3	2.50	40	1.77
59	2.7	37.0	1.69
62.1	2.84	35.2	1.64
64.5	2.7	37.0	1.69
67.4	2.81	35.6	1.65
71.5	2.75	36.4	1.66
72.8	2.65	37.75	1.70
75.5	2.87	34.85	1.63
78.8	2.77	36.1	1.67
81.8	3.2	31.25	1.53

## FLOATS RESULTS.

P I S T A N C E  F E E T.	Run D1		Run D2		Run D3		Run D4			D5	
	FRONT	FLOAT I	FLOAT II	I	II	FRONT	I	II	FRONT	I	
	Time (T) sec.	T	T	T	T	T	T	T	T	T	T
1	12.5	36	59.1	23.45	63.8	6.8	20.2	34.8	5.6	14.2	
2	24.6	50.5	72.1	41.8	76.5	13.1	28.7	42.2	12	21.5	
3	35.8	64.7	84.3	54	90.7	21.1	-	-	18.9	28	
4	46.7	78.0	99.3	-	102.8	27.0	-	56.7	25	35	
5	59.3	93.4	-	78	-	33.5	50.5	-	32	42	
6	71.5	108.7	128.4	-	129.5	39.5	-	71.2	38	48.7	
7	83.5	123.2	148.0	105.8	146.5	45.5	63	-	43.6	54	
8	95.1	142	174	121.8	172.5	51.3	-	86.5	50.0	58.8	
9	108.7	170.1	-	-	198.7	57.7	-	-	56.6	66	
10	123.0	-	-	163	-	65	81.5	103.6	63	71.6	
11	140.6	-	-	-	-	71.2	-	-	69.5	78	
12	164.0	-	-	-	-	79	96.8	-	77.9	86	
T <sub>1</sub>	56.1°F	56.1°F	56°F			64°F			64°F		
T <sub>2</sub>	-	-				87			87		
H	.3'	.3'	.3'			.6'			.6'		
T <sub>ym</sub>	S <sub>o</sub>	S <sub>o</sub>	S <sub>o</sub>			Th <sub>o</sub>			Th		
Date	27-3-61	"	"			29-3-61			"		

## DYE TRACES RESULTS.

DISTANCE	TIME (SEC.) FROM LIFTING OF THE BARRIER.												
	1D'	2D'	3D'	4D'	5D'	6D'	7D'	8D'	9D'	10D'	11D'	12D'	13D'
1	13.1	11	-	32.2	10	35.4	28	34.2	12	55.8	-	83	11.6
2	25.5	21	-	42	20.3	48	39.5	46.7	24.1	68	45	95	23.2
3	39	33	-	53.2	30.9	-	49.5	58.5	-	81	5.6	108.2	35.5
4	52.5	45.7	-	64	42	-	59	67.5	47.7	91.8	66	-	46.8
5	64.5	56.2	64.5	74.3	56	-	-	81.0	59.2	103.5	-	-	58.4
6	76.1	68.1	76.9	85.3	68	-	-	91	71	114.6	-	147	69.5
7	89.3	80.9	89.5	94.2	81.5	-	-	104	84	126.5	-	-	81.9
.8	102.5	92.2	104.5	107.5	94.1	-	-	117.5	95	140.2	-	-	94
9	121.1	106.0	121	125	107	-	-	-	108.7	158.9	127	-	106.1
10	140.6	124.0	138.5	142.1	121	-	-	166	125.5	-	-	-	121.7
11	161.3	141.3	159.3	-	138.5	-	-	-	144	-	-	-	139.2
12	-	161.7	182	-	-	-	-	-	-	-	-	-	162
13	-	-	-	-	-	-	-	-	-	-	-	-	-
Date	4-4-61	S-4	5-4	-	11-4	11-4	11-4	12-4	"	"	13-4	"	14-4
T	Th <sub>0</sub>	"	"	"	S <sub>0</sub>	"	"	"	S <sub>0</sub>				
H	.3'	"	"	"	"	"	"	"	"	"	"	"	"
T <sub>1</sub> °F	62.5	61.8	62.5	-	67.7	67.7	67.5	65.7	67	67.5	67.5	67.5	67.5
T <sub>2</sub> °F	72.5	80.8	79.0	-	66.5	67.7	67.5	-	65.7	66.5	65.7	"	65.7

Th<sub>0</sub>      Thermal Overflow  
 S<sub>0</sub>      Saline

$T_1$  = cold water temperature ;  $T_2$  = tepid water temp. ;  $T$  = recorded layer temp.

RUN NO.	Rack's Readin g	Actual Depth	temper- ature of	$\frac{T-T_1}{T_2-T_1} \%$	1	2	3	4	5	1	2	3	4	5
E. 4	surface	3.484	66.2	88.62	E.G.	Surf.	3.286	65.8 +65.8	87.1		.22	1.315	63.1	54.0
	.35	2.731	66.5	92.8	Th. 15'	.35	2.696	66.2	92.2		.18	.955	61.3	29.7
Th. at 4.5'	.30	2.131	66.5	92.8	F 9'	.30	2.096	65.3	80.65		.15	.356	60.9	24.3
Frontat 9'	.27	1.771	65.1	87.2		.28	1.856	64.2	66.65		.13	.116	60.8	22.95
	.25	1.531	64.3 +64.2	61.92		.25	1.496	62.6 +62.5	46.15	T <sub>1</sub>			59.1	
	.23	1.293	63.2	46.42		.22	1.136	61.6	33.3	T <sub>2</sub>			66.5	
	.20	.932	62.1	30.95		.18	.656	60.3	16.65	H			.3'	
	.17	.572	61.3	19.7		.15	.296	59.9	11.53	E.12	.41	3.521	66.2 +66.2	90.9
	.15	.332	61.1	16.89		.135	.116	59.9	11.53	Th. 8'	.35	2.801	66.6	96.05
	.132	.116	61.1	16.89	T <sub>1</sub>			59.0		F. 9'	.30	2.201	66.5	94.8
T <sub>1</sub>			59.9		T <sub>2</sub>			66.8			.25	1.604	65.2 +65	78.15
T <sub>2</sub>			67					.3'			.22	1.245	64.1	54.02
H			.3'		E.8	.413	3.486	65.8	82.75		.18	.763	62.5	43.6
E. 5	surface	3.484	66.455	85.8	Th. 15'	.35	2.732	66.1 +65.7	87.1		.15	.404	62.0	37.15
Th. 3	.35	2.696	66.2	88.61	F 4.5	.30	2.132	64.3	61.4		.126	.116	61.8	34.6.
F 9'	.30	2.096	65	71.75		.27	1.776	63.0	42.8	T <sub>1</sub>			59.1	
	.28	1.856	63.8	54.9		.23	1.291	62.1 +62.3	29.99	T <sub>2</sub>			66.4	
	.25	1.496	62.8	40.77		.2	.931	61.5	21.41	H			.3'	
	.22	1.136	61.6	23.94		.15	.332	61.1	15.7	E.13	.412	3.498	66 +66	88.25
	.18	.656	60.5	8.45		.132	.116	61.1	15.7	Th. 4'	.35	2.753	66.4	93.47
	.15	.296	60.1	2.92	T <sub>1</sub>			60		F. 4.5	.30	2.153	66.0	88.25
	.135	.116	60.1	2.92	T <sub>2</sub>			67			.25	1.556	63.5 +63.8	55.82
T <sub>1</sub>			58.9		H			.3'			.22	1.197	62.2	39.95
T <sub>2</sub>			67		E.9	.41	3.535	66.2	95.83		.18	.715	61.2	25.97
H			.3'		Th. 63'	.35	2.756	66.3	97.15		.15	.356	61.2	25.97
					F 9'	.30	2.156	66.3	97.15		.13	.116	61.1	24.66
						.25	1.8	64.8	77	T <sub>1</sub>			59.2	
										T <sub>2</sub>			66.9	
										H			.3'	

Run No.	Rack #	Actual Depth inch.	Temp. °F	$\frac{T\%}{T-T_1}$	1	2	3	4	5	1	2	3	4	5	
E14	surf.	7.084	67.1	89.6		.45	4.039	651	71.4	E.17	surf	7.084	67.1	95.25	
Th. 3'	.55	5.136	67.5 +67.1	97.65		.40	3.439	64.0	57.1	Th. 45'	.55	5.064	67.3 +67.4	97.6	
F. 9'	.50	4.536	67.2	90.8		.37	3.08	63.9	56.8	F. 9'	.5	4.46	67.1	95.25	
	.45	3.931	66.1	78.15		.30	2.224	63.1	45.43		.45	3.86	65.7	78.75	
	.40	3.331	63.8 +64.1	51.7		.25	1.639	62.2	33.75		.4	3.259	63.9 +64.1	57.65	
	.37	2.972	62.5	36.8		.20	1.04	61.7	27.25		.35	2.658	63.2	49.45	
	.30	2.116	61.9	29.9		.123	.116	61.2	20.76		.3	2.04	62	35.3	
	.25	1.531	61.1	20.7	T <sub>1</sub>			59.6			.25	1.459	61.1	24.7	
	.20	.932	60.6	14.95	T <sub>2</sub>			67.3			.2	.86	60.7	20	
	.132	.116	60.2	10.35	H			.6'			.138	.116	60.3	15.3	
T <sub>1</sub>			59.6		E.16					T <sub>1</sub>			59		
T <sub>2</sub>			67.3		Th. 1.5'	surf.	7.084	66.2	84.6	T <sub>2</sub>			67.5		
H			.6'			.55	5.16	66.8	91.65	H			.6'		
E11		3.55	66.12	95	F. 9'	.50	4.56	66.2	84.6	E.18	surf.	7.084	66.8	95.83	
Th. 64'		2.76	66.36	98		.45	3.955	64.2	61.15	Th. 6	.55	5.16	67	98.6	
F. 9'		2.15	66.36	98		.40	3.36	62.2 +63.1	37.62	F. 9'	.50	4.56	66.9	97.2	
		1.8	64.85	78		.35	2.756	61.7	31.75		.45	3.955	66.5 +66.2	91.6	
		1.32	63.12	54		.30	2.14	61.3	27.05		.40	3.355	65.1	72.2	
		.96	61.4	28.5		.25	1.56	60.7	20.0		.35	2.756	64.0	56.9	
		.35	60.3	23		.20	.96	60.1	12.93		.30	2.14	63.1	44.45	
		.116	60.3	23		.15	.36	60.0	11.77		.25	1.56	62.1	30.55	
T <sub>1</sub>			59			.13	.116	60.0	11.77		.20	.96	61.5	22.2	
T <sub>2</sub>			66.5		T <sub>1</sub>			59.6			.15	.36	61.1	16.66	
H			.3'		T <sub>2</sub>			67.3			.13	.116	61.1	16.66	
E15					H			.6		T <sub>1</sub>			59.9		
Th. 8'	surf.	7.084	66.8	93.45						T <sub>2</sub>			67.1		
F. 9'	.55	5.244	67.1 +66.8	97.3						H			.6'		
	.50	4.644	66.1	84.4						Date			3-7-1961		

Run No.	Rack's Reading	Actual Depth	Temp. F	t % $\frac{T-T_1}{T_2-T_1}$	1	2	3	4	5	1	2	3	4	5		
E19				E.21	sunt.	7.08	68.7	83.5		E.23	sunt.	7.08	68.1	92.15		
Th. 1.5	sunt.		68.3	86.9	Th. 3'	.55	5.87	68.5	81.0	Th. 8'	.55	5.51	68.6	98.6		
F. 9'	.35	2.83	68.8	94.1	F. 9'	.50	5.27	68.8 ↑68.3	84.7	F. 9'	.50	4.91	68.1 ↑68.0	92.15		
	.30	2.12	68.1	84.0		.45	4.67	68.7	83.5		.45	4.31	67.3	81.75		
	.27	1.87	66.5	60.8		.40	4.07	68.1	75.9		.40	3.71	66.5	71.4		
	.24	1.41	65.3	43.45		.35	3.47	66.2	51.8		.35	3.11	66.0	64.9		
	.20	.93	64.1	26.07		.30	2.88	65.0 ↑64.8	36.7		.30	2.52	65.2 ↑65.1	51.55		
	.15	.33	63.2	13.03		.25	2.28	63.5	17.7		.25	1.92	64.6	46.7		
	.132	.116	63.2	13.03		.20	1.68	63.0	11.39		.20	1.32	63.3	29.85		
T1			62.3			.15	1.08	62.7	7.59		.15	.72	62.4	18.18		
T2			69.2			.07	.116	62.7	7.59		.10	.116	62.4	18.18		
H			.3'		T1			62.1		T1			61.0			
E.20	sunt.	7.08	69.2	98.5	T2			70		T2			68.7			
Th. 1.5	.55	5.38	69.1	97.15	H			.6'		H			.6			
F. 9'	.50	4.78	69.1 ↑68.5	97.15	E.22	sunt.	-	68.6	94	E.25	sunt.	7.08	68.5	92.2		
	.45	4.18	68.0	81.9	Th. 4.5	.55	5.09	68.8 ↑68.5	96.4	Th. "	.55	5.48	68.9 ↑68.4	97.4		
	.40	3.58	66.2	56.9	F. 9'	.50	4.49	68.8	96.4 ↑64.3	F. 9'	.50	4.88	68.8	96.1		
	.35	2.98	65.0 ↑65	40.25		.45	3.88	67.8	84.5		.45	4.29	68.5	92.2		
	.30	2.38	64.2	29.15		.40	3.29	66.2	65.45		.40	3.69	67.3	76.8		
	.25	1.78	63.5	19.43		.35	2.69	64.5 ↑64.1	45.25		.35	3.09	66.2	62.75		
	.20	1.18	63.0	12.5		.30	2.10	62.7	23.8		.30	2.49	65.0 ↑65	47.4		
	.111	.116	62.9	11.1		.25	1.50	62.1	16.65		.25	1.89	64	34.6		
T1			62.1			.20	.90	61.7	11.9		.20	1.29	63.1	23.05		
T2			69.3			.135	.116	61.7	11.9		.15	.69	62.7	17.93		
H			.6'		T1			60.7		T2			.102	.116	62.7	17.93
Date	3-7-1961				T2			69.1		T1			61.3			
					H			.6'		T2			69.1			
										H			.6'			

RUN. N.O.	Rack's Reading	Actual Depth	Temp. °F	t%											
1	2	3	4	5	1	2	3	4	5	1	2	3	4	5	
E.26	surf.	7.08	68.2	84.2	E.29	surf.	3.484	67	98.0		.30	243	64.9	62.25	
F. 9'	.55	5.46	69.1	97.1		.35	3.04	67.1	100		.25	1.83	63	47.5	
Th. at middle	.50	4.86	68.9	94.15		.30	2.44	67.1	100		.20	1.23	61.8	11.47	
Le. at bulidge (8'-5")	.45	4.26	68.1	82.75		.25	1.848	66.8	94.15		.107	.116	61.1	0	
	.40	3.66	66.6	61.45		.20	1.245	65.1	61.5	T <sub>1</sub>			61.1		
	.35	3.06	65.5	45.65		.15	.644	63.7	34.6	T <sub>2</sub>			67.2		
	.30	2.46	64.8	35.7		.106	.116	63.2	24.98	H			.6'		
	.25	1.86	64.1	25.7	T <sub>1</sub>			61.9		E.32	.54	5.261	68	100	
	.20	1.26	63.5	17.15	T <sub>2</sub>			67.1		F.4.5	.50	4.77	76.5	53.75	
	.105	.116	63.3	14.29	H			.3'		Th. 9'	.45	4.171	65.7	43.75	
T <sub>1</sub>			62.3		E.30	surf.	7.08	66.7	93.4	↓	.40	3.57	64.6	30.0	
T <sub>2</sub>			69.3		Th. at	.55	5.15	67.1	98.6	not reliable	.35	2.97	63.7	18.75	
H			.6'		1.5'	.5	4.56	66.7	93.4	Instead E.4.0 Was Constructed	.30	2.37	63.0	10.0	
D			6-7-1961		F. 9'	.45	3.96	65.3	75.25		.25	1.77	62.6	5.0	
E.28	F at 9' Th. at 8'-5"					.4	3.36	63.3	49.35		.20	1.17	62.3	1.25	
	surf.	7.08	67.1	89.8		.35	2.76	61.9	31.15		.112	0	62.2	0	
	.55	5.46	67.5	94.3		.30	2.16	61.0	19.45	T <sub>1</sub>			60.2		
	.50	4.86	67.3	92.1		.25	1.556	60.5	12.98	T <sub>2</sub>			68.2		
	.45	4.26	66.7	85.3		.20	.956	60.4	11.68	H			.6'		
	.40	3.66	65.0	66.25		.13	.116	60.4	11.68	E.33	surf.	3.48	67.8	93.3	
	.35	3.06	63.8	52.75	T <sub>1</sub>			59.5			.35	2.97	68.2	100	
	.30	2.46	62.7	40.9	T <sub>2</sub>			67.2			.30	2.37	68.1	98.3	
	.25	1.86	62.0	32.57	H			.6'			.25	1.77	67.3	85	
	.20	1.26	61.4	25.82	E.31	surf.	7.084	66.7	91.7		.2	1.17	65.0	46.6	
	.105	.116	61.1	22.45	F. 9'	.55	5.43	67.1	98.25		.15	.57	62.5	5	
T <sub>1</sub>			59.1		Th. at	.5	4.83	67.1	98.25		.112	0	62.3	1.67	
T <sub>2</sub>			68		8'	.45	4.23	66.9	95.0	T <sub>1</sub>			62.2		
H			.6			.35	3.03	65.9	78.6	T <sub>2</sub>			68.2		
										H			.3'		



## DAM-BURST ANALOGY

Distr. FT.	F1 T <sub>100%</sub>	F2 T	F3 "	F4 "	F5 "	F6 "	F7 "	F8 "	F9 "	F10 "	F11 "	F12 "	F13 "	F14 "	F15 "	F16 "	F17 "	F18
1	5	11	5	11	8.5	7.5		14	5	8.	7	4.6	4.6	6	6	5	6-8	
2	10	24.5	10	22.5	16.5	14		27	9.5	14	13	8.5	8.6	11.2	10.3	10	13 11.8	
3	14.5	36.4	14.6	33.5	24.5	20	35.2	39	13.5	20.5	20	12.8	12.9	16	15	14.3	20 17.5	
4	19.9	48.5	19	44	31.3	26.5	47	50	18	27	26	17.4	17.6	20.8	20	18.5	24.5 22.1	
5	24.8	61	23.5	55.2	39	31.6	59.3	63.5	23	34.5	33	22	22.2	25.9	24.7	23.5	29 28.5	
6	29.3	73.3	28	67	46.3	37.5	72	76	27	41	39.5	27	27	30.2	-	28.7	37.1 34.6	
7	34	85.5	33	72.5	53	43.5	82.5	88.5	31.5	48.5	46.5	31.5	31.5	35.6	36	33.8	37.5 40	
8	38.5	97	37.5	91	61	50	96	103	36.5	55.5	54	37	37	40.7	41.5	39.3	42.2 46	
9	44	107.5	42.2	103.2	-	55.5	108.7	116	41.5	64	61	42.2	42.2	46.2	47.7	45.1	47 52.5	
10	48.5	123.5	46.5	116	-	61.5	122	30.5	46	71.5	68	47.7	47.7	52	54.2	51.0	52 58.7	
11	54	138	52	129.2	-	67	136	144.5	51.5	78.5	76	53.5	53.6	58.5	60.6	56.6	57.5 66.5	
12	58.5	152	57.5	144	-	75	150.5	158.5	55	86.5	83.3	59	59	65	67.3	63.6	62.2 74.1	

RUN	TYPE	$\Delta Q$	H	K	K <sub>Rd</sub>
F. 1	S <sub>o</sub>	.01155	.3'	.623	5115
F. 3	"	"	"	"	"
F. 6	"	.00693	"	.625	4000
F. 5	"	.00462	"	.622	3240
F. 2	"	.00231	"	.58	2135
F. 4	"	"	"	"	"
F. 14	"	.0231	.15'	.605	2540
F. 18	"	.01733	"	.608	2180
F. 19	"	"	"	"	"
F. 9	S <sub>u</sub>	.0155	.3'	.561	5440
F. 10	"	.00693	"	.57	3700
F. 11	"	"	"	"	"
F. 8	"	.0023	"	.523	1949
F. 12, 13	"	.0031	.15	.563	2725
F. 16	"	"	"	"	"

D	G.1 T	G.2 "	G.3 "	G.4 "	G.5 "	G.6	G.7	G.8	G.9	G.10	G.11	G.12	G.13	G.14	G.15	G.16	G.17	G.18	G.19	G.20	G.21
1'	4.5	4.6	4.6	5	4	3.5	-	-	16.8	28	28	27.8	16.5	16.6	16.6	46.6	46.8	37.6	37.2	77.3	77
2'	10	10.5	9	-	-	-	-	-	-	-	-	-	-	-	-	-	-	-	-	-	
3	15.5	16.8	14	10.5	8.5	8.8	30.7	30	-	31	-	30	-	-	50	-	41	-	80.8	80	
4	22	23.8	20.5	14	11.3	-	-	-	20.5	-	31.6	-	20.3	20.6	-	51.5	-	-	83.1	83	
5	29.5	29.5	27.5	18.5	-	11	34	33.9	-	34.1	33.8	33	-	-	53.6	53.5	-	-	85.2	84.9	
6	35.5	38.5	35	23	21	22	36	-	23.6	36.5	-	35.2	24.8	25	56.1	55.8	48.1	45.6	87.8	88.8	
7	44	46.2	43	-	-	28.5	38	38.5	26	38.5	38.1	39.8	29	28.7	58.5	58.4	51.8	48.8	91.2	92.5	
8	55.5	57.3	54.3	32.6	33.5	34	40.7	41	29.7	41.9	-	-	35	33.9	61.2	61	56	53	97.5	96.9	
9	65.2	73	68.3	40.6	40	40.7	44.3	44.2	35	46.5	44	44.4	41	39.6	65	64.7	59	55.6	102.2	100.8	
10	79.5	89	83	47.7	48	50.5	48.7	48.5	43.2	55.5	50.5	54.9	48.5	47.3	68.8	68.3	63.7	60.5	108.3	105.8	
11	98	106	97.3	60.2	60	65.5	53	53.2	48.8	64.8	59.2	58.7	57.5	55.5	73	72.7	68.1	67.5	118	112.5	
12	116	-	113	69	69.1	77.3	61.7	60.7	54.2	76.7	69.2	64.4	67	65.2	79.5	79.7	74.5	74.7	-	119.5	
13	135	-	130	80.5	83.6	91.5	69.5	69.7	62.7	93	81	74.7	79.8	76.1	87.5	90.9	82.6	81.2	-	126.5	
14	154	-	148.5	-	-	109.5	77.4	78	-	-	-	86.5	93.5	-	95.3	103.3	90.5	-	-	132.8	
15	-	-	168	-	-	-	-	-	-	-	-	-	100.5	-	-	-	-	-	-	140.1	

PP IN	22.2	"	"	25.5	"	"	25.5	"	15	25.5	"	"	15	"	45	"	35	"	75	"	"
SEC																					
ΔP	.0017	"	"	"	"	".0016	".0017	"	"	".0018	"	"	"	"	"	"	".0019	"	"	"	
Q cu SEC	.044	"	".0445	.08	.08	.081	.081	"	"	".082	"	"	"	"	"	"	"	"	"	"	
H FT.	.83	"	"	"	"	"	.83	"	"	"	"	"	"	"	"	"	"	"	"	"	
Date	31-10	1-11	"	2-11	"	3-11	6-12	"	"	7-12	"	8-11	"	"	9-11	9-11	10-11	"	"	13-11	

D	G22	G23	G24	G25	G26	G27	G28	G29	G30	G31	G32	G33	G34	G35	G36
	T <sub>SEC</sub>	T	"	"	"	"	"	"	"	"	"	"	"	"	"
1	4	3.8	3.6	3.5	6.2	5.3	7	6	5.6	64.5	63.7	17.5	17.6	38	37.5
2	6	-	6.3	5.9	10.3	9	11.8	11	10.5	66.9	-	19.2	19.3	40.3	-
3	8.7	9	9	8.5	15.5	13.9	17.5	16	14.8	70	68.8	21.3	42.3	41.3	
4	11	11.1	12	-	20.6	18.5	25.5	21.2	21.1	73	72.4	23.7	25.7	..	44.5
5	14.5	14.3	14.8	-	26.8	24.1	33	27.7	27.2	76.8	76.4	27.5	-	47.5	47.2
6	18.7	18	19	18.5	33	30	39.5	35	34.5	81.2	80.3	34	33.9	53	52
7	22.7	23.2	23.2	23	-	36.5	47	43.3	43.5	86	87	42	41.4	58.2	58
8	28.2	29.8	29.5	29	50	43.5	54.5	51.5	52	91.6	94.8	51.2	51	65.2	65
9	33.3	33.8	36.5	34.2	58.8	52	61.5	60.5	61.3	97.5	101.5	60.4	61.4	71.8	72.8
10	41.1	43	44.2	42	70	60.5	69.5	70.5	73.4	106.6	111.3	71	71.5	81.1	84.3
11	48.2	51.7	52.5	50.5	-	71	76.5	80.6	83.8	116	119	81.7	84	89.9	97
12	56	61.6	61	61.5	97.3	81.6	84	90	93.8	125	124.2	94	97.5	102	108.1
13	63.5	73.4	71	73	-	96	92.3	101.3	102.6	136	-	106.5	110.2	115.3	120.2
14	-	-	79.8	-	-	110.5	102.3	114	114.2	145	-	118.6	123	130.2	136
15	-	-	-	-	-	-	-	-	126.5	-	-	130.3	-	148.5	150
16	-	-	-	-	-	-	-	-	-	-	-	-	-	-	-
$\Delta e$	.0019	.0019	"	"	"	"	"	"	"	.002	.002	"	"		
Q <sub>CUSEC</sub>	.082	"	"	"	"	"	"	"	"	"	"	"	"	"	
H	.83'	"	"	"	"	"	"	"	"	"	"	"	"	"	
DATE	15-11	"	16-11	17-11	20-11	"	22-11	22-11	22-11	23-11	23-11	"	"		
T <sub>S</sub>	59°F	"	59.6	59.6	59.6	"	"	"	"	"	"	"	"	"	
T <sub>F</sub>	66°F	"	68.5	68.5	68.5	"	"	"	"	60.4	"	"	"	"	

S.T. BALANCED	.326' W.D IN INTRODUCT ION BOX.	P.P IN AT 60 SEC. OVERTAKING NEVER TOOK PLACE IN THE AVAILABLE TANK.
.326' WATER DEPTH IN INTRODUCTION BOX		

DEPTH	RUN G 24						G 25					
	D = 1 on E		D = 5'		D = 11'		1'		5'		11'	
	(1)	(2)	(1)	(2)	(1)	(2)	(1)	(2)	(1)	(2)	(1)	(2)
"	59.6	0	60	4.5	59.8	2.25	60.1	5.0	60	4.5	60	4.5
"	-	-	59.9	3.5	-	-	-	-	60	4.5	60.1	5.6
"	59.8	2.25	60.1	5.61	59.9	3.37	60.7	12.4	-	-	-	-
"	-	-	60.3	7.88	-	-	-	-	60.8	13.45	60.9	14.6
"	60.1	5.61	-	-	60.5	10.1	61	15.75	-	-	-	-
"	60.1	5.61	60.3	7.88	60.8	13.45	-	-	61	15.75	61.1	16.82
"	-	-	-	-	-	-	61.7	23.6	-	-	-	-
"	60.5	10.1	60.5	10.1	60.8	13.45	-	-	61.5	21.4	61.5	21.4
"	-	-	-	-	-	-	62.5	32.6	-	-	-	-
"	61	15.7	61	16.85	-	-	-	-	62.2	29.2	62	27
	G 26											
	1'		5'		11'							
	(1)	(2)	1	2	1	2						
"	60	4.5	60.4	9	-	-	Freshwater $68.5^{\circ}\text{F}$					
"	60	4.5	60.5	10.1	-	-	Salinity $59.6^{\circ}\text{F}$					
"	-	-	-	-	-	-	$\Delta \rho$ .002					
"	60.5	10.1	61.9	25.8	-	-	Date 25-11-1961					
"	-	-	-	-	-	-	H .83'					
"	60.9	14.6	61.1	16.82	61.2	18	Q .082 cusec.					
"	-	-	-	-	61.2	18	Water Depth in the Introduction					
"	61.5	21.4	61.8	24.7	-	-	Box .326'					
"	-	-	-	-	-	-	S.T BALANCED.					
"	-	-	62	27	62.2	29.2						

H23

$d_m = .205'$				$d_m = 1.025'$				$d_m = 2.26'$				$.205'$				$1.025'$				$2.26'$				
$h$	$H$	$t_F^{\circ}$	$\frac{T-T_f}{T_2-T_f} \%$																					
1	2	3	4	2	3	4	2	3	4	2	3	4	2	3	4	2	3	4	2	3	4	2	3	4
SURF ACE	-	65	36.4	-	-	-	-	-	-	-	65.2	36.6	-	64.2	20	-	64	16.65						
2.1	8.01	-	-	8.01	64	18.2	8.01	64.3	23.6	8.01	64.6	26.6	8.01	64.8	30	-	64	16.65						
1.6	6.12	-	-	6.12	-	-	6.12	-	-	6.12	63.8	13.5	6.12	-	-	6.12	-	-	6.12	-	-			
1.1	4.21	64	18.2	4.21	63.5	9.1	4.21	64	18.2	4.21	63.3	5	4.21	64	16.65	4.21	63.7	11.65						
0.6	2.3	-	-	2.3	-	-	2.3	-	-	2.3	63.2	3.34	2.3	-	-	2.3	-	-	2.3	-	-			
0.1	383	-	-	383	63.5	9.1	383	63.2	3.64	383	63.2	3.34	383	63.6	10	383	63.2	3.34						
$T_1$	63°										$T_1$	63°												
$T_2$	68.5										$T_2$	69°												
Date	12-12										Date	12-12												
$\Delta P$	.002										$\Delta P$	.002												

H 25

$d_m = .205'$				$1.025'$				$2.26'$																
$h$	$H$	$t_F^{\circ}$	$\frac{T-T_f}{T_2-T_f} \%$																					
1	2	3	4	2	3	4	2	3	4	2	3	4	2	3	4	2	3	4	2	3	4	2	3	4
Surf A	-	66	33.4	-	-	-	-	-	-	65.5	22.2													
2.1	8.01	66	33.4	8.01	65.5	22.2	8.01	-	-															
1.6	6.12	-	-	6.12	-	-	6.12	-	-															
1.1	4.21	65.1	13.3	4.21	65.3	17.8	4.21	65.3	17.8															
0.6	2.3	-	-	2.3	-	-	2.3	-	-															
0.1	383	65	11.1	383	65	11.1	383	65	11.1															
$T_1$	64.5																							
$T_2$	69																							
Date	12-12																							
$\Delta P$	.002																							

